RUSSIAN SPACE SYSTEMS

Scientific and technical journal

ROCKET-SPACE DEVICE ENGINEERING AND INFORMATION SYSTEMS

Volume 3. Issue 2. 2016

Contents

Vol. 3, Iss. 2, 2016

ROCKET-SPACE DEVICE ENGINEERING AND INFORMATION SYSTEMS
Vol. 3, Iss. 2, 2016, pp. 2–19

Photonic Technologies in Space Device Engineering

A. K. Ponomarev[1], A.A. Romanov[2], A.E. Tyulin[3]

[1,3]candidate of engineering science, [2]doctor of engineering science, professor,
[1]Scolcovo Institute of Science and Technology (Scoltech),
[2,3]Joint Stock Company "Russian Space Systems"

e-mail: romanov@spacecorp.ru

Abstract. The article provides an overview of the basic technologies where products of photonics and optoelectronics are used or potentially can be used to create a target and service equipment of navigation, communication, and Earth remote sensing space-craft. The possible range of technology solutions needed to ensure precision satellite positioning, creation of optical communication technologies used for information exchange on the lines of "spacecraft-spacecraft" or "spacecraft-Earth", as well as the choice of ma-terials for photodetectors and measuring sensors is presented. Moreover, technological trends of modern and advanced developments based on the use of photonic technologies, providing record characteristics that meet the global standards in the development of space device engineering are shown. The main recommendations for the development and intensification of the introduction of photonic technologies in the space industry of the Russian Federation are given in the conclusion.

Keywords: Photonics, optoelectronics, fiber optics and optical communications, onboard time scales, coordinate-time and navigation support, frequency instability, optical frequency standards, small-sized atomic clock, optical gyroscope, annular resonator on "whispering waves", photoelectronic receivers, hyperspectral devices, photon sensors

Introduction

Photonics in recent years has become one of the important directions in development of innovative economy in different countries. The development of this high-tech area is considered a priority for the global aerospace industry. NASA [1,2], ESA [3], JAXA and space agencies of the BRICS countries [4] identified this trend in the national programs of development of advanced space systems and complexes for various purposes as a priority.

The emergence of photonics as a scientific field, encompassing problems of generation, collection, dissemination and processing of optical signals, in itself marked a strong potential for the introduction into the information systems created for different purposes, used in various industries.

Despite the fact that the space industry does not have large amounts of commercially available high-tech products, the industry itself can certainly become the locomotive for the introduction of modern photonic technologies into the space complexes and systems under development. This circumstance is due to the fact that the functioning of space-based information systems for various purposes is provided by the processes of generation, emission, reception, processing and transmission of electromagnetic signals throughout the electromagnetic spectrum, from ultraviolet optical to microwave radio band.

Constantly growing volumes of data produced by space systems, as well as the requirements for miniaturization of target and service equipment for spacecraft, define the urgent need for the developers to search for promising technologies used in space device engineering for creating new types of target and service equipment.

The demand for implementation of photonic technologies is increasing in space applications, since with increasing volumes produced by space data facilities, the infrastructure for generating, collecting, processing, digestion and dissemination of optical data to the end user rests on purely physical limitations associated with the use of electrons as the information carriers. Photonics is the direct successor to the electronics [5]. Its main difference is that in place of electrons, photons are used as information carriers. Nevertheless, the development of photonic technologies largely repeats the stages of development of electronics. Today, photonics combines areas such as optical photonics, microphotonics, nanophotonics and radiophotonics, covering the range of the electromagnetic spectrum from UV to microwave.

In [6] it is shown that in the future remote sensing systems, the amount of generated data on board the spacecraft will increase by at least three orders of magnitude due to the increase in the spatial resolution of the target imaging equipment to the submeter size and the use of several thousand spectral channels of survey. The currently employed on-board computing power will not be sufficient to collect, process and exchange data without the use of photonic technologies.

Note that the functionality usually implemented with one “big” spacecraft, complexing a large number of target devices, in the future can be distributed among a certain number of interacting with each other “small” spacecraft [7]. Each spacecraft in such groups developed on the principle of “companion device” may have different limited functionality, but, on the whole, the cluster will function as a single unit. At the same time, in order to maintain the secure borders for each of the interacting elements, joint control and synchronization of spacecraft maneuvers within the cluster is required.

Optical inter-satellite links are a great tool for solving problems of interaction of the elements of such a distributed system, especially in view of the need to transfer large amounts of data from each party [8]. For the components of this distributed spacecraft to act as the “main server” and “router” a link with a capacity of not less than several Gbit/s is required [9].

When designing a spacecraft for deep space exploration, it is necessary to create the on-board equipment that meets the extremely stringent requirements for weight, power consumption and the geometric dimensions. Therefore, the large and power-inefficient antenna complexes are based on the ground to compensate for the limitations imposed on the on-board equipment of the spacecraft. In accordance with Article [10], the optical communication terminals are lighter than the traditional radio systems. Provided a repeater station is installed on the ISS or other spacecraft (outside the Earth’s atmosphere), optical communication can be used for control, as well as for the target channels of communication with spacecraft designed for deep space exploration.

Creating data transmission hardware in the optical range of the spectrum in the long term will almost completely solve the whole complex of the current problems. On the one hand, there is a technical possibility to considerably (at least by an order) increase the bandwidth of on-board radio lines, on the other hand, several devices can simultaneously operate in the optical range without compromising their functionality [11] due to the absence of electromagnetic compatibility problems.

Modern space systems and complexes used for a variety of national economic goals, actively employs the methods and tools for measuring the time and frequency characteristics of the signals detected by them. In [12] it is noted that since time and frequency are the most frequently measured physical quantities, one of the main applications of modern metrology, ensuring the proper functioning of satellite equipment, is the creation of standards of various physical quantities on the basis of the fundamental physical constants (FPC) and precision frequency measurements.

The relative instability of the on-board frequency standards used as a part of the on-board spacecraft equipment, significantly impacts the accuracy of satellite-based positioning of ground targets. Existing tools with an instability of around 10^{-14} make it possible to establish the coordinates of objects with meter accuracy. The transition to the centimeter or millimeter accuracy requires the use of on-board standards of time with an instability better than 10^{-16}. Such precision will be ensured by the optical atomic frequency standards currently under development both in the Russian Federation and abroad.

Thus, the precise metrology of frequency and time measurements is vital to make progress in the following space applications [13]:

– basic research, using precise measurements of distances;

– communication, including space communication, using high speed data transmission over long distances;

– global satellite navigation systems GLONASS/GPS, requiring accurate measurement of time.

Optical-electrical (photonic) components have been widely and for long implemented in modern space systems of remote sensing as photosensitive detectors, as well as in solar batteries, providing power to spacecraft. In addition to these obvious applications, the developers of space systems show an increased interest in the use of photonic technology in carrying out various measurements on board the spacecraft, as well as for the collection, processing and transmission of measurement information obtained.

Paper [14] provides an overview of the storage systems and devices for large volumes of digital data, including CD drives and photonic data storage devices based on the use of holographic methods.

According to the report presented by the International Data Corporation (IDC) in 2011, the total amount of data generated globally is growing exponentially and will reach 35 ZB by 2020 (1 zetabyte (ZB) = $5*10^3$, 1 exabyte (EB) = $5*10^6$, 1 petabyte (PB) = $5*10^{12}$GB) [15], while, for example, only the amount of data from a daily survey of the Earth surface with sub-meter spatial resolution of potential space-based systems [16] could make $5*10^{14}$ digitized points or over 10^{15} bytes = 10^6 GB or 73 EB yearly. It is noted that the provision of storage of such data volumes is only possible when using new photonic principles underlying the development of advanced means of data storage.

One of the earliest publications on the use of photonic technologies in spacecraft [17] declares the need for a wider band of frequencies for information signals, their on-board processing in the harsh conditions of the outer space, and makes serious demands to improve the technologies of creating an electronic component base and new materials.

The purpose of this article is to analyze possible areas of application of photonic technologies in the development and creation of future equipment for space-based information systems and complexes for various purposes, to identify the main problematic issues, as well as to formulate the recommendations and proposals for their solution.

Assessment of global trends in the use of photonic technologies in space systems of communication, navigation and remote sensing

The first employment of photonic technologies for space applications included radio signal distribution circuits, delayed signal lines, on-board frequency generators, analog-to-digital conversion with the photonic signal processing, as well as fast analog-to-digital signal conversion. Along with the listed areas of space applications of photonic technologies, the employment of nanophotonic components has been started to create advanced designs of space technology [18].

To implement technically exigent mission of deep space exploration at an acceptable cost, NASA has developed a special technology program known as X2000. The program implied that beginning with 2000, every two or three years the upgraded subsystems, as well as

Table 1. Roadmap of spacecraft avionics until 2030

	Descent module of the “Mars exploration” mission	1st generation X2000	3rd generation	5th generation	Future
Volume, cm^3	50000	10000	1000	10	1
Mass, kg	80	40	1	0.01	0.002
Power consumption, W	300	150	30	5	0.05
	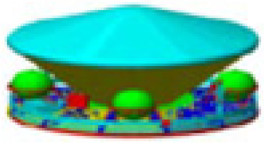	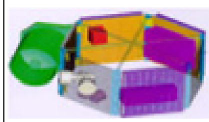		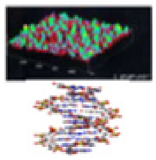	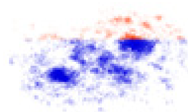
Year	1999	2003	2010	2020	2030

Source: Nanotechnology Research Directions: IWGN Workshop Report, Vision for Nanotechnology R&D in the Next Decade, September 1999.

elements of the spacecraft design, will be developed and implemented. One of the objectives of the program was a significant reduction in the size of the spacecraft avionics with each new generation of X2000 products, partly through the implementation of the nano- and microtechnologies. Table 1 contains the road map of development of spacecraft avionics, which shows that the projected volume, weight and power consumption of avionics has reduced by about one order of magnitude in the last 10 years. The parameters of Martian spacecraft avionics as of 1999 are taken as the base level.

Notably, even the first upgrade in the framework of X2000 is an integrated avionics system that combined command telemetry and data processing functions, attitude control, energy distribution and management, as well as the interface of the scientific payload. The use of automated technologies of development and design of equipment has made it possible to create a highly integrated modular block architecture, which provided a greater degree of design reliability for long missions in deep space.

Currently, great hopes are put on the use of the “system on chip” technology, that allows in the future to create of avionics modules in a single chip – an integrated circuit. At the same time such a crystal may include power consumption management, sensors and telecommunications modules, combined with the on-board computer and memory. Today’s success of the global space device engineering fully confirmed the predictions given.

The goal set for 2020 involves the development of revolutionary computer technology that could not only overcome the limitations of a simple scaling of semiconductor technologies, but also make the concept of “intelligent spacecraft” feasible. Such a spacecraft should be a fully self-contained, highly integrated spacecraft with superb capabilities and ultra-low power consumption. To achieve these goals it is necessary to ensure the widespread use of photonics technology in general and nanophotonics in particular. This circumstance is due to the fact that the phenomenal advances in digital computer technology in recent years, even using supercomputers, will not be able to compete with biological systems in the accomplishment of such ill-conditioned tasks as image recognition, processing of multisensor systems data, failsafe control, and adaptive adjustment for environment conditions.

Creation of new multifunctional materials based on quantum technologies with extraordinary properties will allow to achieve a faster (tens of Tbit/s) data transfer, secure storage and processing of information, replacement of the hardware components of microchips, as well as space and transport equipment.

The use of the next generation microphotonic integrated circuits permits the integration of various optical components into a common photonic chip, which minimizes the number of external connecting optical fiber cables and reduces the overall size and weight of a space system, at the same time substantially increasing its reliability.

Table 2. Interests of the European space industry in the use of photonic technologies and metamaterials

Technology	Technology level	Development horizon	Priority	Usage
Photonics-on-chip	Level C	Medium-term	Highest	Protection against radiation, communication
Photonic FOCL	Level C	Medium-term	High	Devices, radiation resistance
Aerogel packaging of photonic components	Level C	Long-term	High	Thermal protection
FOCL on sapphire	Level C	Medium-term	High	Temperature control
Microresonators	Level A	Long-term	High	Spectroscopy
Nanocrystals	Level A	Medium-term	High	Sensors
Photon beacon	Level B	Medium-term	High	Spectroscopy
Vector vortex coronagraphy	Level C	Medium-term	High	Detectors
Infrared metamaterials	Level A	Long-term	High	Cyclic changes in temperature
Metasurfaces	Level A	Long-term	High	Sensors
Interferometer with tunable pupil	Level B	Medium-term	High	Interferometry
Quickly tunable metamaterials	Level A	Medium-term	Highest	Communications, sensors, detectors
Frequency selective surfaces	Level A	Medium-term	High	Design of antennas, sensors, detectors
Plasmonic enhancement of photosensitivity	Level A	Medium-term	Highest	Sensors, detectors
Frequency selective surfaces	Level A	Long-term	High	Cyclic changes in temperature
Metamaterials with a negative index	Level A	Long-term	High	Detectors
Phase changing films	Level A	Long-term	High	Radiation protection
Flat tunable lenses	Level A	Long-term	High	Sensors
Plasmonic color separation	Level A	Long-term	High	Sensors

Source: Technological Breakthroughs for Scientific Progress (TECHBREAK)// Brussels, ESF Forward Look, 2014.

In [19] the interests of the space industry in Europe have been identified in the field of photonic technologies and metamaterials, which are listed in the Table 2. It gives expert assessment of the current level of readiness for each technological trend. The level A corresponds to TRL 1-3 of the standard scale of technology readiness [20]; level B corresponds to TRL 4; level C, to TRL 5.

Thus, for all these technologies and their applications, the main advantages of photonic systems that make it possible to successfully use them in space missions through a combination of built-in micro-, nano- and fiber optics, include:

– low susceptibility of the systems under development to electromagnetic interference, electrical discharges and the impact of charged space particles;

– a significant reduction in the weight of signal lines (<1/20 compared to traditional cable electrical connections);

– high throughput data transfer capability (up to tens of THz);
– galvanic isolation of critical subsystems of spacecraft (SC);
– high-speed processing of optical, radio and microwave signals;
– high-speed transmission/reception of useful information;
– sensitization and expansion of operating ranges for sensors and detectors;
– increase in the active life time of SC.

The realization of such benefits and the application of photonics products in the on-board spacecraft equipment dramatically improves the performance:
– reduce the weight of the signal cable lines by 20 times;
– reduce electric power consumption by 30%–50%;
– increase the speed of information processing by 20–200 times;
– reduce the cost of the equipment manufacturing by 20%–50%;
– increase the active lifetime of space devices by 1.5–2 times.

Based on the analysis of these photonic technologies and their applications in space devices, critical photonic technologies, topical for the Russian space industry can be identified:
– infotelecommunication technology (optical inter-satellite links and downlinks, fiber optic and wireless information networks inside the spacecraft, hybrid computing devices);
– remote sensing technology (receivers of optical and infrared signals, optical aperture synthesis);
– technologies of development and implementation of sensor, measuring and converting devices (temperature and pressure sensors, accelerometers, ADC/DAC, optical accelerometers, optical gyroscopes, solar sensors);
– quantum calculators technology;
– optical laser detecting and ranging systems technology;
– technology of small on-board transceiver antennas made of metamaterials;
– wireless power transfer technology;
– information storage technology, holographic memory;
– quantum technology of satellite navigation and orientation systems (compact on-board atomic clocks, optical accelerometers, optical gyroscopes, solar sensors, terrestrial radiation sensors).

We now estimate the current state of development of photonic technologies for space applications and the main trends of their development.

Basic requirements for the emerging technologies of satellite navigation through the application of photonic technology

The final report of the US National Security Space Management "National Positioning, Navigation, and Timing Architecture Study" [21] presents the development trends and recommendations for the assessment of development alternatives of PNT systems. The development team, challenged with the task of identifying potential tools and technologies for solving future problems of PNT, have used the procedures accepted in the US National Security Space Management that take into account any non-standard ideas that now may seem extreme or unusual, but by 2025 can become feasible. The analysis shows that the most promising are the 3 technologies that can lead to significant changes:
– Chip Scale Atomic Clocks (CSAC)
– high-precision optical atomic clock;
– cost-effective units of inertial sensors based on microelectromechanical systems (MEMS) – extremely high-precision interferometric inertial navigation systems, etc.

The total scope of the experiment covered 50 technologies of which the following areas were selected as priorities for the development of global navigation systems:
– the use of small-sized atomic clock;
– the use of optical clocks based on atomic transitions at optical frequencies;
– installation of laser retroreflectors on all spacecraft and the use of ground-based laser tracking in order to improve the satellite orbit models to enhance the accuracy of determining the orbit parameters;
– precise calibration of devices that transmit time signals, including the equipment on-board the spacecraft, transmitting the information about the time in the navigation signal;
– communication of the elements of GNSS through inter-satellite laser data channels;
– provision of additional sources of airborne PNT;
– the formation of timing support tools, that transmit timing information over the fiber optic link;

– creation of a single GNSS service that could provide centimeter accuracy in real time or close to it, and millimeter accuracy in post-processing mode, as well as the integrity data in real time;

– the organization of high-precision ephemeris timing support for the consumers using all available signals for navigation tasks.

Using the radiation of pulsars for synchronization of satellite navigation systems

The accuracy of mutual synchronization of satellite navigation systems is influenced by three main factors:

– the accuracy of the system time scale itself, which is determined by the technology of its realization: the stability of its constituent time keepers, methods of their comparison and the creation of the group time scales;

– synchronization accuracy of the on-board time scales (OTS) and the system time scale is determined by the technology of the synchronization process;

– the accuracy of prediction in consumer equipment on-board time scales for a predetermined interval, that is determined by the stability of the on-board clock device based on the on-board frequency standards with specified accuracy characteristics.

One of the possible development directions of time synchronization of satellite navigation systems in the long term is its building on the basis of a pulsar time scale, actively developed in recent years both in Russia and abroad [22, 23]. A detailed overview of various methods of navigation in deep space is discussed in [24].

The idea of using a highly stable pulse repetition observed in pulsar emission at virtually unlimited space-time extent by transforming it into a reference (pulsar) time scale arose almost immediately after the discovery of pulsars in 1967. The relative instability of proper rotation of pulsars is 10^{-14} and higher at a time interval of several years. The best value is shown by the pulsar J0437-4715 with an instability of $\sigma_y(\tau) < 10^{-15}$ on a time scale of over 3 years (unpredictable deviation is 10 ns in 3 years). Thus, the stability of a pulsar time scale (PTS) is potentially high and essentially can be used for highly stable and precise timing.

The pulsar based scales, however, have several advantages compared to the existing atomic time scales:

– the means for a reliable observation of the source with the existing or future astronomical instruments with the accuracy sufficient for the tasks of potential consumers;

– the lifetime the source, sufficient for the customer requirements (depending on the task);

– high-precision extrapolation of the pulse arrival times by the analytical model (high stability of the observed emission period, or predictability);

– shorter radiation period than required for the consumer time scale synchronization;

– a high degree of recognizability of electromagnetic radiation variations.

Studies, including those conducted in Russia, have shown that, due to the presence of a sufficiently large number of bright stable pulsars, it is possible to build a pulsar group time scale based on their observation, with higher stability than that of each of its constituent individual pulsars. The stability of a pulsar group time scale is estimated to be in the order of 10^{-16} over long periods of time (years, decades), which is much more reliable than existing nuclear group time scales.

In this context, the future competitiveness of the PTS in comparison with the atomic time scale it is of considerable interest. The question is very important owing to the fact that the development of ground-based atomic frequency standards is rapid, and during the last 50 years their stability was improved by about an order of magnitude every 7 years. Now they have characteristics comparable to the stability of the very stable pulsars. For example, the most massive cesium clock of the 5071A type, used for the creation of the TAI global time scale, has an instability of $\sigma_y(\tau) \le 5\times10^{-15}$ in the sampling intervals of 72–120 hours. The instability of the clock based on the best hydrogen masers with a sampling interval of 120 hours is $\sigma_y(\tau) \le 5\times10^{-16}$. The group time scales (TAI, UTC) are even more accurate: according to the results received from 220 atomic clocks from almost 50 time laboratories around the world, those scales have an instability of about 2×10^{-15}.

Spaceborne optical time standards

Optical atomic clocks will be widely employed both in ground and in spaceborne segments of global navigation satellite systems, which will improve the accuracy of the spaceborne time standards by 2–3 orders of magnitude. This, in turn, reduces the need to update the satellite time standard parameters and thus improve the autonomy of navigation satellites. With better understanding of the influence of the atmosphere on the passage of the navigation signal this will eventually lead to a significant increase in the accuracy of positioning systems for consumers.

A detailed review of the application of the European research results in the field of satellite navigation is presented in [25].

The work on optical atomic time standard provides guidance on the parallel development of four different variants of optical atomic clocks [26]:

1. Optical atomic clocks with ion baffles based on 88Sr+ [27].
2. Optical atomic clocks based on strontium atomic lattice [28].
3. Optical atomic clocks with ion baffles based on quantum logic using 27Al+.
4. Optical atomic clocks based on the mercury space lattice.

The development of these devices is expected to be performed in broad international cooperation of companies from the European Union countries, including the UK, Germany, France, Austria, Italy and Switzerland that hold the leading positions in the optical radiation metrology. Certainly, professionals from the companies specialized in space system integration should be involved in these projects from a very early stage.

Small atomic clock

Development of small-sized optical frequency standards lies in line with the miniaturization of the lasers used for these purposes. Such research projects first took place in the National Institute of Science and Technology (Boulder, US) [29]. Similar projects are under way, in particular, at the Institute of Laser Physics SB RAS [30] ("generator of optical frequencies based on femtosecond forsterite laser"). The size of the laser developed here is 20 by 30 cm; the ILP I2/532 – 1 optical frequency standard is created on its base. Together, LPI, Fiber Optics Research Center, and the Avesta company (LPI subsidiary) were the first to develop a compact femtosecond optical clock, capable of operating on board of an artificial satellite after the necessary fine-tuning (stability of 10^{-14}).

To date, the efforts in the field of optical frequency standards are for the most part on the stage of research and advanced development; the commercial use of such devices is limited. It is believed that under the condition of overcoming their inherent shortcomings such equipment will have a very positive market outlook.

Main research areas in the field of optical communication systems

In general, studies of the open lines of the optical range are aimed at solving problems in several areas. Finding the optimal bands for data transmission in the atmosphere, as well as factors affecting the speed of data transmission, are the goals of many research projects. The possibilities of increasing the transfer rates and development of new signal modulation schemes are studied [31]. Transmitters and receivers of optical signals are being developed [32]. Analytical research, justifying the need to introduce optical technologies to replace the traditional radio engineering, also plays a major role.

The idea of information transmission in the optical range was proposed in the 1960s [33]. Specialists of the Hughes Corporation proposed to use for this purpose the newly developed rubidium laser. Subsequent experiments have had little success over the following 50-60 years. Only in the beginning of the 21st century the first space experiment on the transmission of information in the optical range, SILEX, was held [24].

In 2001, as a part of the SILEX, information has been transmitted from the low-Earth orbit (SPOT-4 spacecraft) to the geostationary orbit (ARTEMIS spacecraft). Transfer rates of up to 2 Mbit/s at the 819 nm wavelength have been achieved [34].

Simultaneously with the transfer of information in open space with the ARTEMIS spacecraft, the information transmission through the atmosphere was carried out. In 2001, data rates up to 50 Mbit/s through the 847 nm channel were also achieved. Presently, data rates as high as 5-6 Gbit/s have been achieved. Such an optical link functions aboard the TerraSAR-X and NFIRE spacecraft using the 1064 nm channel.

For transmission of information in the optical range modern equipment uses two frequencies, which lie in similar atmospheric transparency windows: 1064 nm (282 THz) and 1550 nm (193 THz). For optical satellite links the 1550 nm channel seems more preferable than the 1064 nm channel, as the background noise in this channel is 4 times lower. In addition, the turbulence, which increases the signal-to-noise ratio, has less effect [36].

At present, the possibility of creating optical terminals with speeds from 30 to 100 Gbit/s is considered. Preliminary calculations show that the aperture of the "mirrors" of such terminals will be 200 mm and 1000

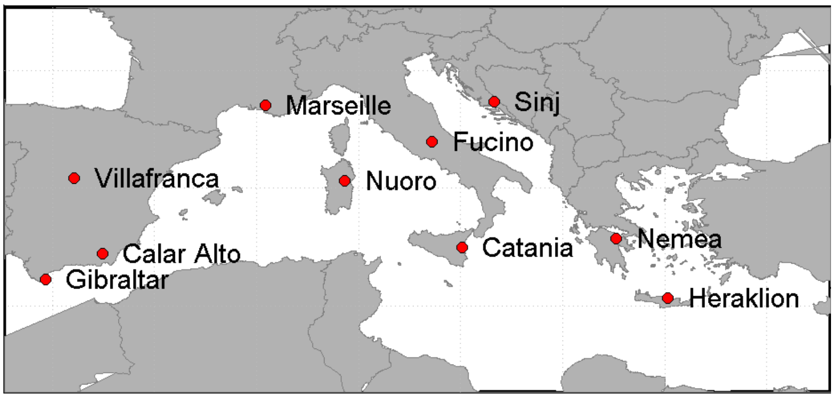

Figure 1. Prospective placement of the European terrestrial optical stations network
Source: Adapted from [31].

mm respectively. In accordance with the energy budget of the radio link, it can be stated that the minimum viewing angle must be at least 30° above the horizon, without the use of antinoise signal coding technologies [31].

Work [31] shows the results of an experiment on information transmission in the optical range in the atmosphere at a rate of 1 Tbit/s. It is shown that information can be transmitted and received at such transfer rate, but the transmission distance does not exceed a few hundred meters. This study examines the possibility of using the new technology of Erbium-Doped Fibre Amplifers (EDFA), which may increase the characteristics of both the receivers and the transmitters of optical signals. In addition, it is proposed to consider the possibility of multiplexing of the channels with different wavelengths, which will increase the energy potential of the optical line.

It is well known that the ability of the optical data transmission lines is limited by the presence of clouds in the path of the optical signal. The European Union established a geographically distributed network of stations, which provides spatial diversification of the receivers and is the most reasonable way to ensure the continuous availability of the communication channel. Along with the spatial distribution of the receivers (by analogy with conventional radio systems), research is conducted in the field of multiantenna receiving stations, which are meant to reduce the traffic of optical lines in order to increase the system capacity [37].

Possible distribution of ground stations in Southern Europe is shown in Figure 1 (10 stations) [31]. The following reasons (alongside with cloudiness) can result in the lack of communication: strong turbulence in the atmosphere above the receiving station, the presence of the sun in the area of visibility, the technical condition of the station or of safety considerations (for example, the presence of aircraft in the signal propagation path). This cloudiness is still the dominant cause.

The average annual availability of this network, which is determined by the probability that at least one station is not obscured by clouds and is available for the exchange of information, is 99.89% [31]. A detailed statistical analysis of the cloudiness in Europe shows the situation when all the stations are covered by clouds may occur mainly in winter, i.e. to further increase the percentage of availability, one station must necessarily be placed in the southern hemisphere.

One of the main problems in the construction of space optical communication systems is to provide a technology for the data transition from one ground station to another directly in the course of a session. To prevent data loss when switching, it is necessary to provide a data feed to the stations, at least as long as the data stream is not synchronized.

The technology can be created with the application of the duplicated line, which implies the presence of two transceivers on board of the geostationary spacecraft. Such apparatus may be arranged in the form of two independent terminals or as a single telescope with an enhanced focal plane in order for two stations to be multiplexed. Furthermore, for the successful implementation of this technology, the information about the actual and forecasted availability of ground stations, taking into account all factors (clouds, turbulence, etc.), is required.

The use of optical links for the transmission of information from spacecraft has some fundamental advantages over the conventional radio technology. Namely, higher large data transfer rates and smaller apertures of

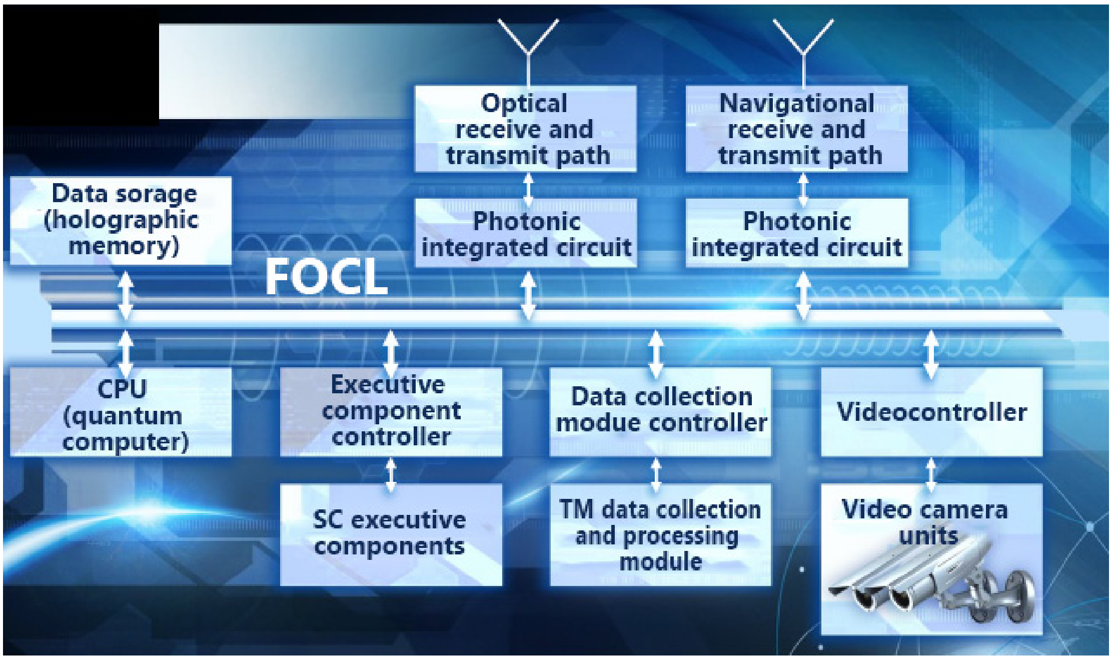

Figure 2. A generalized block diagram of the SC information system

the transceiver complexes. These factors increase the effectiveness of such solutions.

In the open space the problem of cloudiness is absent and, therefore, an alternative approach to the data transfer implies that the data from low-orbit satellites can be broadcast through the optical channel to a geostationary satellite, which will transmit the data to a ground station in the radio frequency range, which is not obstructed by the atmosphere.

Key research areas for the application of photonic technologies in the target and service equipment for space information systems

Now let us consider the basic technology of building the information infrastructure of space information systems.

The block diagram of the on-board segment of space information system is shown in Figure 2.

It is seen that the number of data connections in the space information system is large and includes both the data transfer within satellites and the SC-SC and SC-ground communication links. As the complexity of the equipment increases, the amount of information grows exponentially, and this fact becomes a bottleneck for space device engineering.

Photonic technologies, specialized for space applications, are used to create a wide range of payloads and service systems of the spacecraft:

- fiber optic gyroscopes;
- integrated micro- and nanooptics;
- photodetectors for visible and infrared ranges;
- acoustic and optical filters and dispersive elements;
- diffraction antenna arrays;
- small antennas based on metamaterials;
- high-frequency micromechanical and electro-optic modulators;
- organic energy converters;
- radiation-resistant ECB of the new generation;
- magneto-optical holography products;
- microelectronics element base with on-the-chip elements of photonics-based galvanic isolation.

Work [41] indicates that the optoelectronic components are increasingly used in Earth remote sensing missions due to their high integrability and the ability to provide better performance while reducing weight and dimensions of the target devices, as well as improve the quality of the images of the Earth's surface. However, the technology readiness level of innovative technologies is not always sufficient for use in the engineering development, which leads to unnecessary risks that must be considered at the earliest stages of development. The cited paper also attempts to identify these risks and propose the ways to reduce them.

It is noted, that during the development of the Pleiades space mission, a number of fundamentally new optoelectronic technologies were implemented, which provided a new level of the total system performance for the time. The characteristics are listed in Table 3. Highlighted in green are those that require the mandatory application of photonic technology to achieve specified requirements for the mission. At the same time, other technologies used optoelectronic components for the traditional functions of the spacecraft equipment.

It should be noted that despite the fact that Tables 2 and 3 were compiled at different times, their contents are somewhat correlated. This means that the development of advanced photonic technologies is carried out in a coordinated manner with the experience obtained in the course of the ongoing missions.

The main risks identified during the development of optoelectronic components have been associated with the innovativeness of the research, so the main recommendation for the developers was to advance the development of the critical components to ensure the overall success of a new mission as a whole.

Work [42] shows the results of the efforts of the French Space Agency (CNES) in development of photodetectors operating in different spectral ranges: ultraviolet (UV), visible (VLR), the near (c), middle (MIR) and the far infrared (FIR). Major progress in this direction is achieved by:

– the coordination of the R&D based on the requirements identified by the thematic road maps;
– the existing possibilities of achieving a record performance of the optoelectronic devices that use single-element-cooled infrared detectors, as well as the large-format CCD sensors;
– taking into account the cosmic radiation at ground tests by comparing the results of the flight and ground tests.

All these works are carried out in close cooperation with the developers of the Photonis, LETI/LIR, SOFRADIR, Cypress, e2v technologies, CMOSIS companies.

Work [43] lays out the need for opto-electronic components for space purposes. It is noted that these components have reached the required level of technological readiness in telecommunications and land infrastructure, clearly increasing the use of photonic technologies in the promising methods of telecommunications, which is associated with a number of advantages, including:

– virtually unlimited bandwidth of frequencies;
– lossless;
– low weight;
– small size of the printed circuit boards;
– mechanical flexibility for components such as optical fiber;
– immunity to electromagnetic interference;
– simple electrical isolation.

However, for space applications the readiness of the listed optoelectronic technologies is still very limited, primarily due to problems with the reliability associated with the harsh environments of the outer space. Article [43] analyzed the needs in different types of optoelectronic components used in a wide range of space applications, from signal generation to signal processing on board the spacecraft, signal reception, its processing and routing. It can be argued that the implementation of photonic technologies in space technology is still in its infancy, primarily because a considerable amount of work is required to achieve the readiness level comparable to the terrestrial applications, while ensuring an acceptable level of quality and reliability.

Today, ESA is already using photonic technology for different purposes in a number of space projects, for example, SMOS, GAIA, DARWIN, Herschel, Bepi-Colombo and others. It should be noted that the major space companies are reluctant to proceed with the development of photonic components for space applications mainly because the market for space products is very limited, as compared, for example, to telecommunications.

Another important, but so far not studied enough application of fiber optic technology, is the possibility of modulation of optical signal with the microwave radiation used in radar, communications, electronic warfare systems, as well as in device engineering [44]. This article details the broadband detectors and waveguides for the photonic generation of high-frequency signals, because they are the key components for ensuring the effectiveness of the implementation of fiber optic systems of the millimeter and submillimeter range. The article examines and discusses several technologies, systems, and applications in which the fiber optic technologies provide a competitive advantage against their electronic counterparts, which will significantly expand the field of applications for the microwave frequency range.

Currently, new opportunities are emerging in the field of information and measurement systems for aerospace hardware, including the ability to replace a significant number of sensors of the traditional sensor-transducer devices (STD) with fundamentally new sensors

Table 3. New technologies on board the Pleiades ERS satellites.

	Equipment	Technology	Enhancement
Surveying equipment	Panchromatic detector	Precise CCD receiver with reverse exposure and antich-arge loss structure	More efficient exposure and no image blurring due to the charge loss
	Highly integrated focal plane	Highly integrated FPGA technology	High density of integration
	Lens	Carbon/carbon structure	Low weight, high temperature stability
Image processing and telemetry	Very high speed digital communication	Commercially available 1 Gbit/s	Reduction of mass and energy consumption
	Data compressor	Wavelet transform algo-rithm at a rate of 2 bits/pixel	Minimizing the weight of on-board memory and the input data rate
	Telemetry modulator	Treyllis codes in X-range with the 8 PSK modulation	High-speed low-error data line
Guidance and stabili-zation system	Inertial navigation system	Fiber optic gyroscope	Low noise, high stability
	Gyroscopic torque control	Bearing technology	High connection with high torque, providing high dynamic stability
Power system	1500 W Solar battery	Gallium arsenide triple junction	High efficiency (26%) and a small area
	150 a/h battery	Lithium ion	High specific energy density

Source: data of [41].

based on photonic technologies for measuring electrical and non-electrical parameters with a previously unattained level of precision.

One of the critical components of such devices are analog-to-digital converters (ADCs) used in the development of advanced digital (software controlled) signal receivers and directly convert sensor signals to digital data for subsequent processing. However, the improvement of the ADC modules is progressing slowly due to the large number of problems associated with manufacturing very high resolution (with large number of signal quantization levels) and high conversion speed electronic circuits. The wide bandwidth and high resolution of the ADCs allow all kinds of measurement sensors to produce analog signals directly on the carrier frequencies of radio signals, eliminating the need for lowering the frequency of the analog signal. Currently, such solutions have already been found by means of photonic conversion technologies that implement record characteristics compared with the best electronic ADC. The capabilities of optical and optical-electrical devices make it possible to use 12-14 bit signal quantization at a rate of about 10 gigasamples per second (GS/s) in comparison with the best parameters of electronic ADC, providing only 3 bit conversion at a speed of 8 GS/s.

Work [45] analyzed almost 30 years of experience in the creation of photonic ADCs, simultaneously describing modern electronic ADC to illustrate the principles of their operation, their fundamental properties, as well as the analog optical communication lines used in many photonic ADCs. Thus, 4 classes of photonic ADCs are examined: 1) ADCs with elements of photonic technology, in which photonic devices added to a purely electronic ADC to improve the performance, 2) ADCs with photonic sampling and electronic quantization, 3) ADCs with an electronic sampling circuit and a photonic quantizer, and 4) ADCs with fully photonic sampling and quantization. In conclusion, the possibilities of the future photonic ADCs are discussed. Note that even at the beginning of the second decade of the 21st century, the maximum rate of electronic quantization achieved was 18 GHz, while the optical sampling circuits provided a rate of 100-200 GHz.

The results of the laboratory studies of the photonic ADC for space applications are presented in Work [46]. It is shown that in comparison with a traditional electronic ADC, the photonic ADC has a 200% advantage, especially in energy consumption and weight.

The simulation proved the proposed approach to be very promising, bearing in mind the fact that the sample tested in the laboratory has achieved a performance similar to traditional analog systems with significantly reduced complexity, size, weight and power consumption.

Work [47] covers the effective use of photonic technologies in a number of fiber optic sensors to measure various environmental parameters: temperature, pressure and humidity. These devices are based on different spatial arrangement of the sensor active region. Fluctuations of pressure, temperature, geometric deformations of the hull of a spacecraft affect the properties of the light beam propagating through the optical fiber, its phase, polarization, amplitude or range. The measurement accuracy of such devices, however, is unattainable for conventional DPAs.

In the built-in sensors, the optical signal modulator is used as a component of the optical fiber proper, one or more physical properties of which are subject to external influences and changing. External influences affect the optical fiber, which, in turn, changes some of the characteristics of the light beam within the optical fiber.

Recent advances in the development of the photonic sensor and transducer devices (PSTD) have attracted a stable interest of developers to their use for space applications both the on-board and ground-based.

Initially, the main advantage of the PSTD was their high-speed performance. With the improvement of the PSTD the following advantages are becoming increasingly relevant:

- passivity (the sensors do not require power supply);
- high sensitivity;
- small size and weight;
- high noise resistance;
- ability to operate in harsh environmental conditions (resistance to temperature, mechanical stress, etc.);
- multiplexing of electrical and optical signals.

Since the 2000s, special attention is paid to scientific research and designs based on various properties of magnetic fields and the effects associated with their impact on optical media [48]. Such measuring devices are already used in industrial process control systems, measuring and computing equipment, fault detection, etc. [49]. The Russian Federation has also seen an increasing interest in the development and research of such PSTDs. Developments carried out in Institute of Radio Technologies and Electronics of the Russian Academy of Science, National Research University of Electronic Technology, Moscow State University, Moscow Power Engineering Institute, Moscow State Technical University and others.

The application field for magnetic optical-electronic structures, relevant for the rocket and space industry, is development of the electric current sensors for non-contact measurement and current control in signal and power circuits of electronic equipment, power wires and cable of the devices, etc. These sensors would provide reliable electrical isolation of current carrying circuits of different voltages on the measuring circuits. They also will eliminate the need of discontinuities in the current-carrying circuits to include a measuring device (especially important for high-current lines and cables); they provide resistance to the effects of ionizing radiation of the outer space. The sensors do not require power supply and allow direct interfacing with fiber optic communication lines of the telemetry systems. Creating these current sensors can qualitatively improve the reliability and service life of products the industry backbone enterprises: FSUE “NPC AP”, JSC “Energia”, FSUE “Khurynichev State Research and Production Space Center”, JSC Progress, etc.

Another promising application of the photon technologies close to the practical implementation is creating microcavisies in the “whispering gallery” mode [50]. The range of applications extends from the creation of high-Q resonators for the optical and microwave range [51] to ensure the effective broad area radiation input into single-mode optical fiber [52].

Work [53] reported that a group of young specialists of the Russian Federal Agency of Technical Regulating and Metrology that manufactured and studied the prototype of ultra low-noise microwave oscillator based on the type of resonator disk leucosapphire a "whispering gallery", operating at a frequency of 6.8 GHz. The developed technology enables the production of these resonators in the frequency range of 6.0–10.0 GHz. The studied sample demonstrates a Q-factor as high as 450000 in the microwave frequency range at about -40°C. It is planned to continue studies at lower temperatures to increase the Q-factor of the resonator. It is expected that by 2025 it will be possible to start a mass production of such microcavities with a record Q-factor of about 1000000.

A very important application area of photonic technologies in the creation of space vehicles is the use of fiber optic gyros (FOG). Fundamentals and principles of operation of FOGs and sensors based on fiber optic technology are detailed in a number of papers, such as, [54, 55]. Moreover, according to US experts, in the near future FOGs will replace the widely employed mechanical gyros [56].

The latest research focuses on the development of miniature versions of FOGs for use in small-sized spacecraft, among other applications [57]. It is noted that FOGs have significant advantages compared to other technologies. Thus, in contrast to mechanical gyroscopes, FOGs contain no moving parts, therefore they are more compact, lighter and do not have a counter orientation in space. Compared to the ring laser gyros, FOGs do not require precise adjustments, are better suited for use on the spacecraft, do not require a vibration anti-lock mechanism. Finally, in contrast to the MEMS gyros, FOGs have a better resistance to impact and vibration, and show much better performance. So, the FOGs designed for onboard use (NG LN-200) have better stability (<<1°/hour) and much better noise resistance parameters (<<0.05°/hour). Key technological advantages of FOGs over laser gyros are given in [58], where their common and distinctive characteristics are discussed; some advantages of the FOG technology are presented.

Works [59, 60] provide an overview of the current state of development of fundamentally new materials, called metamaterials, artificial electromagnetic media, the structure of which is scaled in proportion to the wavelength of the radiation propagating in them. They were originally intended for the production of lenses with negative refractive indices. They then became the basis for development of the electromagnetic environment for the controlled wave propagation, which encouraged the revision of the laws of classical geometric optics.

Work [61] considers reflective coatings of silicon carbon. Their main task is to protect the spacecraft from the strong electromagnetic radiation of gas in the shock layer during the re-entry. The structures of silicone carbon and glass carbon that increase the reflected radiation are presented. The numerical simulation and optimization of photonic structures are conducted. Among the materials considered, the resonant structures of layer-by-layer, stacking volume, porous and waveguide type, which evaluated the role of the existing structural defects. It is expected that in future these materials may form the basis of the protective coatings applied in space technology.

Conclusion

The analysis of photonic technologies relevant for space applications demonstrated that photonic technologies can be prioritized both by the levels of technological readiness and demand as follows:

– on-chip photonics: the technologies correspond to the 3-5 TRL levels and have the highest priority for space applications with a relatively short implementation time (about 3 years);

– photonic FOCL and sapphire FOCL used in space device engineering and thermal control, and airgel array packaging of photonic elements used for the thermal protection of spacecraft;

– all technologies with the levels of technological readiness of 3-5 with 3-5 years of implementation;

– interferometers and spectroscopes in early development and requiring fairly long periods of implementation (5-10 years).

Of particular note is the high potential of large-format photosensitive multielement receivers, especially in IR and UV spectral ranges, as well as a variety of metamaterials. The development of such devices is very viable in the medium term (3-5 years).

It is necessary to constantly bear in mind the increased requirements on the reliability and radiation resistance of the components based on photonic technologies, as well as the obligatory flight qualification of such products, to provide a guarantee of their implementation in the target and service SC hardware.

Given the almost completely exhausted potential of the traditional technologies, to support sustainable development and a competitive level of the Russian space technology it is necessary to master modern methods and design tools and develop new technologies, currently not available in the Russian market.

To accomplish this task it is necessary to develop a comprehensive industry target program "Photonics for space", that should include a clear roadmap of creation and implementation of a specific product range of photonic devices, primarily for the space device engineering. After the development of this program is complete, it is advisable to conduct its in-depth discussion at the Scientific Technical Council of the Roscosmos, as a result of which it can be approved for realization by the space industry organizations.

Creating such a program will consolidate the efforts of the industry development, as well as various departments in order to create elemental component base for a new generation of space industry.

The main problem in accelerating the development of this direction in the Russian Federation is associated with a complete lack of inter-departmental coordination. Roadmap of photonics has been in development for several years, but has never formed into a program of mass production. Various agencies are trying to solve problems independently, even realizing that their own efforts are not enough to fully implement the technology.

A coordinated program of development and manufacturing of photonic products should be drafted as the main recommendatory document for the development of photonic technologies for space applications. It should be tightly focused on the creation of the products with a guaranteed demand in various sectors of the Russian economy. Of course, the baseline work must be carried out with the participation of the universities and institutes of the Ministry of Education, as well as development institutions (Skolkovo, Rosnano, etc.). At the same time, the Ministry of Industry of the Russian Federation, Roscosmos and Rosatom will act as customers of those works.

Given the limited funding opportunities offered by the work in the conditions of economic crisis, possible solution could be the adoption of a set of ADC agencies, allowing them to focus limited resources on the breakthrough development projects.

Finally, it is extremely important to organize the international cooperation, i.e. with the BRICS countries.

References:

1. Space Flight Requirements for Fiber Optic Components; Qualification Testing and Lessons Learned. Photonics Group, April 2006, SPIE Europe, Vol. 6193SPIE.

2. *Optics and Photonics: Essential Technologies for Our Nation.* The National Academic Press, Washington D.C., 2013, 341 p.

3. *Draft Horizon 2020 Work Programme 2016-2017 in the area of Leadership in Enabling and Industrial Technologies – Space*. Available at: http://ec.europa.eu/research/participants/data/ref/h2020/grants_manual/hi/oa_pilot/h2020-hi-oa-data-mgt_en.pdf.

4. Available at: http://www.csir.co.za/dpss/conference/docs/Space_photonics.PDF.

5. *Microphotonics for Space Application*. Full report. Available at: http://seminarprojects.org/t-microphotonics-for-space-application-full-report.

6. Antikidis Jean-Pierre. A new business paradigm for Earth Observation with the e-CORCE programme. *3rd Symposium on Earth Observation Business.* September 15–16, 2011, Paris. Available at: 5SEOBPanel8BluePlanet_0.pdf.

7. Romanov A.A., Romanov A.A., Urlichich Yu.M., Buravin A.E. Kontseptual'nye podkhody k sozdaniyu perspektivnykh kosmicheskikh sistem [Conceptual approaches to development of advanced space systems]. *Mekhanika, upravlenie i informatika* [Mechanics, control and informatics]. 2011, No. 5, pp. 92–104. (in Russian)

8. Leeb W.R., Kalmar A., Kudielka K.H., Winzer P.J. Optical terminals for microsatellite swarms. *Proc. SPIE 4635.* 2002, pp. 202–214.

9. Nishinaga N., Takayama Y., Takahashi T., Ogawa Y., Kubooka T., Umehara H. Study for HDR cross-link for formation flight satellite systems. *Proc. SPIE 4975.* 2003, pp. 45–56.

10. Wilson K., Enoch M. Optical Communications for Deep Space Mission. *IEEE Commun. Magazine*. 2000, No 38, pp. 134–139.

11. Korolev B.V. Tekhnologiya raboty kosmicheskoy opticheskoy linii svyazi dlya povysheniya operativnosti upravleniya i polucheniya informatsii potrebitelem v protsesse funktsionirovaniya kosmicheskikh sredstv [Technology for space optical links to improve the efficiency of management and information receive for consumer in the operation of space vehicles]. *Kosmicheskaya tekhnika i tekhnologii* [Space engineering and technology]. 2014, Vol. 1, No. 4, pp. 39–47. (in Russian)

12. Krasovskiy P.A. Metrologiya kosmicheskikh navigatsionnykh sputnikovykh sistem [Metrology of space navigation satellite systems]. Monograph. Mendeleyevo: FGUP "VNIIFTRI", 2009, Ill. 44, Tab. 7, Bibl. 22, 216 p. (in Russian)

13. National Research Council, 2013, Optics and Photonics: Essential Technologies for Our Nation.

14. Min G., Xiangping L., Yaoyu C. Optical storage arrays: a perspective for future big data Storage. *Light: Science & Applications*. 2014, 3, e177; DOI: 10.1038/lsa.2014.58.

15. Gantz J., Reinsel D. *The Digital Universe in 2020: Big Data, Bigger Digital Shadows, and Biggest Growth in the Far East*. Framingham. MA: IDC, 2012. Available at: http://www.emc.com/ leadership/digital-universe/index.htm.

16. Antikidis Jean-Pierre. Serving the whole planet with metric resolution data: The e-CORCE program status. WGISS 27, Toulouse, May 12, 2009.

17. Bernstein N.P., Rrost G.A., Hayduk M.J., Hunter J.R., Nichter J.E., Payson P.M., Repak P.L. Why photonic systems for space? *Radio Frequency Photonic Devices and Systems*. Eds. Pinch A.R., Goutzoulis A.P., Repak P.L. *Proceedings of SPIE*, 2000, Vol. 4112.

18. Nanotechnology Research Directions. *IWGN Workshop Report, Vision for Nanotechnology R&D in the Next Decade*. September 1999.

19. *Technological Breakthroughs for Scientific Progress (TECHBREAK)*. Brussels, ESF Forward Look, 2014.

20. *Technology Readiness Assessment (TRA) Guidance.* DoD, April 2011. Available at: http://www.acq.osd.mil/chieftechnologist/publications/docs/TRA2011.pdf.

21. *National Positioning, Navigation, and Timing Architecture Study.* Final Report, National Security Space Office. September 2008.

22. Ray P.S., Wood K.S., Phlips B.F. Spacecraft Navigation Using X-ray Pulsars. Featured research, 2006, *NRL REVIEW*, pp. 95–102.

23. Aref'ev V.A., Pavlinskiy M.N., Fedotov S.N., Lutovinov A.A., Semena N.P., Levin V.V. Rentgenovskie pul'sary – mayaki avtonomnoy sistemy navigatsii kosmicheskikh apparatov [X-ray pulsars – the lighthouses of the autonomous navigation system of spacecraft]. *Mekhanika, upravlenie i informatika. Sbornik trudov vserossiyskoy nauchno-tekhnicheskoy konferentsii "Sovremennye problemy opredeleniya orientatsii i navigatsii kosmicheskikh apparatov"* [Mechanics, control and informatics. Proceedings of All-Russian scientific and technical conference "Modern problems of attitude and navigation of spacecraft"]. Izd. IKI RAN, 2009, pp. 210–218. (in Russian)

24. Rad A.M., Azar L.V. Determining Attitude and Position in Deep Space Missions Using X-Ray Pulsars. *International Journal of Astronomy and Astrophysics*. 2014, No. 4, pp. 628-648. Available at: http://www.scirp.org/journal/ijaa, http://dx.doi.org/10.4236/ijaa.2014.44058.

25. Overview of Results from GNSS Research under the FP7 R&D Programme (2007-2013). *Research Applications to Market, European GNSS Agency (GSA)*. 2015. Available at: http://www.gsa.europa.eu/rd-for-galileo-egnos-app.

26. Gurov M.G., Gurova E.G. *Opticheskie chasy na ionakh i neytral'nykh atomakh* [Optical clocks on ions and neutral atoms]. [Electronic resource]. Gurov M.G., Gurova E.G. *Contenant*: *scientific and technical journal*, 2014, Vol. 1, No. 4. Available at: http://www.contenant.ru/1electron_mag/magazine/. (in Russian)

27. Bloom B.J. *Building a Better Atomic Clock.* A thesis submitted to the University of Colorado in partial fulfillment of the requirements for the degree of Doctor of Philosophy Department of Physics, 2014. Available at: https://jila.colorado.edu/sites/default/files/assets/files/publications/BenBloom_Thesis447.pdf.

28. Poli N., Schioppo M., Vogt S., Falke St., Sterr U., Lisdat Ch., Tino G.M. A transportable strontium optical lattice clock. *Appl. Phys.* DOI: 10.1007/s00340-014-5932-9. Springer-Verlag Berlin Heidelberg, 2014. Available at: http://coldatoms.lens.unifi.it/tino/images/personal/articles/tino/2014-a-transportable.pdf.

29. Kitching J., Knappe S., Liew L., Moreland J., Robinson H.G., Schwindt P., Shah V., Gerginov V., Hollberg L. Chip-Scale Atomic Clocks at NIST. *NCSL International Workshop and Symposium.* 2005. Available at: http://tf.boulder.nist.gov/general/pdf/2067.pdf.

30. Pivtsov V.S., Nyushkov B.N. Razrabotka mobil'nykh pretsizionnykh femtosekundnykh opticheskikh chasov dlya metrologii i sputnikovykh navigatsionnykh system [Development of the mobile precision femtosecond optical clocks for metrology and satellite navigation systems]. Otchetnaya sessiya po programme Prezidiuma RAN 16 dekabrya 2013 [A report session on the program of RAS Presidium dated December 16, 2013]. FIAN im. P.N. Lebedeva. (in Russian)

31. Perlot N., Dreischer T., Weinert C., Perdigues J. Optical GEO Feeder Link Design. *Future Network & Mobile Summit*. 2012, Berlin. (in Russian)

32. Hilbert S., Krutz D. *BTDI CCD21122 Optical Performance Test Report*. DLR-OS. 2014.

33. Lindgren N. Optical Communications - A Decade of Preparations. *Proceedings of the IEEE.* 1970, Vol. 58, No. 10, pp. 1410–1418.

34. Sbardellati A., Sassorossi T., Marinelli M., Guibilei R. The communication payload of the ARTEMIS European satellite. *Proceedings of AIAA Conf. AIAA-94-0905-CP.* 1994, pp. 22–32.

35. Lunde C., Fields R., Wong R., Wicker J., Kozlowski D., Skoog J., Muehlnikel G., Hartmann J., Sterr U., Lutzer M. Joint United States-Germany Satellite Laser Communications Project: NFIRE-to-TerraSAR-X ISLs and NFIRE-to-Ground SGLs. *International Workshop on Ground-to-OICETS Laser Communications Experiments*. 2010, May 13–15, 2010, Tenerife, Spain. Paper: GOLCE2010-08.

36. DIN; VDE; DKE (Hrsg.). Optische Strahlungssicherheit und Laser 2. 2010. DIN-VDE-Taschenbücher Band 526, 2, Auflage.

37. Wilson K., Enoch M. Optical Communications for Deep Space Mission. *IEEE Commun. Magazine*. 2000, No. 38, pp. 134–139.

38. Dat P.T., Bekkali A., Kazaura K., Wakamori K., Matsumoto M.A. Universal Platform for Ubiquitous Wireless Communications Using Radio Over FSO System. *J. Lightwave Technol.* 2010, No. 28, pp. 2258–2267.

39. Kudielka K., Pribil K. Transparent optical intersatellite link using double-sideband modulation and homodyne reception. *Int. J. Electron. Commun*. 2002, Vol. 56, 254 p.

40. Lim W., Yun C., Kim K. BER performance analysis of radio over free-space optical systems considering laser phase noise under Gamma-Gamma turbulence channels. *Optics Express*, 2009, No. 17, pp. 4479–4484.

41. Perret L. Optoelectronic demands on Earth Observation Satellites: Example of the Pleiades Mission. *ISROS*, May 14–16, 2009.

42. Materne A., Bardoux A., Penquer A., Bernard F. Main trends for the development of detectors for space applications at CNES. *ISROS*, May 14–16, 2009.

43. Zahir M. Space needs on optoelectronics. *ISROS*, May 14–16, 2009.

44. Vidal B., Nagatsuma T., Gomes N.J., Darcie T.E. Photonic Technologies for Millimeter- and Submillimeter-Wave Signals. *Advances in Optical Technologies*. Vol. 2012, Article ID 925065, 18 p. DOI: 10.1155/2012/925065.

45. Valley G.C. Photonic analog-to-digital converters. *Optics Express*, March 2007, Vol. 15, No. 5, 1955 p.

46. Pantoja S., Piqueras M.A., Villalba P., Martínez B., Rico E. High performance photonic ADC for space applications. *ICSO 2010 International Conference on Space Optics.* Rhodes, Greece, October 4–8, 2010.

47. Parikh Meera J. and Gharge Anuradha P. A Survey Paper of Optical Fiber Sensor. *International Journal on Recent and Innovation Trends in Computing and Communication*. ISSN: 2321-8169, Jan. 2014, Vol. 2, Iss.1, pp. 33–39. Available at: http://www.ijritcc.org/download/A%20Survey%20Paper%20of%20Optical%20Fiber%20Sensor.pdf.

48. Ioppolo T., Ötügen M.V. Magnetorheological polydimethylsiloxane micro-optical resonator. June 15, 2010, Vol. 35, No. 12. *Optics letters*. 2037 p. Lubkowski G., Suhrke M. Metamaterials for Optical and Photonic Applications in Space. *Final Report ESA AO/1-6187/09/NL/AF.* Euskirchen, March 2011.

49. Wolinski T.R., Lesiak P., Domanski A.W., Polarimetric optical fiber sensors of a new generation for industrial applications. *Bulletin of the polish academy of sciences technical sciences.* 2008, Vol. 56, No. 2, 125 p.

50. Vinogradov A.V., Oraevskiy A.N., Volny shepchushchey galerei [Whispering gallery waves]. *Sorosovskiy educational journal*. Vol. 7, No. 2, 2001.

51. Foreman M.R., Swaim J.D., Vollmer F. Whispering gallery mode sensors. *Advances in Optics and Photonics.* 2015, No. 7, pp. 168–240. DOI: 10.1364/AOP.7.000168 168. (in Russian)

52. Gorodetskiy M.L., Rodin A.V., Benderov O.V., *Shirokoaperturnyy vvod izlucheniya v odnomodovoe opticheskoe volokno pri pomoshchi asfericheskikh rezonatorov na mode shepchushchey galerei* [A wide-aperture radiation input into the single-mode optical fiber using spherical resonators based on the whispering gallery mode]. Presentation, Apatity, 2013. (in Russian)

53. *Molodye uchenye iz "VNIIFTRI" predstavili razrabotku na osnove rezonatora tipa "shepchushchaya galereya"* [Young scientists from "VNIIFTRI" presented the development based on the whispering gallery mode resonator]. Available at: http://www.ria-stk.ru/news/detail.php?ID=97769&SECTION_ID=. (in Russian)

54. Merlo S., Norgia M., Donati S. *Fiber gyroscope principles. Handbook of Fibre Optic Sensing Technology.* Ed. José Miguel López-Higuera. John Wiley & Sons Ltd., 2000.

55. Lecler S., Meyrueis P. Intrinsic Optical Fiber Sensor. *Fiber Optic Sensors.* Ed. Yasin M., Harun S.W., Arof H. InTech. 530 p. Chapters published February 22, 2012 under CC BY 3.0 license. DOI: 10.5772/1379.

56. *ASTRIX200 – A Very High Performance FOG Inertial Measurement Unit for Accuracy demanding Satellites*. EADS-ASTRIUM & IXSEA, 2002.

57. Costa J. *Miniaturizable High Performance Fiber Optic Gyroscopes for Small Satellites.* Presentation to NASA Early Stage Technology Workshop. March 2015.

58. Napolitano F. *Fiber-optic gyroscopes key technological advantages*. 2010. Available at: http://www.industrycortex.com/datasheets/profile/1254703121/fiber-optic-gyroscopes-f.-napolitano-102010-fiber-optic-gyro.

59. Lubkowski G., Suhrke M. Metamaterials for Optical and Photonic Applications in Space. *Final Report ESA AO/1-6187/09/NL/AF*, Euskirchen, March 2011.

60. Zheludev N.I., Kivshar Yu.S. From metamaterials to metadevices. *Nature Materials*. Vol. 11, November 2012, pp. 917–924. Available at: www.nature.com/naturematerials.

61. Komarevskiy N., Shklover V., Braginskiy L., Hafner C., Lawson J. Optimal design of reflecting photonic structures for space applications. *Journal of Electromagnetic Analysis and Applications*. 2012, ISSN Print: 1942-0730. Available at: http://scee2012.ethz.ch/abstracts_new/SCEE12_Abstract_22_talk_Komarevskiy.pdf.

ROCKET-SPACE DEVICE ENGINEERING AND INFORMATION SYSTEMS
Vol. 3, Iss. 2, 2016, pp. 20–25

Estimation of NDVI Calculation Error When Using Empirical Methods for Atmospheric Correction

K.I. Zubkova, T.G. Kurevleva, L.I. Permitina[1]

[1]*candidate of engineering science*
Joint Stock Company "Russian Space Systems", Russia

e-mail: zubkova.k@ntsomz.ru

Abstract. The paper presents the results of the analysis of different empirical atmospheric correction method applicability to the Resurs-P spacecraft hyperspectral data for the NDVI calculation. The methods such as FF (Flat Field), DOS (Dark Object Subtraction), DOS-1% (Improved Dark Object Subtraction) and COST (Cosine Approximation Model with atmospheric transmittance taken into account), as well as the atmospherically corrected value calculation using the Lambert's formula, are considered and used. The paper analyses the merits and drawbacks of each method. It is concluded that the empirical methods taking into account the atmospheric effects improve the NDVI calculation accuracy. The atmospheric correction effect of DOS1-% and COST is the best; the mean deviation values do not exceed 5%. The results obtained in this study may be applied for solving the problems requiring the knowledge of underlying surface spectral radiance factors.

Keywords: Earth remote sensing, atmospheric correction, hyperspectrometer, spectral radiance, NDVI

Introduction

To solve the tasks of the Earth remote sensing (ERS), it is necessary to know the spectral brightness factors (SBF) of the underlying surface calculated according to radiometrically calibrated data allowing for the atmospheric influence. Accurate atmospheric correction of the ERS data in majority of cases is impossible due to the lack of a complete set of the necessary atmospheric parameters. Thus, many methods for empirical atmospheric correction have been developed.

The paper gives the analysis results for applicability of the following methods: DOS (Dark Object Subtraction), COST (Cosine of the Solar Zenith Angle, COS (TZ)), Flat Field, and so on [1, 2, 3] for hyperspectral data received from the Russian spacecraft (SC) Resurs-P No.No. 1, 2.

Methods of empirical atmospheric correction

1. ***Flat Field***. A method implies a reference object, for which SBF is known a priory. A reference spectrum for correction is determined as averaged values of spectral density of energy brightness (SDEB) on the uniform surface area of the reference object. SBF in each pixel with the coordinates (i, j) is determined in the form of (1):

$$\varrho_{i,j} = \frac{L_{i,j}}{L_{i,j}^{prot}} \times \varrho_{i,j}^{ref} \tag{1}$$

where is the SDEB on the upper boarder of the atmosphere (UBA), is the average spectrum of SDEB on UBA of the reference object, is the SBF on UBA of the reference object.

A prototype area should have the following characteristics:

1. A surface area should be flat (near to the Lambert one) for the correct averaging of the SDEB values.

2. A surface area should be bright (for example, a light-colored sand) to increase a signal-to-noise ratio.

2. ***Lambertian Reflectance*** (calculation by the Lambert formula). In this method, calculation of SBF is carried out by the formula for the Lambertian surface (2):

$$\varrho_k = \frac{\pi L_k}{S_k \cos \Theta_S} \tag{2}$$

where is the SDEB on SBF, is the SBF on UBA,is the solar constant (solar irradiation on UBA within the limits of the function of the channel spectral sensitivity κ), and is the zenith angle of the Sun.

The method is applied at the complete absence of knowledge on the atmosphere under the area of interest [4].

3. ***DOS*** (subtraction of "the dark background"). The method is for recording the atmospheric haze. A value of a dark object on the underlying surface is taken as the value of SDEB of the haze. The haze value is subtracted from SDEB to UBA, and than calculation of SBF onto UBA by the formula (3):

$$\varrho_k = \frac{\pi(L_k - L_{dark})}{S_k \cos \Theta_S} \tag{3}$$

where is the SDEB onto UBA, is the UBA onto SBF,is the solar constant for the channel *k*, is the zenith angle of the Sun, and is the SDEB of the dark object.

4. ***Modified DOS***. The DOS method [4, 5] suggests that there are no reflections from the object, but the energy got by the pupil of the target equipment is due to the presence of the atmospheric haze. However, in later works dedicated to the atmospheric correction, the SBF of the dark object is not considered equal to zero, and the value of the atmospheric haze is calculated as the difference between SDEB of the dark object and SDEB corresponding to 1–2% from SDEB of the dark object. After subtraction of the haze influence, the calculation of SBF onto UBA is carried out by the formula (4) [4]:

$$\varrho_k = \frac{\pi(L_k - L_{1\%})}{S_k \cos \Theta_S} \tag{4}$$

$$\text{where } L_{1\%} = \frac{0.01 * S_k \cos \Theta_S}{\pi} \tag{5}$$

where is the SDEB onto UBA, is the UBA onto SBF, is the solar constant, is the zenith angle of the Sun, and is the SDEB of the dark object.

5. ***COST***. In this method, an atmospheric haze is calculated the same way as in the "Modified DOS" method. However, apart from considering the atmospheric haze, the method suggests an empirical record of the atmosphere transparency [4]. The transparency factor of the atmosphere is calculated as the cosines of the zenith angle of the Sun and the cosines of the zenith surveillance angle from the spacecraft. Primary, the method was used only for the data of the survey in the nadir [4], that is why only the cosines of the zenith angle of the Sun (a cosines of the viewing angle equals to 1) was taken into account.

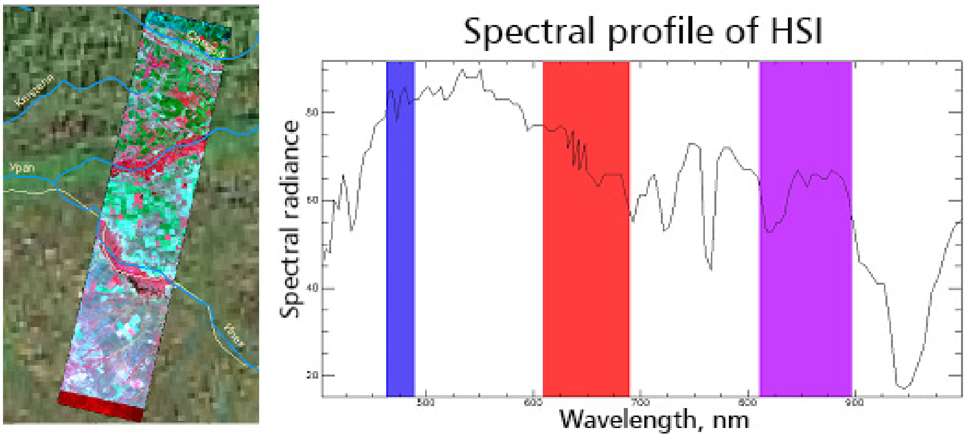

Fig. 1. The survey data the HSE (hyperspectral equipment)/Resurs-P No. 1. A synthesis of the channels 106 (859 nm), 60 (636 nm), 40 (550 nm) (on the left) and the spectrum of the central point of the hyperspectral survey (on the right).

Nowadays calculation of SBF is made by the formula (6):

$$\varrho_k = \frac{\pi(L_k - L_{1\%})}{S_k \cos^2 \Theta_s \cos\Theta_{viz}} \qquad (6)$$

where is the SDEB onto UBA, is the SBF onto UBA,is the solar constant for the channel *k* under analysis, is the zenith angle of the Sun, is the SDEB of the dark object, and is the cosines of the viewing angle.

Description of the input data for research

The research has been carried out based on the data of the hyperspectral survey of the spacecraft Resurs-P No. 1 dated May 16, 2014, 10:27 Decreed Moscow Time (07:27 UTC) of the territory of the Orenburg region and the data of the survey MODIS of the Terra spacecraft dated May 18, 2014, 07:45 UTC (Fig. 1).

The survey data are visualized in pseudocolors, vegetation is shown in red, and soil is in blue that is due to the combination of the chosen channels: near infrared, red, and blue.

Crosscalibration of the data

Since there are problems with radiometric calibration of hyperspectral data [6], it was not possible to study the methods of atmosphere correction based on narrow band indices.

Estimation of NDVI calculation error was made based on the wide band NDVI through the operation with wide spectral ranges formed by means of averaging the hyperspectral ranges into three spectral ranges corresponding to the functions of spectral sensitivity of the channels 3, 2, 1 of the MODIS equipment (Fig. 1).

To obtain a correct value of SDEB onto UBA, radiometric crosscalibration of the HSE data according to the MODIS data (in the form of the MOD02 product – the data on SDEB of the underlying surface) was carried out. After spatial data combination, building of 100 test facilities on the similar surface area was performed. Moreover, average values of SDEB of HSA and MODIS for each of the test sites was made. Crosscalibration was made by the formula (7):

$$L_R = L_M \ \frac{S_R}{S_M} \ \frac{\cos\Theta_{sR}}{\cos\Theta_{sM}} \qquad (7)$$

where , are the SDEB of MODIS and HAS respectively, is the ratio of solar constants (Exoatmospheric Solar Irradiance) for a pair of the channels taking into account the width and form of the functions of spectral sensitivity of the channels of HSE and MODIS, and is the ratio of the cosines of the zenith angle of the Sun during the survey allowing for survey asynchrony.

Fig. 2 shows the crosscalibration results: the *x* axis carries the values of SDEB of HSE, the *y* axis has the values of SDEB of MODIS lead to the survey conditions of HSE. Based on the crosscalibration results, correction of the SDEB values in the averaged blue, red, and near infrared channels of HSE was carried out. A calibration function corresponding to the SDEB scaling for each of the three channels is given in the upper part of each graph. Further, only the calibrated HSE data were used.

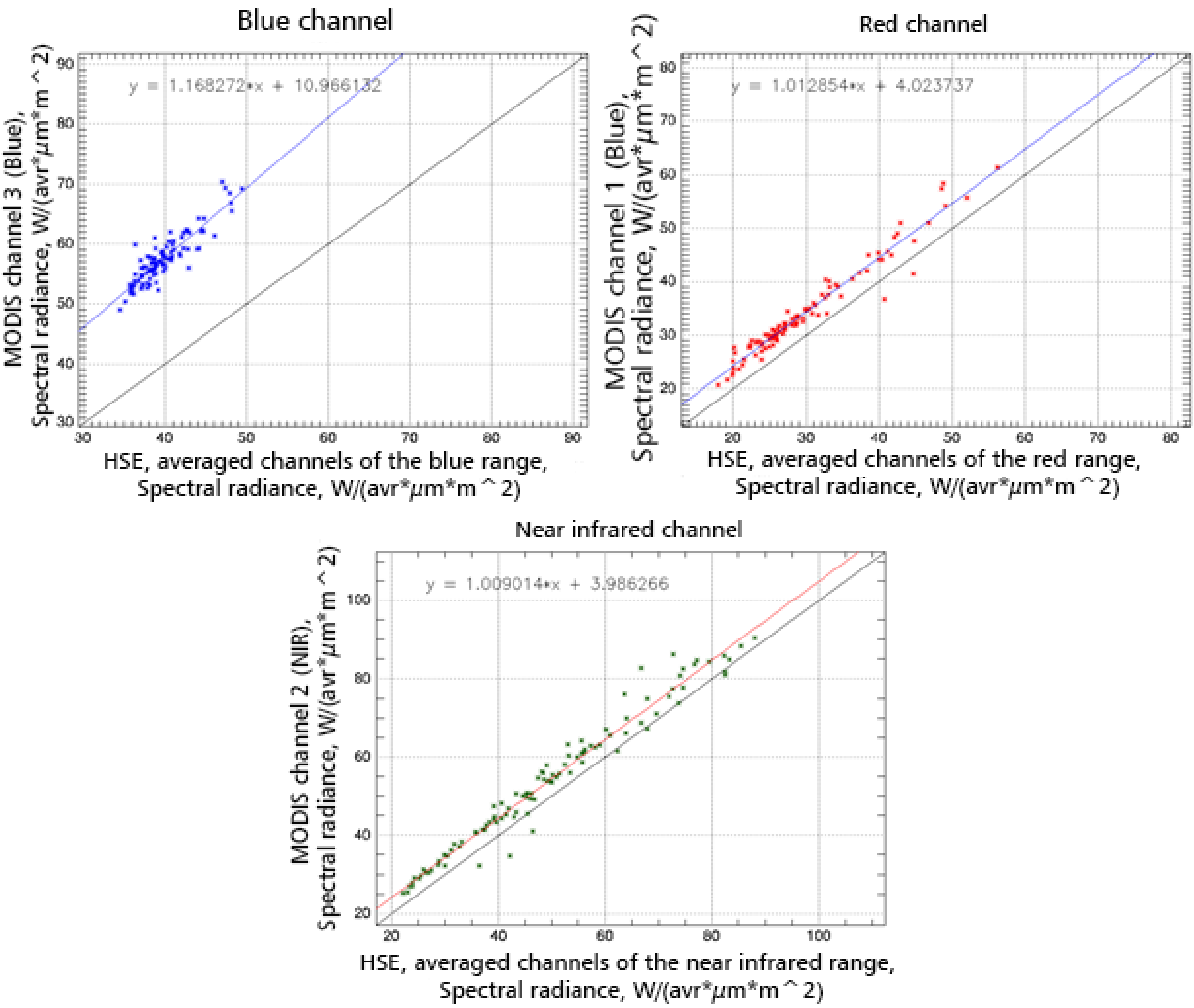

Fig. 2. Comparison of the SDEB values of the averaged HSE channels/Resurs-P No. **1** (x axis) and SDEB MODIS of the Terra spacecraft (y axis) lead to the conditions of the HSE survey.

Atmospheric data correction

Atmospheric correction of the averaged HSE channels is carried out after crosscalibration through a software package 6S taking into account the following parameters:

1. A model of the atmosphere is a user one requiring an input of the value of a total content of vapor (2.20 g/cm^2) and a total content of ozone (356 DU). The data are obtained from the product MOD09 of MODIS.

2. A model of the atmospheric aerosol is continental; a content of aerosol on the wavelength of 550 nm (according to the 6S requirement) is obtained according to the data of the nearest AERONET station in Yekaterinburg (AOT = 0.13, AOT (Aerosol Optical Depth of the atmosphere).

3. An average altitude of the underlying surface above the sea level is 120 m.

NDVI calculation

After atmospheric correction, NDVI calculation was performed. Its values became a standard when evaluating the NDVI calculation error by empirical methods.

Fig. 3 gives the comparison result of the NDVI values calculated by empirical methods, with the standard – the NDVI values calculated after crosscalibration and atmospheric correction of the HSE data. As during crosscalibration, comparison of NDVI in the form of scattergrams is made for the average NDVI values on each of 100 test facilities. The graph carries the NDVI values calculated by the formula (2).

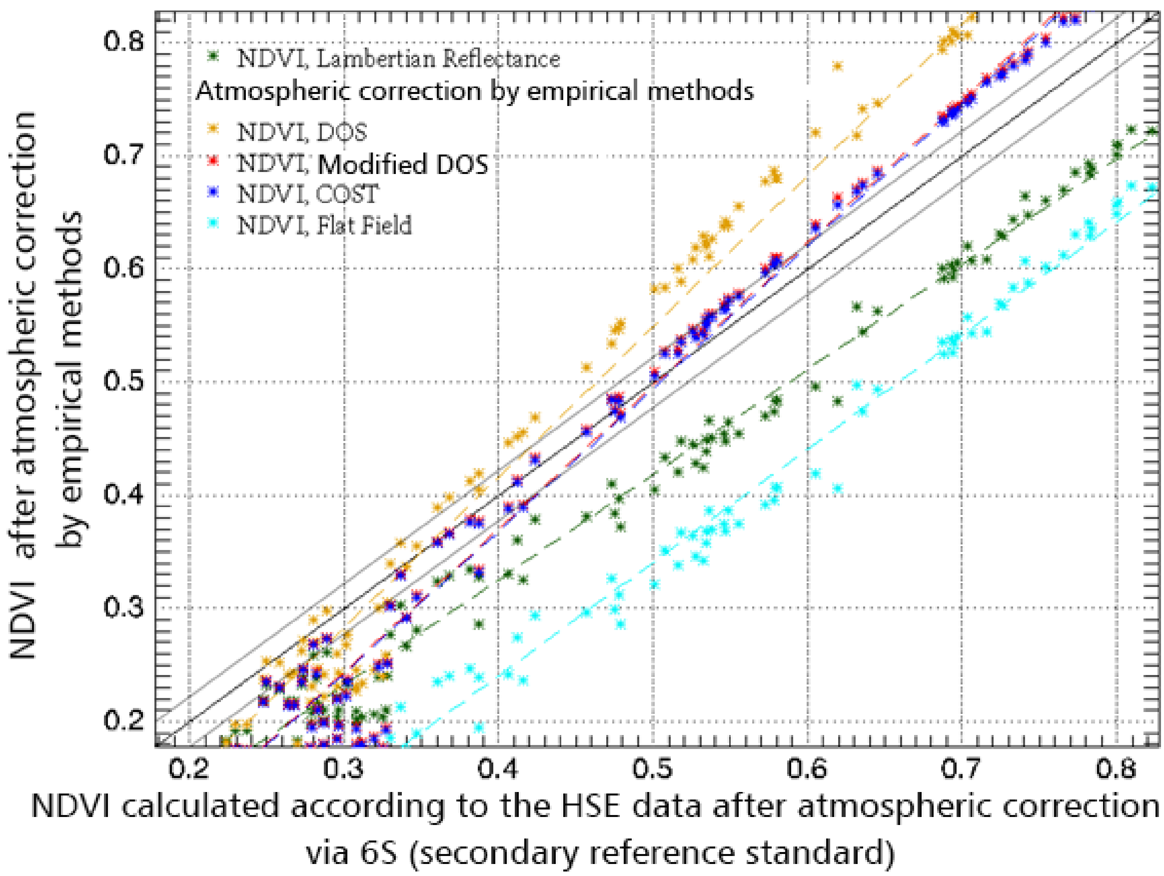

Fig. 3. Comparison of the NDVI calculated after the atmospheric correction by empirical methods with a reference object.

Ideally, the scatterogram of the NDVI values should lie squarely at angle 45° (along the black line). The results of the analysis have shown that a modified DOS method gives the minimum deviation from the reference object. In particular, an average deviation from the prototype does not exceed 2% in the range of the NDVI values from 0.3 to 0.6. In the method "Modified DOS", the value of the atmospheric haze is less than in the DOS method. Hence, overcorrection of the SBF values has a not so explicit effect; it is noticeable only for the small (up to 0.3) NDVI values.

In the COST method, an atmospheric fog is calculated the same way as in the method "Modified DOS". The transparency of the atmosphere is calculated as cosines of the zenith angle and does not depend on the wavelength. Therefore, the COST method does not give additional information into the NDVI method in comparison with the "Modified DOS" method: a constant value of the transparency of the atmosphere decreases.

Great deviations from the reference values (not less than 20%) make it possible to calculate NDVI according to the Lambertian Reflectance method. However, the DOS method also results in a great relative deviation. This happens because in the nearest IR channel, the DOS method leads to overcorrection of the SBF values: an atmospheric haze is significantly less than that of in the red channel and in the SDEB value being deducted; along with an atmospheric haze, it has a part of the "useful" solar energy reflected from the surface.

Using the Flat Field method resulted in deviation from the NDVI reference object more than 30%. First of all, is can be due to the incorrect choice of the reference spectrum Q_{ref} from the soils.sli library prepared by the Johns Hopkins University (Brown loamy fine sand, Hapulstalf 87P3468): a test site with a dry soil the spectrum of which was further compared with the spectrum of the dry soil after atmospheric correction of the HSE data was chosen for the analysis. Under such conditions, an average deviation does not depend on the NDVI value compared to the "Modified DOS" method.

Table below gives the values of the average deviation from the reference object for each of the methods of the empirical atmosphere correction.

Table. The values of the average deviation from the reference object for each of the methods of the empirical atmosphere correction

A method's name	A value of the average deviation
Lambertian reflectance	> 20%
DOS	10–15%
Modified DOS	In the range from 0.3 to 0.6 – 3%, in other intervals – 5%
COST	In the range from 0.3 to 0.6 – 3%, in other intervals – 5%
Flat Field	> 30%

Conclusion

In the course of work, the areas where the empirical methods of the atmosphere influence during the processing of the hyperspectral ERS data based on the evaluation of the NDVI error were determined.

The results obtained can conclude the following:

1. Using the empirical methods of the atmosphere correction results in decrease in evaluating of the NDVI error in comparison to the calculation without the atmosphere correction. The results with the least deviation are obtained employing the "Modified DOS" method, where the calculation of the atmospheric haze is performed using a "dark" object with the deduction of SDEB corresponding to SBF of the object 0.01. In the range of the NDVI values from 0.3 to 0.6, the deviation of the NDVI calculation is in the range of 0.02 that corresponds to the nominal value of the error for the MOD13Q MODIS product containing the composites of the NDVI values during 10 days.

2. The COST method gives the same results as the "Modified DOS" method because reducing a constant influence of the atmosphere.

3. The largest average deviation from the reference object calculated by means of 6S demonstrated the Flat Field method. The disadvantages of the Flat Field method is that an operator has to choose the above-mentioned object. Moreover, the method is not useful for the area of the underlying surface containing only vegetation. However, it can be employed for the analysis of the territories of urban settlements, roads, and concrete structures. "Employed" in this context means "using this method leads the hyperspectral data to the most convenient view and greatly increases the calculation accuracy of the NDVI" [4]. During comparison of the spectra with true values of the measurements on the area, the errors of the atmospheric correction can be too large (more than 30%).

4. Additional correction of the SBF occurred when using the DOS method because of the deduction of the "useful" information during processing along with the atmospheric influence. In the region of the high NDVI values (more than 0.4), an average deviation from the reference object was about 20%.

The best results were achieved using the "Modified DOS" and COST methods. Their application is limited by the fact that "dark" objects (water areas, heavy vegetation or strongly shaded regions) should be present on the underlying surface of the "dark" objects.

References

1.Liang S., Fang H., Chen M. Atmospheric correction of Landsat ETM+ land surface imagery: I. Methods. *Geoscience and Remote Sensing, IEEE Transactions on Geoscience and Remote Sensing*. Vol. 39, No. 11, 2001, pp. 2490-2498.

2.J. Ju, et al. Continental-scale validation of MODIS-based and LEDAPS Landsat ETM+ atmospheric correction methods. *Remote Sensing of Environment*. Vol. 122, 2012, pp. 175-184.

3.Lu D., et al. Assessment of atmospheric correction methods for Landsat TM data applicable to Amazon basin LBA research. *International Journal of Remote Sensing*. Vol. 23, No. 13, 2002, pp. 2651-2671.

4.Pat S. Chavez. Image-based atmospheric corrections revisited and improved. *Photogrammetric Engineering & Remote Sensing*. September 1996, Vol. 62, No. 9, pp. 1025-1036.

5.Wooley J.T. Reflectance and transmittance of light by leaves. *Plant Physiol*. 1971, Vol. 47, pp. 656-662.

6.Grishantseva L.A., Emel'yanov K.S., Kurevleva T.G., Markov V.S. Problemy radiometricheskoy kalibrovki KA GSA "Resurs-P" No.No. 1, 2 [Problems of the radiometric calibtration of the hyperspectral equipment of the "Resurs-P" No.No. 1, 2 spacecraft]. *Aktual'nye problemy raketno-kosmicheskoy otrasli* [Current problems of rocket and space industry]. 2015, Vol. No. 1. 280 p. (in Russian)

ROCKET-SPACE DEVICE ENGINEERING AND INFORMATION SYSTEMS
Vol. 3, Iss. 2, 2016, pp. 26–32

Algorithm of restoration for short exposure of the ERS image spatially-non invariant to atmospheric distortions

K. N. Sviridov

doctor of engineering science, professor,
Joint Stock Company "Russian Space Systems", Russia

e-mail: sviridovkn@yandex.ru

Abstract. Negative influence of the atmospheric turbulence on the ERS systems is noted. Hardware and software technologies for partial correction of atmospheric influence are reviewed. New algorithm for recovering of an image not distorted by atmosphere, which has a diffraction-limited resolution of the ERS telescope in its broad field of view is proposed and substantiated.

Key words: turbulent atmosphere, problems of vision and isoplanacity, spatial filtration, image restoration.

Introduction

Optical images of objects observed through the turbulent atmosphere, are distorted both by the imaging process and the process of their registration. This distortion in the image formation process is caused by spatiotemporal fluctuations of the refractive index of the turbulent atmosphere, and the distortion in the registration process is due to the quantum character of the interaction of light with the photosensitive layer of the photographic material and nonlinearity of the process of photoexposure. To correct these distortions several image filtering algorithms have been developed [1]. These algorithms are based on the assumption of linearity and spatial invariance of the imaging systems. However, if the non-linearity of the registration process in some cases may be disregarded and consider the imaging system as linear, the spatial invariance (isoplanaticy) of the systems that form images through the turbulent atmosphere, is limited [2]. This restriction is significant in filtering of instant (short exposure) images of the extensive tracts of the Earth's surface and those images cannot be handled by the known spatial filtering algorithms [1].

This paper proposes a new statistical processing and recovery algorithm for the short-exposure remote sensing images, spatially noninvariant to the atmospheric distortions.

Effect of the turbulent atmosphere on the remote sensing systems

The presence of turbulent atmosphere between the surveyed region of the Earth surface and the earth remote sensing spacecraft significantly limits the information capabilities of the earth remote sensing systems [3]. Two problems arise: the problem of "vision" through the turbulent atmosphere and the problem of "isoplanaticy" of the surveyed region. The core of those issues is that the "vision" imposes restrictions on the minimum size of the detail resolvable by the atmosphere-remote sensing telescope system on the sensed region of the Earth's surface, and the problem of "isoplanaticy" limits the maximum size of the sensed region of the Earth's surface which is spatially invariant to atmospheric distortions, i.e. this problem limits the field of view of the atmosphere-remote sensing telescope system.

These issues substantially depend on the conditions of observation and, in particular, from the conditions of the remote sensing images registration.

If the registration (exposure) time t_E exceeds the interval of temporal correlation of the atmospheric fluctuations t_A (so-called time of "frozen" atmospheric turbulence), the registration time is considered long-exposure, and if the registration t_E is less than t_A, then it is considered a short-exposure registration. These two extremes significantly differ in nature of atmospheric distortion. If the long exposure picture, averaged over atmospheric distortions during the time $t_E>t_A$ has a lower resolution than instant short-exposure image register during the time $t_E<t_A$, it is spatially invariant to atmospheric distortions in the whole field of view of the atmosphere-remote sensing telescope system, unlike the short-exposure image, consisting in this field of a series of instant regions of isoplanaticy spatially invariant to atmospheric distortions.

In accordance with this, at the early stages of development of ERS technologies, the pursuit of a wider field of view stimulated the application of long-exposure ERS imaging both on Russian ERS SC: "Resurs-DK1" [4] and "Resurs-P", and the American ERS SC: "QuickBird", "WorldView" and "GeEye" [6].

The technology of time delay and integration, used in surveying, leads to registration of a long-exposure ERS image, averaged by the atmospheric distortions.

This image is characterized by a medium (long-exposure) optical transfer function (OTF), defined [7] as

$$\langle t(\vec{f})\rangle_{\text{l-e}}=\langle t(\vec{f})\rangle = t_0(\vec{f})\exp\left\{-3{,}44\left[\bar{\lambda}F\vec{f}/r_0\,(\bar{\lambda},\mathrm{H})\right]^{5/3}\right\} \quad (1)$$

With the development of ERS equipment, new technologies emerge that allow identifying and correcting the atmospheric distortions. Those technologies can be conventionally categorized into two classes: hardware and algorithmic technologies. Let us review them.

Hardware technologies of correction of the effect of the atmospheric turbulence in remote sensing systems

The first hardware technology of increasing of the spatial resolution of the ERS systems is based on a modification of the ERS telescope, namely, the replacement of the glass refractor telescope with a mirror reflector telescope and the increase of the diameter of the receiving aperture of the telescope D to $D>2r_0(H)$. This technology allows in the conditions of atmospheric vision and long exposure ERS image registration to reach limit resolution of 4.6 cm. The main problem of the practical implementation of this technology is the necessity of creation of the aperture synthesis multi-mirror telescope with a diameter of aperture D=7 m at H=350 km or D=10m at H=500 km, where H is the altitude of the ERS spacecraft. This ERS technology was considered in [8], which proposes an alternative possibility to reach the maximum ERS resolution for aviation altitudes H=10–20 km with a continuous aperture reflector telescope with a diameter of D = 20–4) cm, respectively.

Another hardware technology for increasing the spatial resolution of the remote sensing systems based on pre-sensor adaptive compensation of random wave tilt, caused by the influence of atmospheric turbulence. This technology proposed in [9] and explored in [10]. It makes it possible to receive an averaged short-exposure image characterized by medium short exposure optical transfer function, which is defined [7] as

$$\langle t(\vec{f})\rangle_{s\text{-}e}=t_0(\vec{f})\exp\left\{-3{,}44\left[\bar{\lambda}F\vec{f}/r_0\left(\bar{\lambda},H\right)\right]^{5/3}\cdot\left[1-\left(\bar{\lambda}F\vec{f}/D\right)^{1/3}\right]\right\} \quad (2)$$

In expressions (1) and (2) $\vec{f}=(\vec{\rho}_1-\vec{\rho}_2)/\bar{\lambda}F$ – spatial frequency vector in the aperture $\vec{\rho}$ of the ERS telescope, $\bar{\lambda}$ - is the average wavelength of solar illumination radiation ($\bar{\lambda}$= 0.5 μm), F - focal length of the ERS telescope, $\tau_0(\vec{f})$ - optical transfer function of the ERS telescope and $r_0(\bar{\lambda},H)$, - spatial correlation radius of atmospheric fluctuations of light at an altitude H of the ERS spacecraft, which is defined [8] as

$$r_0(\bar{\lambda},H)\approx\frac{H}{L}\ r_0(\bar{\lambda},L), \quad (3)$$

where $r_0(\bar{\lambda},L)$ = 0.1 m - is the magnitude of spatial radius of correlation of atmospheric fluctuations of light on the border of the turbulent layer L (L ≈ 10 km).

It is easy to see that at the altitude H = 350 km the value $r_0(\bar{\lambda}, H)$ is equal to 3.5 m, at H = 500 km $r_0(\bar{\lambda}, H)$ = 5 m and with H = 750 km $r_0(\bar{\lambda},H)$ is equal to 7.5 m. Thus, the value of $r_0(\bar{\lambda},H)$ is significantly larger of the diameter D = 1.1 m of the existing remote sensing telescopes [5], and atmospheric wave front distortion on the receiving aperture of the ERS telescope represent random tilts of the wavefront, compensated in the adaptive system. It is obvious that the resulting average short-exposure OPF (2) prevails over the medium and long exposure OPF (1) in the entire field of frequencies, providing a gain in resolution of the averaged short-exposure ERS image. Studies have shown that at the optimum aperture diameter D = 3.5r_0, a system with adaptive compensation of random wavefront tilts compared to a system without compensation provides a resolution gain of up to 4 times [10].

In General, hardware technology, providing theoretically good results in resolution, practically require a substantial upgrade of ERS equipment. Algorithmic technologies provide a simpler way to achieve the improvement of spatial resolution and increase the isoplanatic field of view of ERS systems.

Algorithmic correction technologies of the effect of the atmospheric turbulence in remote sensing systems

The first algorithmic technology proposed in [11] is based on receiving and processing of a series of N spectrally-filtered short exposure ERS images. Studies [12] have shown that as a result of detecting and recording a series of instant ERS images, affected by various atmospheric distortions, and their subsequent statistical processing, a secondary short exposure image is received, which has a resolution of the averaged short-exposure OTF (2) and an field of view isoplanaticy of the averaged long exposure OTF (1). In this manner the algorithmic technology helps to improve the spatial resolution while increasing the spatially invariant field of view of the ERS systems. The complexity of the practical implementation of this technology results from the need to change the process of ERS image detection and the transition from the traditional detection of medium and long exposure TDI images to the selective detection of instantaneous short exposure ERS images, independent from each other for atmospheric distortions.

Another algorithmic technology of increasing the spatial resolution of the ERS systems proposed in [13] requires no changes to the methods of detection of TDI and is based on the post-detection adaptive filtering of the registered long exposure ERS image spatially invariant to the atmospheric distortions. Studies [14] of this algorithmic technology confirmed the effectiveness of the algorithm of adaptive filtering of a long exposure image to improve its spatial resolution. The gain in resolution does not exceed 2 times, but may be sufficient to improve the spatial resolution of Russian remote sensing data (1 m) to match the level of foreign ERS systems (0.5 m).

The algorithmic technology considered above is less efficient than the new ERS algorithmic technology based on statistical processing of subimages and fragments of one short-exposure ERS image not spatially invariant to atmospheric distortions, a posteriori determining of the instant OTF of the atmosphere-telescope system for each area of isoplanaticy of the source image, their use for further spatial filtering of the relevant subimages and merging the results of filtering to restore the undistorted atmosphere time limited images of the surveyed region of the terrain. Let us review this technology

Statistical processing of subimages and their fragments of a short-exposure non-isoplanatic ERS image

When surveying areas of the Earth's surface illuminated by the sun, the distribution of intensity of spectrally filtered in the $\Delta\lambda < \Delta\lambda_A$ band short-exposure $t_E < t_A$, image of the object (an area of the Earth's surface) $I_i(\vec{I})$ if the additive noise is negligible, is determined by the following superposition integral:

$$I_i(\vec{I})=\int I_O(\vec{r})I_A(\vec{r},\vec{I})d\vec{r}, \quad (4)$$

where $I_C(\vec{r})$ is the true intensity distribution of the object, $I_A(\vec{r},\vec{I})$ is the instant impulse response of the atmosphere-telescope system (point blurring function), $\Delta\lambda_A=\lambda/\sigma_Q$, and σ_Q, is the root mean square deviation of atmospheric fluctuations of the phase Q_A of light radiation.

Due to the spatial noninvariance of the registered image, the function $I_A(\vec{r},\vec{I})$ is different for different points of the $\vec{r}$ object $_O(\vec{r})$, which does not allow applying the convolution theorem of the theory of Fourier Transforms to expression (4) and get its corresponding description in the spatial-frequency domain.

For the spatial filtering of the received nonisoplanatic images, they are broken down into N subimages, commensurate with the size of the isoplanaticy area of the atmosphere-telescope system, i.e. for N independent areas, within each of which the spatial system invariant. Then, for each j-th subimage, expression (4) can be written as convolution integral

$$I_i^j(\vec{I})=\int I_O^j(\vec{I})I_A^j(\vec{I}-\vec{r})d\vec{r}, \quad (5)$$

where j = 1, 2, ... N is the index indicating the number of a subimage and the atmospheric realization, which took part in the formation of the subimage.

Now that each subimage is spatially invariant, by converting both parts of the equation (5) by Fourier, its description in the spatial frequency domain is given by:

$$|\tilde{I}_i^j|\exp(i\tilde{\Theta}_{Im}^j)=|\tilde{I}_0^j|\exp(i\tilde{\Theta}_0^j)|\tilde{I}_A^j|\exp(i\tilde{\Theta}_A^j) \quad (6)$$

Here $|\tilde{I}_{im}^j|$ - is the spatial frequency spectrum modulus of the distorted j-th subimage, $|\tilde{I}_O^j|$ and $|\tilde{I}_A^j|$ is the modulus of the spatial spectrum of the true j-th subimage of the object and the OTF modulus of the atmosphere-telescope system of the j-th area of isoplanaticy, $\tilde{\Theta}_{Im}^j,\tilde{\Theta}_O^j,\tilde{\Theta}_A^j$ are the phases of the relevant spectra and OTF of the atmosphere-telescope system.

Subsequently, each subimage is divided into M fragments corresponding to the number of elements of resolution of the atmosphere-telescope system within the isoplanaticy field.

By analogy with (5) and (6), an expression for the i-th fragment of the j-th subimage is given by

$$I_{Im}^{ij}=I_O^{ij}*I_A^j \quad (7)$$

and its spacial spectrum by

$$|\tilde{I}_{Im}^{ij}|\exp(i\tilde{\Theta}_{Im}^{ij})=|\tilde{I}_O^{ij}|\exp(i\tilde{\Theta}_O^{ij})|\tilde{I}_A^j|\exp(i\tilde{\Theta}_A^j) \quad (8)$$

Here i = l, 2,..., M is the number of fragments in an isoplanaticy area (subimage), $|\tilde{I}_{Im}^{ij}|$ and $\tilde{\Theta}_{Im}^{ij}$ respectively are the modulus and the phase of the spatial spectrum of the -th fragment of the registered image, $|\tilde{I}_0^{ij}|$ and $\tilde{\Theta}_0^{ij}$ are the modulus and phase of the spatial spectrum of the ij-th fragment of true distribution of the object's intensity, * denotes the convolution operation, similar to (5). Further the processing of the phase and amplitude information will be performed separately.

1. Recovery of moduli of instant OTF subimages

Square modulus of the spatial spectrum of each ij-th fragment of an image is defined as

$$|\tilde{I}_{Im}^{ij}|^2=|\tilde{I}_O^{ij}|^2|\tilde{I}_A^j|^2 \quad (9)$$

Were this value by index i, i.e. find the average square of the spatial spectrum module each piece within the j subizobrazhenija also.

$$\langle|\tilde{I}_{Im}^{ij}|^2\rangle_i = \frac{1}{M}\sum_{i=1}^{M}|\tilde{I}_{Im}^{ij}|^2 = \langle|\tilde{I}_O^{ij}|^2\rangle i|\tilde{I}_A^j|^2, \quad (10)$$

where$\langle.\rangle = \frac{1}{M}\sum_{i=1}^{M}|\tilde{I}_{Im}^{ij}|^2$ denotes an averaging operation.

Now we shall average (9) over the index j, i.e. average different fragments over all the N subimages

$$\langle|\tilde{I}_{Im}^{ij}|^2\rangle_j = \frac{1}{N}\sum_{j=1}^{N}|\tilde{I}_{Im}^{ij}|^2 = \frac{1}{N}\sum_{j=1}^{N}|\tilde{I}_O^{ij}|^2\,|\tilde{I}_A^j|^2 = \langle|\tilde{I}_O^{ij}|^2\rangle_j\langle|\tilde{I}_A^{ij}|^2\rangle_j \quad (11)$$

Function $\langle|\tilde{I}_A^j|^2\rangle_j$ represents the average square of the OTF modulus of the atmosphere-telescope system and is in general known for the given conditions of atmospheric vision [15]. Then, by inverse filtering [16] $\langle|\tilde{I}_{Im}^{ij}|^2\rangle_j$ of the definiendum (11), we have

$$\frac{\langle|\tilde{I}_{Im}^{ij}|^2\rangle_j}{\langle|\tilde{I}_A^{ij}|^2\rangle_j} = \langle|\tilde{I}_O^{ij}|^2\rangle_j \quad (12)$$

Since the vast majority of real long objects of ERS are statistically homogeneous [17] the following equality is true

$$\langle|\tilde{I}_O^{ij}|^2\rangle_j = \langle|\tilde{I}_O^{ij}|^2\rangle_i = \langle|\tilde{I}_O^{ij}|^2\rangle. \quad (13)$$

By substituting the value received given (12) and (13) $\langle|\tilde{I}_O^{ij}|^2\rangle$ in (10), after the inverse filtering, the square modulus of the instant OTF for the j-th region of isoplanaticy (of the j-th subimage)

$$\frac{\langle|\tilde{I}_{И}^{ij}|^2\rangle i}{\langle|\tilde{I}_0^{ij}|^2\rangle} = |\tilde{I}_A^j|^2 \quad (14)$$

and by taking the square root, the modulus of the instant OTF of the atmosphere-telescope for the j-th subimage is received

$$\sqrt{|\tilde{I}_A^j|^2 =}\ \ |\tilde{I}_A^j|. \quad (15)$$

2. Recovery of moduli of instant OTF subimages

Simultaneously with the modulus of the instantaneous OTF it's phase should be recovered. It is easy to see from (8) that

$$\tilde{\Theta}_{Im}^{ij} = \tilde{\Theta}_O^{ij} + \tilde{\Theta}_A^j \quad (16)$$

To obtain the phase of the instantaneous OTF it is necessary to average the phases of the fragments belonging to one subimage, i.e. over i

$$\langle\tilde{\Theta}_{Im}^{ij}\rangle_i = \frac{1}{M}\cdot\sum_{i=1}^{M}\tilde{\Theta}_{И}^{ij} = \frac{1}{M}\sum_{i=1}^{M}\tilde{\Theta}_O^{ij} + \tilde{\Theta}_A^j = \langle\tilde{\Theta}_O^{ij}\rangle_i + \tilde{\Theta}_A^j \quad (17)$$

Further, in order to resolve the (17) the average phase of an object, we shall average (16) over j, i.e. sum the phases of the fragments belonging to different subimages

$$\langle\tilde{\Theta}_{Im}^{ij}\rangle_j = \frac{1}{N}\cdot\sum_{j=1}^{N}\tilde{\Theta}_{Im}^{ij} = \frac{1}{N}\sum_{j=1}^{N}\tilde{\Theta}_O^{ij} + \frac{1}{N}\sum_{j=1}^{N}\tilde{\Theta}_A^j. \quad (18)$$

Given that $\frac{1}{N}\cdot\sum_{j=1}^{N}\tilde{\Theta}_A^j = \langle\tilde{\Theta}_A^{ij}\rangle_j \equiv 0$[18], and subtracting (18) from (17) with regard for the statistical homogeneity of the object $\frac{1}{N}\cdot\sum_{j=1}^{N}\tilde{\Theta}_O^{ij} = \frac{1}{M}\sum_{i=1}^{M}\tilde{\Theta}_O^{ij}$,received is

$$\langle\tilde{\Theta}_O^{ij}\rangle_i + \tilde{\Theta}_A^j - \langle\tilde{\Theta}_0^{ij}\rangle_j = \tilde{\Theta}_A^j. \quad (19)$$

3. Filtering of subimages and recovery of an image of a region of the Earth's surface undistorted by the atmosphere

So we have recovered the modulus (15) and the phase (19) of the instantaneous OTF of the atmosphere-telescope system for the j-th subimage. Its instantaneous OTF is synthesized as

$$\tilde{I}_A^j = |\tilde{I}_A^j|\exp(i\tilde{\Theta}_A^j) \quad (20)$$

By inverse filtering the spatial spectrum of the j-th subimage (6), we obtain the diffraction-limited spatial range of the n-th filtered subimage of the object

$$\frac{\tilde{I}_{Im}^j}{\tilde{I}_A^j} = \tilde{I}_0^j = |\tilde{I}_0^j|\exp(i\tilde{\Theta}_0^j) \quad (21)$$

by reverse Fourier transforming it an undistorted by the atmosphere diffraction-limited subimage of the j-th isoplanatic area of the surveyed Earth's surface is restored

$$F^{-1}I0j = I0j \quad (22)$$

Performing a similar treatment for all N isoplanatic regions of the registered short-exposure image (4), we reconstruct the N subimages of the form (22), and by merging them, we reconstruct the diffraction-limited image of the probed non-isoplanatic object (of section of the earth's surface) I_0.

In conclusion, note that in the case when the original recorded image turns out to be substantially distorted by additive noise of background and registration, in place of inverse filtering, it is necessary to perform linear Wiener filtering in (12), (14) and (21) [19].

Thus, the proposed algorithm for processing of one short-exposure image spatially non-invariant to atmospheric distortions solves both the problem of "vision" and the problem of "isoplatality" caused by the presence of atmospheric turbulence. The algorithm can be effectively used to reconstruct undistorted images of extended areas of the Earth's surface when solving many ERS problems.

References

1. Tsujinchi J. Correction of optical images by compensation of aberrations and by spatial frequency filtering. *Progress in Optics*. Ed. by E.Wolf. North-Holland, Amsterdam, v. 2, p. 130, 1963.

2. Fried D.L. Varieties of isoplanatism. *Proc. of SPIE* v. 75, r.20, Imaging through the Atmosphere, 1976.

3. Bakut P.A., Sviridov K.N., Ustinov N.D., Khomich N.Yu. Problema izoplanatichnosti opticheskikh sistem, formiruyushchikh izobrazheniya cherez turbulentnuyu atmosferu [Problem of isoplanaticity of optical systems forming images through a turbulent atmosphere]. *Optika i spektroskopiya* [Optics and spectroscopy] Vol.60, No. 3, p. 611, 1986. (in Russian)

4. Sviridov K.N. *Tekhnologii vysokogo razresheniya opticheskikh sistem atmosfernogo videniya* [High Resolution Optical Systems for Atmospheric Vision]. LAMBERT Academic Publishing, GmbH, ISBN 968-3-65969-676-3, 2015. (in Russian)

5. Petri G. Rossiyskiy sputnik «Resurs-DK1»: al'ternativnyy istochnik dannykh sverkhvysokogo razresheniya [The Russian satellite Resurs-DK1: an alternative source of ultrahigh resolution data], *Geomatika* [Geomatics], No 4, p. 38, 2010. (in Russian)

6. Kirilin A.N. et al. Kosmicheskiy apparat Resurs-P [Resurs-P Spacecraft], Geomatika, No 4, p.23, 2010. (in Russian)

7. Lavrov V.V. Kosmicheskie s"emochnye sistemy sverkhvysokogo razresheniya [Space survey systems of ultrahigh resolution]. *Geoinformation portal of GIS Association*, No 2, 2010. (in Russian)

8. Fried D.L. Optical Resolution through a Randomly Inhomogeneous Medium for Very Long and Very Short Exposures, *JOSA*, v. 56, p. 1372, 1966.

9. Sviridov K.N. O predel'nom razreshenii aerokosmicheskikh sistem distantsionnogo zondirovaniya Zemli (DZZ) [Limiting Resolution of Aerospace Systems in Earth Remote Sensing (ERS)]. *Raketno-kosmicheskoe priborostroenie i informatsionnye sistemy* [Rocket-space device engineering and information systems]. Vol. 1, No. 1, p. 34, 2014. (in Russian)

10. Sviridov K.N., Volkov S.A. Sposob distantsionnogo zondirovaniya Zemli [Method of remote sensing of the Earth], application for an invention №2015129353 from 17.07.2014, applicant JSC "Russian Space Systems". (in Russian)

11. Sviridov K.N. Distantsionnoe zondirovanie Zemli s adaptivnoy kompensatsiey sluchaynykh naklonov volnovogo fronta [Remote sensing of the Earth with adaptive compensation of random wavefront inclinations]. *Raketno-kosmicheskoe priborostroenie i informatsionnye sistemy* [Rocket-space device engineering and information systems]. Vol. 2, No. 3, p. 12, 2015. (in Russian)

12. Sviridov K.N. Sposob distantsionnogo zondirovaniya Zemli (DZZ) [Method of remote sensing of the Earth(ERS)]. Patent of RF No. 2531024 from 20.08.2014 from the application for invention No. 2013125540 from 03.06.2013, applicant JSC "Russian Space Systems". (in Russian)

13. Sviridov K.N. O novom podkhode k polucheniyu i obrabotke izobrazheniy DZZ, iskazhennykh turbulentnoy atmosferoy [A New Approach to Obtaining and Processing Earth Remote Sensing (ERS) Images, Degraded by a Turbulent Atmosphere]. *Raketno-kosmicheskoe priborostroenie i informatsionnye sistemy* [Rocket-space device engineering and information systems]. Vol. 1, No.4 , p. 28, 2014. (in Russian)

14. Sviridov K.N. Sposob polucheniya i obrabotki izobrazheniy, iskazhennykh turbulentnoy atmosferoy [Method of obtaining and processing images distorted by the turbulent atmosphere], application for invention No. 2016100934 from t14.01.2016, applicant JSC "Russian Space Systems". (in Russian)

15. Sviridov K.N. Adaptivnaya fil'tratsiya izobrazheniy, iskazhennykh turbulentnoy atmosferoy [Adaptive filtering of images distorted by the turbulent atmosphere]. *Raketno-kosmicheskoe priborostroenie i informatsionnye sistemy* [Rocket-space device engineering and information systems]. Vol. 2, No. 4, p. 40, 2015. (in Russian)

16. Korff D. Analysis of a method for obtaining near-diffraction-limited information in the presence of atmospheric turbulence. *JOSA*. v. 63, p. 971, 1973.

17. Harris J.L., Sr. Image Evaluation and Restoration. *JOSA*. v. 56, p. 569, 1966.

18. Cannon T.M. Blind Deconvolution of Spatially Invariant Image Blurs with Phase. *IEEE Trans. Acoust., Speech, Signal Process.* v 24, p. 58, 1976.

19. Bakut P.A., Sviridov K.N., Ustinov N.D. O vozmozhnosti vosstanovleniya neiskazhennogo atmosferoy izobrazheniya ob"ekta po N ego pyatennym interferogrammam [On the possibility of reconstructing an undistorted by the atmosphere of an image of an object from its N stained interferograms], *Optika i spektroskopiya* [Optics and Spectroscopy], Vol. 50, No. 6, p. 1191, 1981. (in Russian)

20. Hellstrom C.W. Image Restoration by the Method of Least Squares. *JOSA*. v. 57, p. 297, 1967.

ROCKET-SPACE DEVICE ENGINEERING AND INFORMATION SYSTEMS
Vol. 3, Iss. 2, 2016, pp. 33–41

Communication channel for small-size spacecraft on the base of the GLOBALSTAR satellite communication system

I.A. Morozov, N.S. Danilin[1], N.N. Makukhin, A.S. Sergeev

[1]doctor of engineering science, professor
Joint Stock Company "Russian Space Systems", Russia

e-mail: morozov_ia@risde.ru

Abstract. The usage of the available global general purpose satellite communication systems for control of small-size spacecraft is considered a peromising and low-cost direction. The most suitable system to fulfill this task is the GLOBALSTAR. For the first time a communication through this system was carried out by the nanosatellite TNS-0 № 1 in 2005.

The article shows the results of the comparative analysis of the experimental data received from TNS-0 № 1 and computer modeling of the mission conditions using the "Radio coverage zone of TNS-0" software. Favourable communication conditions in which the technology for small-size spacecraft control with use of the GLOBALSTAR system is very effective, low-cost and operationally convenient, as well as realized both in stationary and mobile variants, are defined. It is determined that the area of space where communication can be possible is a so called "cone of communication" in which the small-size spacecraft, a GLOBALSTAR spacecraft and a ground gateway should be simultaneously.

The article describes specific causes of lack of communication. Practical recommendations on increasing the amount and duration of communication sessions are given. A new way for communication channel organization using GLOBALSTAR satellite communication systems is proposed. The results of the ground tests are presented.

Keywords: nanosatellite, small-size spacecraft, GLOBALSTAR, space communication system, zone of radio visibility.

The use of satellite communication systems (SCS) for commercial applications to control small-sized spacecraft (SSS) is currently a promising and low-cost direction.

Among the existing SCS (INMARSAT, IRIDIUM, Orbcomm, Thuraya, Globalstar) the most suitable for the task is the Globalstar System.

The high altitude of the satellites' orbit (H = 1400 km) provides a broad coverage area for the SSS. The weight of the user equipment (a satellite modem and an antenna) does not exceed a few hundred grams, therefore it can be used in the SSS. The system is certified in Russia.

For the first time the CCC Globalstar channel was implemented on the nanosatellite TNS-0 №1 (Fig. 1). This is one of the first Russian nanosatellites. It is made in JCS RSS and on March 25, 2005 has been launched "manually" from the ISS. Active work with the satellite took place till July 6, 2005, when it completely consumed the energy supply of the onboard battery.

One of the main objectives of launching the TNS-0 №1 nanosatellite was to test the possibility of communication sessions between the satellite and the terrestrial MCC using SSS Globalstar, as well as network monitoring to determine the SSS control capabilities through the system.

Fig. 1 Nanosatellite TNS-0 №1

The scheme of information exchange between SSS and MCC using the Globalstar system is shown in Fig. 2

For successful communication sessions with the MCC, the SSS and the ground gateway (GG) must simultaneously be in the radio visibility zone (RVZ) of the Globalstar spacecraft (GS SC). A "cone of communication" is the space where communication is possible, it has the following parameters:

- the vertex is located in the center of mass of the GS SC;

- the semi-apex angle $\boldsymbol{\alpha}_{max}$ is determined by the radiation pattern of the antenna of the GS SC.

Figure 3 shows a diagram of the combined radio visibility zone of SSS - GS SC - GG.

The design of nanosatellite TNS-0 №1 is shown in Figure 4

Communication and management TNS-0 №1 was carried out through GSP 1620 modem of the Globalstar system (Fig. 5). The modem was turned on automatically for 10 min each hour of flight. If it was possible to establish a link, an exchange of information with the ground mission control center was carried out.

At the end of the LCI analysis of the results. During the analysis, the following data were used:

– ***MCC data on the conducted communication sessions;***

– ***catalog numbers of the active satellites in the Globalstar orbital constellation.*** The data were obtained experimentally. It was established, that during the FDT of the TNS-0 №1 of the nominal 48 GS SC only 36 were active, which, of course, reflected in the number of successful communication sessions;

– ***Globalstar data on registrations of the TNS-0 №1 in the network.*** Monitoring of the registrations was performed by the Globalstar service provider in Russia, GLOBALTEL, in accordance with the agreement that had been reached earlier;

– the orbital data (TLE) of the NORAD aerospace control system on SSS and active GS satellites. Data archives are publicly available on the Internet site https: space-track.org.

– coordinates of the terrestrial gateways and their coverage area. The data obtained from the technical description of the SCS Globalstar.

Computer simulation of the conditions of TNS-0 №1 flight was conducted using the RVZ TNS-0 №1 software (Fig. 6).

The communication sessions calculation results are shown in Fig.7.

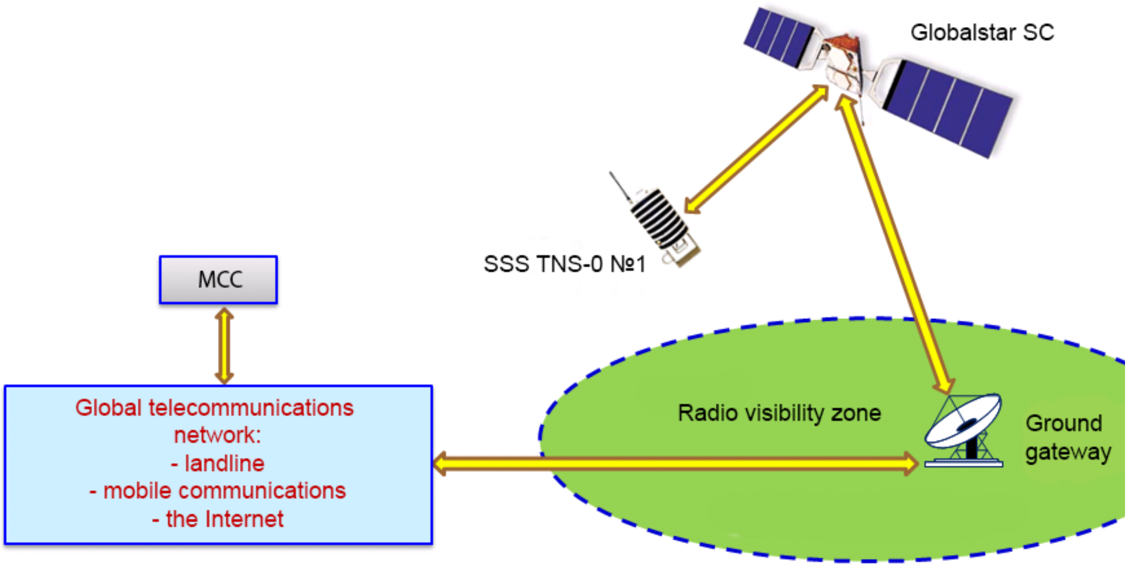

Fig. 2 Scheme of information exchange between SSS and MCC

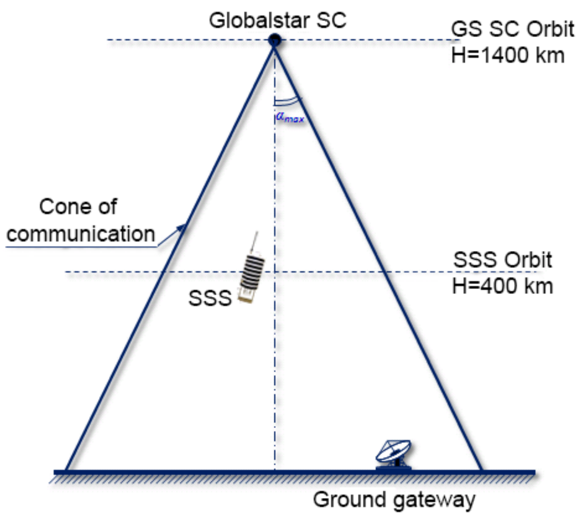

Fig. 3 scheme of the combined RVZ of SSS - GS SC - GG.

Fig. 4 The appearance of the nanosatellite without cover

The results of the FDT post-flight data analysis of TNS-0 №1:

1. The flight design tests (FDT) of the TNS-0 №1 nanosatellite were successful. Active work of the satellite continued 68 days 20 hours 31 minutes (from 09:39 Moscow time 28.03.2005 till 06:10 Moscow time 05.06.2005). During this time, the TNC-0 №1 made 1086 circuits. The satelliet conducted 22 communication sessions, including 11 sessions with the MCC-1 (stationary, Globalstar communication system) and 12 sessions with the MCC-2 (mobile, "MTS" communication system). During the session 8 the link was established alternately with MCC-1 and MCC-2. The total duration of sessions was 34 minutes 49 seconds. The TNS-0 received 561397 bytes (8731 frames), and transmitted 70280 bytes (8770 frames) of information by the means of the MCC. The received signal strength indicators (RSSI) were obtained during the tests.

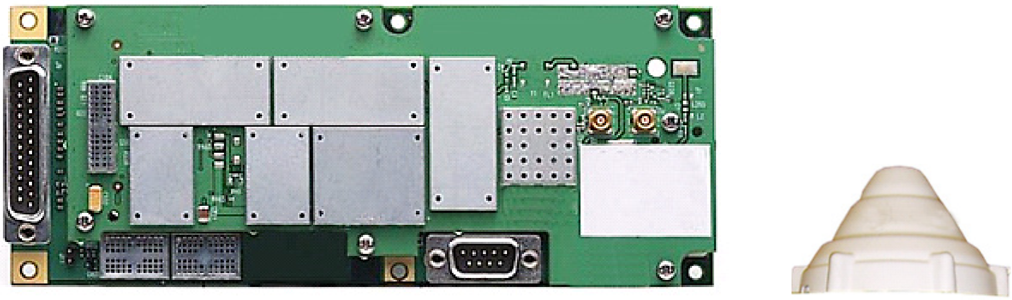

Fig. 5 GSP 1620 modem with the QUALCOMM ANTENNA

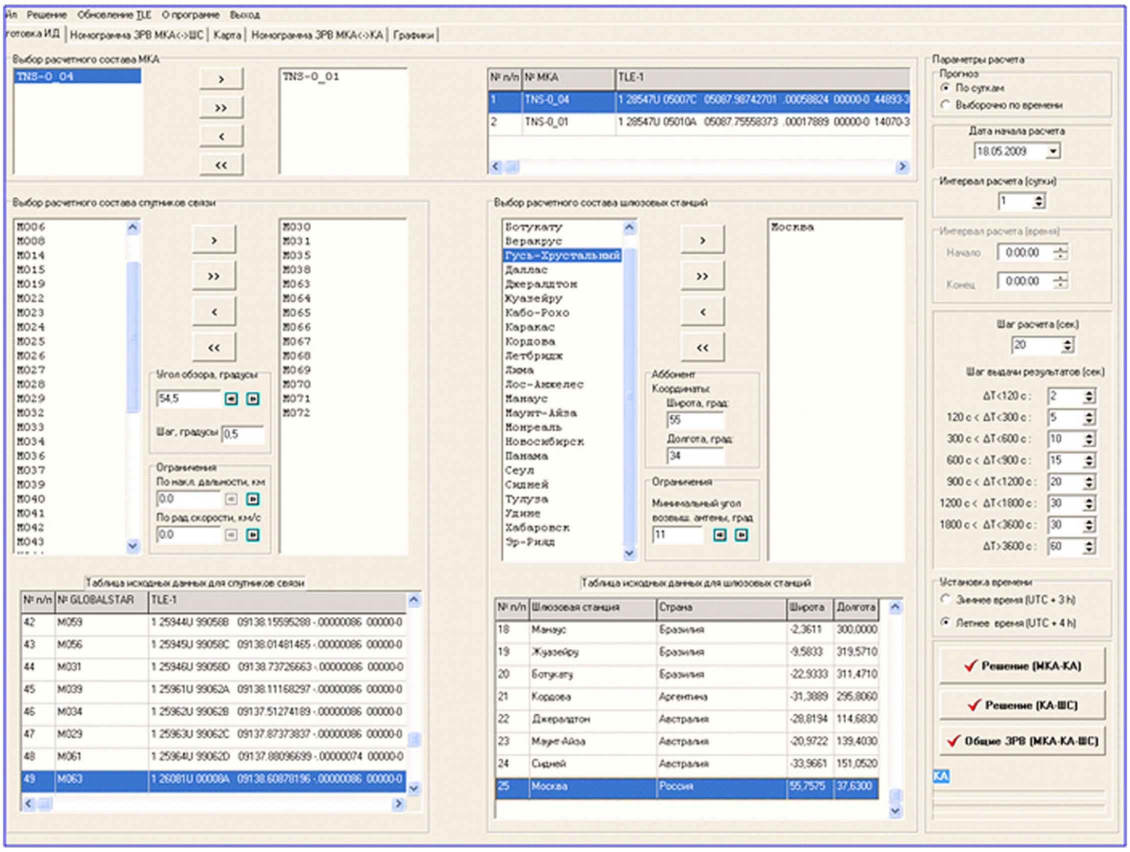

Fig. 6 Central window of the RVZ TNS-0 №1 software

2. Favorable communication conditions under which the SSS control technology using the Globalstar network is highly effective, low-cost and user-friendly, and operationally realizable both in stationary and mobile versions were identified. At the same time, the conditions associated with unstable orientation and stabilization of the spacecraft, the mismatch between the current location of the spacecraft and the service areas of the Globalstar system when such communication is unreliable and it should not be used were identified.

Monitoring of the conditions of communication through the Globalstar system showed that:

- 50% of the activations of the Globalstar modem occured outside the service zones of the regional operators;
- during 12% of the activations roaming was unavailable;
- during 14% of the activations in the link between the TNS-0 №1 and GLOBALSTAR spacecraft was unstable (communication disruption);
- during 24% of the activations the quality of the communication channel was sufficient for the data exchange with the MCC.

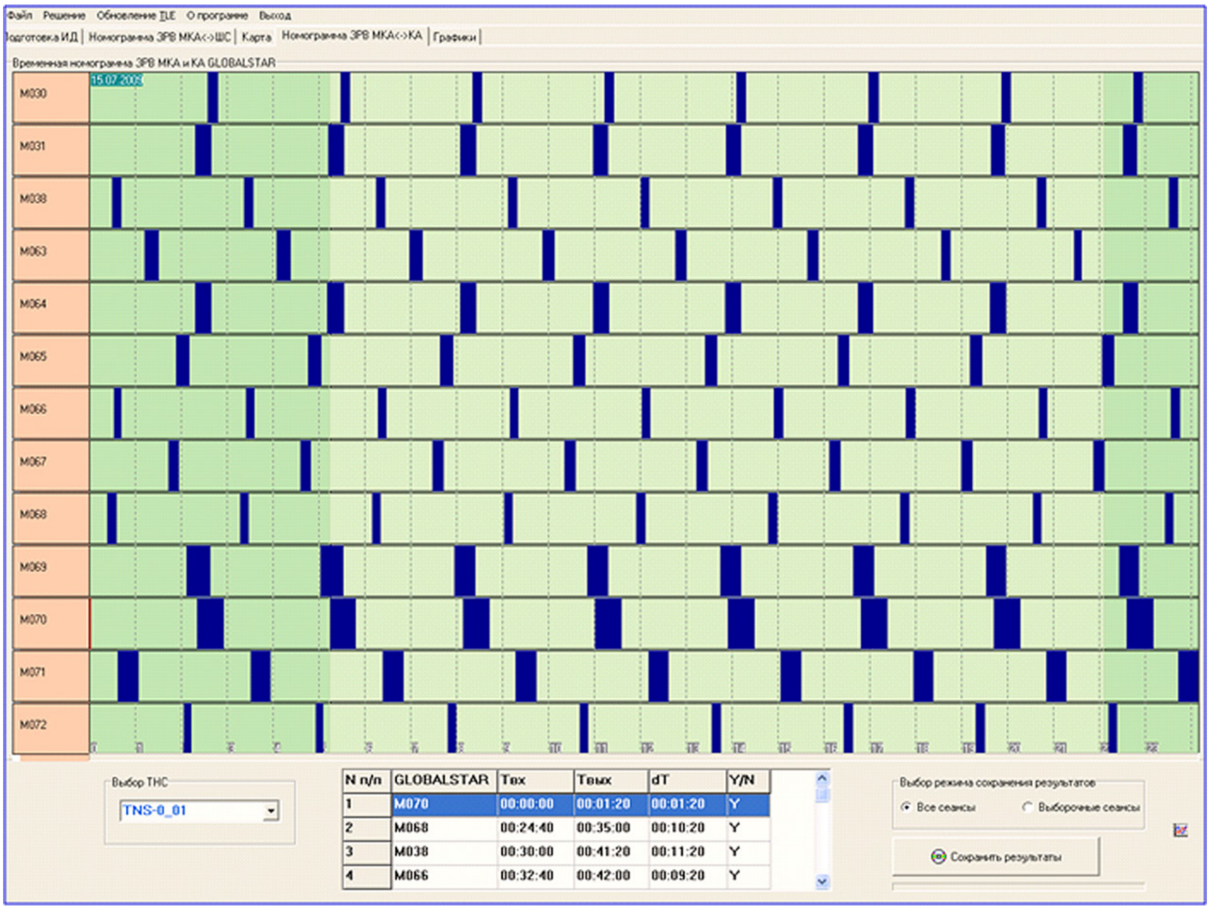

Fig.7 The communication sessions calculation results obtained from the RVZ TNS-0 №1 software

3. the tests of the "RVZ TNS-0" software proved the choice of algorithms for calculation of radio sessions between the MCC and the SSS to be correct. Most of the experimental data received during the monitoring of the GLOBALSTAR network corresponds to the calculations with a sufficiently high accuracy. However, some data does not correspond to the calculations. In particular, RSSI outside the RVZ is detected. Perhaps this effect is due to re-reflections of radio signal in the atmosphere. For a more detailed study of the causes of some data disagreement with the calculation, work needs to continue, including the new space experiment with the use of nano-satellite TNS-0 №2.

Space experiments demonstrated the possibility of using the Globalstar SCS for the SSS Control. However, the number of successful sessions with the MCC (24%) is insufficient. In future devices, measures to improve it must be taken.

Methods of increasing the number and duration of the communication sessions with MCC in the Globalstar network.

1. ***A preliminary calculation of communication sessions.***

The method is as follows. The MCC makes a preliminary calculation of the combined RVZ of the SSS, the active GS SC and ground-based gateways. Such a calculation can be performed using the software package "RVZ TNS-0" on the basis of the current orbital data (TLE) of the spacecraft. Then the long-term schedule of activations (for 3-5 days) is transmitted to the SSS.

Disadvantages:

- error of calculation of sessions is less than 30 seconds. Such accuracy can be considered acceptable for building mission scenarios with communication sessions in the "broad" service areas with the time span of 5-10 min. However, for "narrow" zones (≤ 3 min.) such accuracy is insufficient.

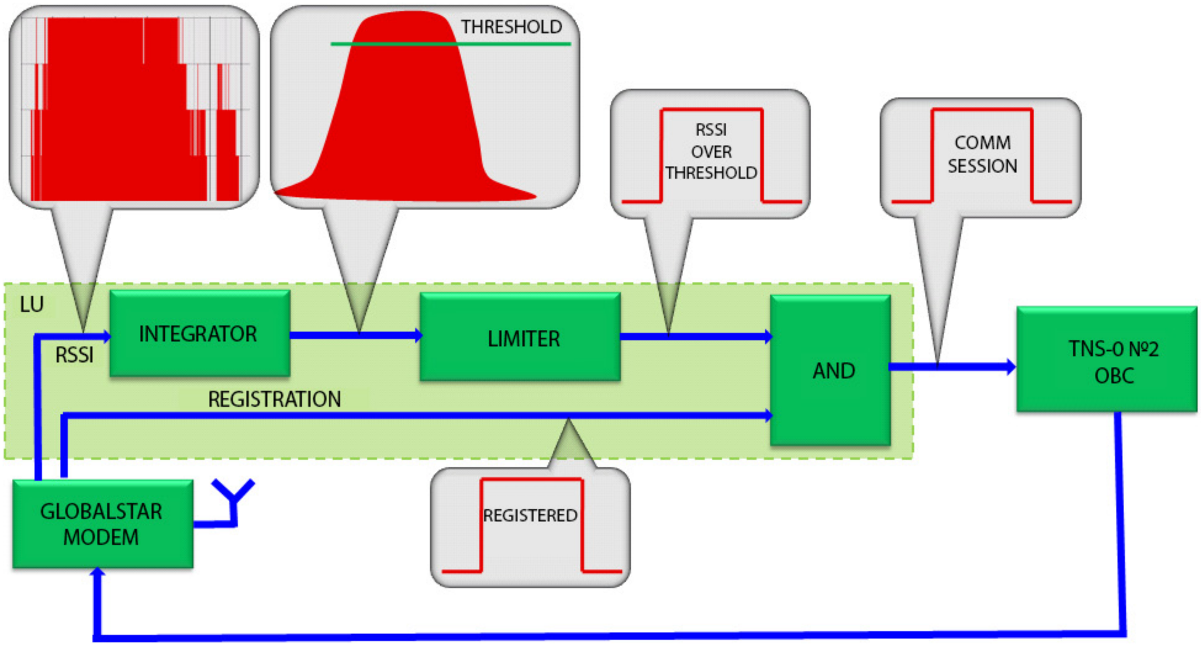

Fig. 8 Schematic diagram of the autonomous operation mode of the Globalstar modem

- the need for regularly updated orbital data and calculations of communications sessions with the subsequent transfer of the data to the satellite.

2. Autonomous activation of the Globalstar modem (patent number 2520352 from 23.08.2012)

The method of autonomous activation of the SSS modem based on analysis of service information from the Globalstar network is deprived of the shortcomings of the first method. The method is as follows.

The general stream of data coming aboard the SSS contains service information (SI), that serves to provide the performance of the Globalstar system. The specially developed software installed on board the satellite, separates the SI signals from the general stream of information. As a result of the subsequent processing of the SI in the logical unit (LU) by pre-worked out algorithms, commands are formed and sent to the satellite computer, which controls the Globalstar modem. Therefore, the start time and duration of sessions is determined by the on-board LU in the automatic mode and does not depend on instructions from the MCC. Calculating RVZ is not required. In this mode, during the communication sessions, in addition to the basic information from the SSS, the SI of the Globalstar network is transmitted to the MCC. The SI will increase the accuracy of the post-flight processing of the SSS FDT results.

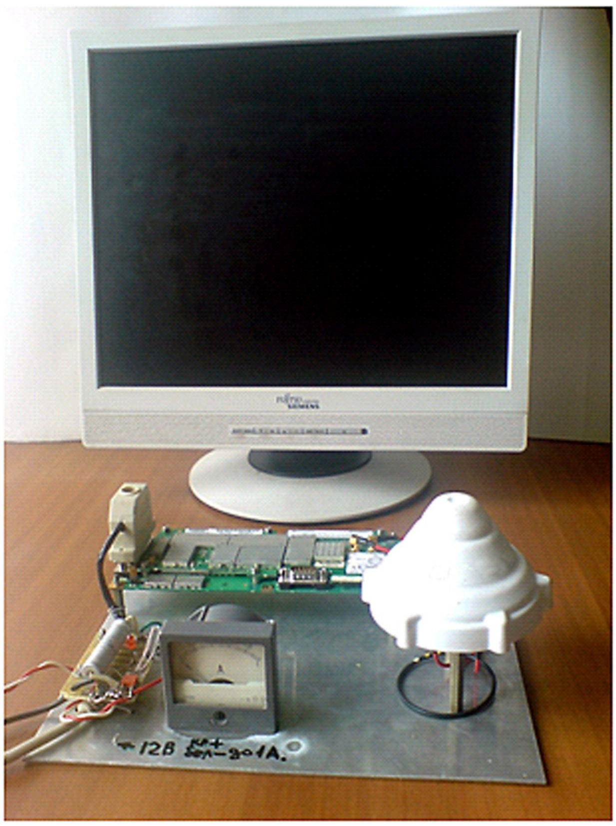

Fig. 9 TNS-0 №2 simulator

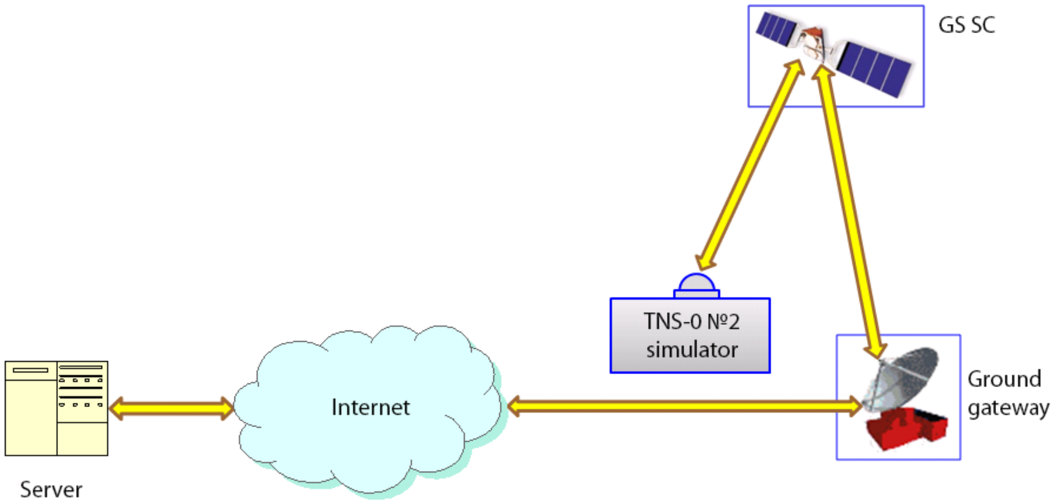

Fig. 10 Scheme of data exchange in the Globalstar network between the TNS-0 №2 simulator and an Internet server in packet mode

The presence of a stable link to the Globalstar system is determined by the following SI signals:

– "RSSI" signal. This is a signal indicative of the quality of the communication channel "Subscriber – Globalstar satellites – terrestrial gateway". It is produced by the modem based on the analysis of the incoming signals from the Globalstar network. The amplitude of the RSSI signal to ensure a stable link must be at least 3 units on the signal strength scale;

– "Registration" signal. Is fed to the modem after the registration process in the Globalstar network. Simultaneously with the "Registration" signal, the modem receives the number of the GG through which it should establish a link.

The user (single-port) mode of the modem does not support the separation of the SI signals. To separate the SI signal, the two-port modem configuration is used.

The schematic diagram of the Globalstar modem operation in the autonomous mode is shown in Fig.8.

The signals from the "Control port" modem are fed to the logic unit (LU), that consists of an integrator, a limiting controller and an "AND" logic circuit. All the constituents of the LU are implemented in software.

The system operates as follows. During the flight of the SSS, the on-board Globalstar modem operates in standby mode with its receiver turned off. When the satellite enters the RVZ, the "Control port" of the modem receives the RSSI signal. Next the RSSI is fed to the integrator. As a rule, the beginning (and the end) of the communication session is characterized by rapid changes in the RSSI level, resulting in unstable communication. To eliminate this phenomenon, an integrating link is included in the scheme of the automatic modem control. The amplitude of the signal at the output of the integrator is equal to the arithmetic mean of the ten current RSSI level readings.

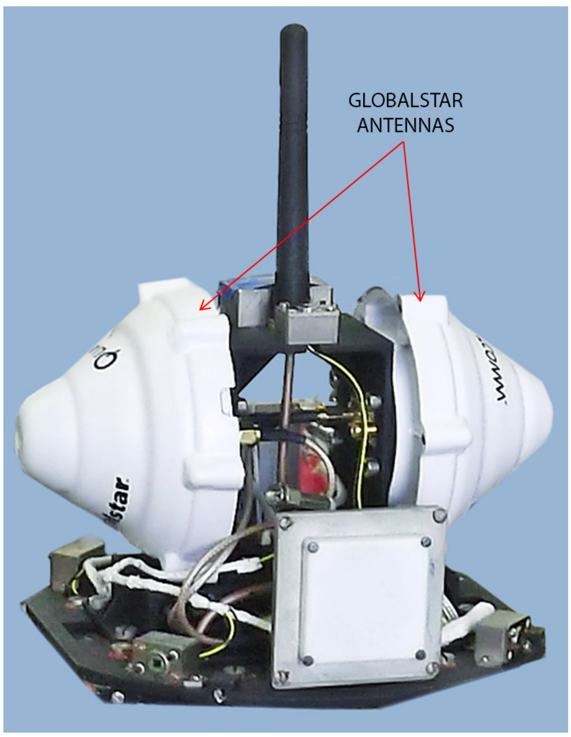

Fig. 11 TNS-0 №2 with an additional antenna

Then the limiter compares the current value of the signal with a predetermined threshold value. When the signal level exceeds the threshold, the limiter sends a logical one to one of the inputs of the "AND" circuit. If the satellite is registered in the network, the modem sends a logical one to the other input of the logical circuit. In this case, the output of the logical "AND" circuit also generates a logical one. Then, a command in the form of positive voltage is sent to the on-board computer for it to activate the operating mode of the modem. A communication session between the SSS and the MCC takes place.

When the satellite leaves the RVZ, the RSSI level drops to zero. The "And**"** logical circuit generates a logical zero. The on-board computer terminates the session and puts the modem in standby mode.

Experimental testing of the automatic operation mode of the modem in the Globalstar - Internet network was carried out in the ground conditions on a TNS-0 №2 simulator. The appearance of the TNS-0 №2 simulator is shown in Fig.9.

In the course of the experiment eleven communication sessions with a remote Internet server with an average duration of 6 minutes were conducted. This time is sufficient for transmitting a test message from the TNS-0 №2 simulator to an Internet server and receiving a response test message (~ 1 min.).

All the test messages were fully transmitted and received, without errors and data loss. The average speed of data transfer is 7 kbit/s. This value is very close to the maximum possible data rate in the GLOBALSTAR network, which is equal to 7.2 kbit/s.

3. Using a packet data transfer mode.

The Globalstar network supports two data transmission modes: the asynchronous mode, when the connection is established via the PSTN and GSM terrestrial networks; and the packet mode, that uses the Internet. Connection with terrestrial networks is carried out using different servers. Obviously, the time of connection establishment will be different for different modes. During the ground experiment on the TNS-0 №2 simulator, the time of connection establishment with the subscriber was measured. The average time taken to establish a connection is T = 34s in the asynchronous mode, and T = 5s in the packet mode. A significant reduction in the time of the connection establishment (≈ 7 times) allows to increase the length of communication sessions. This is especially important for the "narrow" RVZs, lasting less than three minutes.

For the scheme of information exchange in the Globalstar network between the TNS-0 №2 simulator and an Internet server in packet mode, refer to Fig.10.

The results of this experiment show that it is advisable to use the packet mode in the future launches of the SSS. An additional advantage of this mode is that in case the MCC is currently unavailable for communication, the data is stored on an Internet server of the Globalstar provider and can be received by the MCC operator when the communication is restored.

During the flight, TNS-0 №1 used the asynchronous mode, which had a negative impact on the number and duration of sessions.

Fig. 12 VHF modem Roger KD 9600.

Fig. 13 Antenna with circular polarization.

4. Set-up of an additional transceiver Globalstar antenna.

A secondary antenna (diametrically opposed to the primary one) and two couplers will increase the total radiation pattern of antenna feeder device (AFD) approximately twofold that will lead to a substantial increase in the number of communication sessions. Fig. 11 shows a photo of the TNS-0 №2 antenna unit with an additional antenna.

5. Introduction of a backup VHF communication channel.

The Roger KD 9600 modem has the most suitable technical and mass-dimensional parameters. Photos of the modem are shown in Fig.12.

To eliminate the Faraday effect, associated with the change of the polarization plane of the received signal, the terrestrial VHF reception station should employ an antenna with circular polarization (Fig.13).

Conclusions.

1. From the analysis of data obtained during the FDT of TNS-0 №1, it follows that the information field of SCS Globalstar is not global and continuous. The structure of the field depends on the characteristics of the GS spacecraft orbits and the number of active spacecraft in the constellation.

2. FDT of TNS-0 confirmed the possibility of using a communication channel on the basis of Globalstar for the SSS control.

3. To increase the number and duration of sessions is recommended to use a five-item set of design solutions designed after the analysis of data obtained during the flight tests of THC-0 №1 and presented in the article. Experimental ground testing showed their high efficiency. A final check of the new design solutions must perform in a real space flight. Such tests are scheduled to take place on the next nanosatellite, TNS-0 №2.

References.

1. *Spravochnoe rukovodstvo integratora sputnikovogo modema peredachi dannykh GSP-1620 QUALCOMM Globalstar* [A reference guide of the satellite modem integrator for data transmission GSP-1620 QUALCOMM Globalstar].

2. *Otchet po rezul'tatam LKI nanosputnika TNS-0 №1* [A report on the results of TNS-0 № 1 flight development tests].

3. *Arkhivy orbital'nykh dannykh* [Archives of orbital data]. Available at: https: //www. space-track. org.

4. *Patent na izobretenie № 2520352 ot 23.08.2012 g.* [An invention patent № 2520352 dated 23.08.2012].

ROCKET-SPACE DEVICE ENGINEERING AND INFORMATION SYSTEMS
Vol. 3, Iss. 2, 2016, pp. 42–49

The Results of the Modeling and Estimate of the Characteristics of the Signals with Linear Frequency Modulation Reflected from the Spread Objects

S.B. Medvedev, V.I. Shaposhnikov[1], O.A. Chekmazova

[1]candidate of engineering science
Joint-Stock Company "Research Institute of Precision Instruments", Russia

e-mail: v.schaposchnikov@yandex.ru, alter-vista@mail.ru

Abstract. The article contains the study of the algorithms of the weight pulse-type signal processing with linear frequency modulation in the radio engineering measurement system of parameters relative to the movement used for space vehicles docking. The aim of work is to increase the system working capacity through eliminating spurious signals reflected from the large-sized construction elements, for example, from the International Space Station. Such spurious signals are received in the same time interval together with the useful signal that contains the data on the relative movement parameters. This can reduce the measurement accuracy of these parameters. In order to eliminate this effect, there was selected a broadband pulse signal with linear frequency modulation and digital processing of the received signal. Deterioration of the measurement accuracy caused by the side lobes of the correlation function leads to the necessity to examine different ways of their reducing with the help of a so called "mismatched reception", which has a distinctive feature of losses caused by the discrepancy. This work contains the research on measuring these losses depending upon the relation FKV/FDEV = K. Moreover, the best value of K when using this filter was found.

Keywords: space vehicles docking, linear frequency modulation, multipath effect, mismatched filtering, deviation frequency, sampling frequency

Introduction

A combination of a useful signal, sum of the re-reflected signals and receiver noise is transmitted to the output of the filter for processing path to determine the position of large-size space objects (SO). As a result, a spurious signal consisting of a number of signals received from various paths owning to multipath radio waves propagation appears in the reception point. This signal significantly reduces the indicators of the system for mutual measurements and rendezvous-docking search (MMRDSS) in terms of measurement of the parameters accuracy of the rendezvous trajectory for SC and SO.

When developing MMRDSS, there appears a task to minimize the measurement errors due to the side lobes (SL) of the autocorrelation function of an emitted signal. In the literature, works on decreasing the SL response on the time axis are conducted in several directions:

1. Using weight processing methods [4, 5], when the main response lobe widens, and its value decreases in maximum.

2. Signals modification with linear frequency modulation (LFM) introducing a relatively small nonlinearity [1], which makes it possible to achieve the effects similar to weight processing.

3. Carrying out a disagreed processing based on the usage of the special reference function.

In [3], it is concluded that weight processing in the receiver is a more effective method than that of in the receiver, since control of the envelope on the output of power transmitters is considerably difficult.

When using mismatched filtering, there appears a problem to search optimal filter parameters. This task can be found in:

1. Evaluating the signals parameters received under the conditions of a white noise with related re-reflected interferences and multipath.

2. Tracking a great number of noncooperated objects.

3. Designing SAR (synthetic aperture radar).

4. Forming frequency-amplitude distribution according to the aperture of the active phase-array antennas (APAA) with areas of an increased suppression of the re-reflected signals.

The quantization frequency *Fq* is a filter characteristics under investigation. It allowes one to receive minimal loss because of disagreement for different values of the deviation frequency *Fdev* and the pulse duration τ. *Fq* to *Fdev* ratio is taken as $K=F_Q/F_{DEV}$.

Signal extraction principle of this method is based on the model of the received signal in the form of matrix, where the signals are as numeric vectors in a complex space and nonstatic processing methods by evaluating the functions of mutual correlation of the received spaced diversity signals. To search for an optimum solution of the set tasks, computer simulation and series of experiments in the *Matlab* was carried out.

The aim of the paper is to determine optimum parameters of the signal with LFM by computer simulation taking into account the peculiarities of the requirements on the operation of the SC docking system.

Properties of the LFM signal and description of the computer model

A signal with linear frequency modulation (LFM) was used during research. It was taken based on the fact that this signal is employed in the majority of the modern systems, since it has a number of useful properties, including simplicity of realization and opportunity to significantly compress a signal during the reception with increase in its amplitude under the interference level.

Determination of the best parameters of the signal with LFM such as pulse durability τ, deviation frequency F_{DEV}, quantization frequency F_{QUANT} and $F_{QUANT}/F_{DEV}= K$ ratio by means of simulation makes it possible to obtain necessary parameters in the response of the "mismatched" filter, such as:

1. The width of the main lobe (distance between 0 and crossing of the main lobe of the time axis – end point).

2. An integral level of the side lobes on the output of the supression filter.

3. "Mismatch" loss.

4. The maximum size of the peak suppression zone.

5. The minimum level of the side lobes out of the peak supression zone of the compression filter.

The detailed description of the computer model operation is given in [6]. To understand the system operation, further is given a short description of the functioning of the seacrh algorithm for the optimum filter parameters of the signal with LFM.

A model of the emitted signal with LFM: $S(t) = a\cos\left(\omega_0 t + \frac{\pi F_{DEV} t^2}{\tau_{PULSE}}\right);$

An equivalent complex representation is the following:

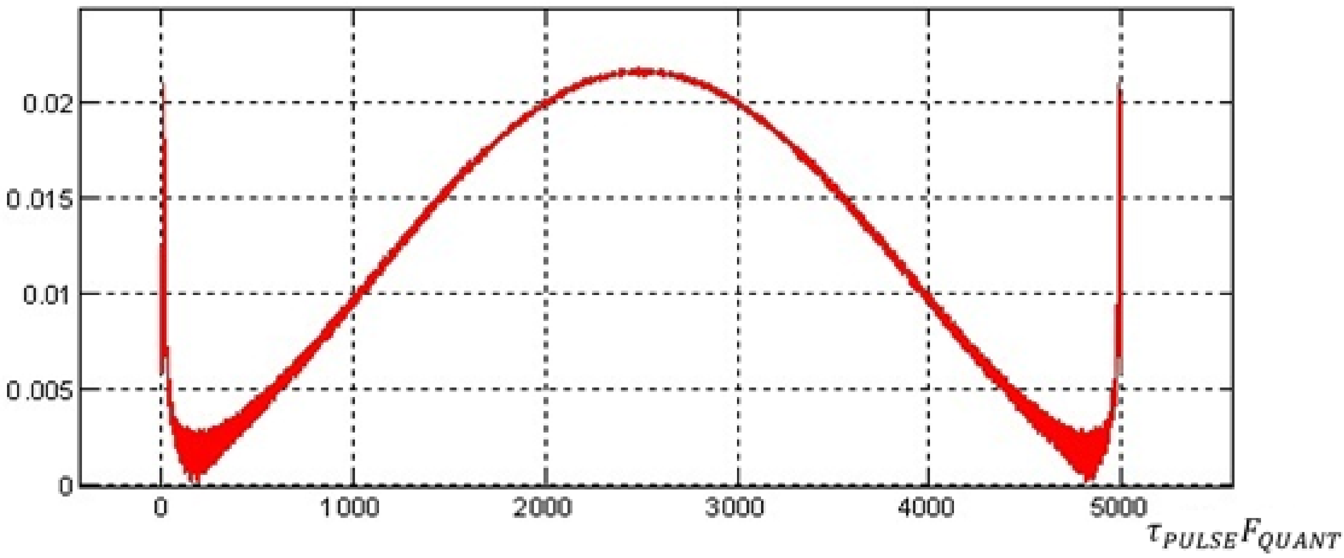

Fig. 1. Amplitude-frequency characteristics of the reference vector.

$$\dot{S}(t) = a\, exp\, \frac{j\pi F_{DEV}t^2}{\tau_{PULSE}}$$

Allowing for digital processing: $\overline{S}(i) = (z_{01}, z_{02}, \dots, z_{0n})$,where $i = 1{,}2 \dots n$, $\bar{S}(i)$ *is* a vector in the complex space.

A model of the reflected signal $\overline{S}_j = [(\alpha_{i1}, \varphi_{i1})\,(\alpha_{i2}, \varphi_{i2}) \dots (\alpha_{in}, \varphi_{in})]$ is a standard, centered emitted signal, where α_{ij} is an unknown amplitude and φ_{il} is an unknown initial signal phase.

In this case a problem of the synthesis can be solved as a problem of the signal resolution $\overline{S}_k$ received together with *m*-other signals: to build an optimum filter (a supporting function) using an optimality criterion, i.e., obtain a response maximum on the signal under analysis when supressing interfering signals up to a some level *ε* (or zero).

A received signal

$$y_k(t_j) = \alpha_k \overline{S}_k + \sum_{i=1;i\neq k}^{m} \alpha_i \overline{S}_j + \overline{\varpi}(t_j),\ \text{where}$$

j=1,2,…2n, m=2n-1.

In the formula, the first summand can be considered as a useful signal, the second one – as an interfering signal, the third – as a noise.

The processing algorithm.

An optimum reference vector should be searched

$$\overline{P}_{0j} = (x_{01}, x_{02}, \dots x_{0n}),\ \text{such that}\ \overline{S}_k, \overline{P}_{0j} = \max$$

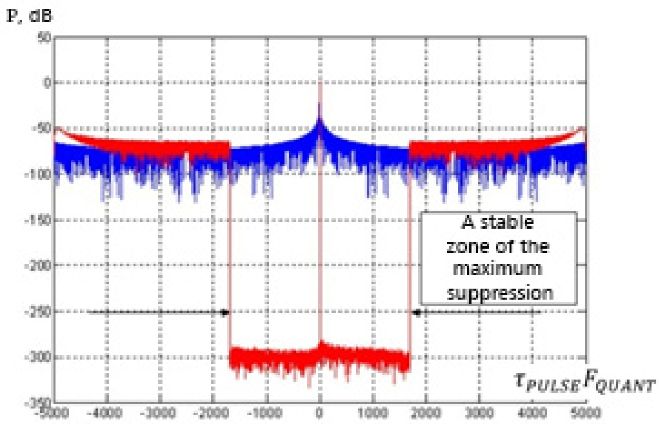

Fig. 2. The responses of the matched (blue) filters and filters under research (red).

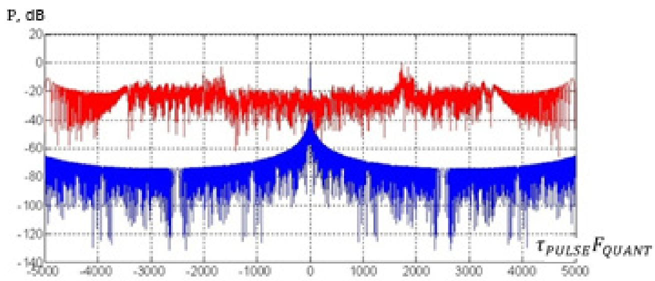

Fig. 3. The responses of the matched (blue) filters and filters under research (red) under the conditions of violating the algorithm for equations solution.

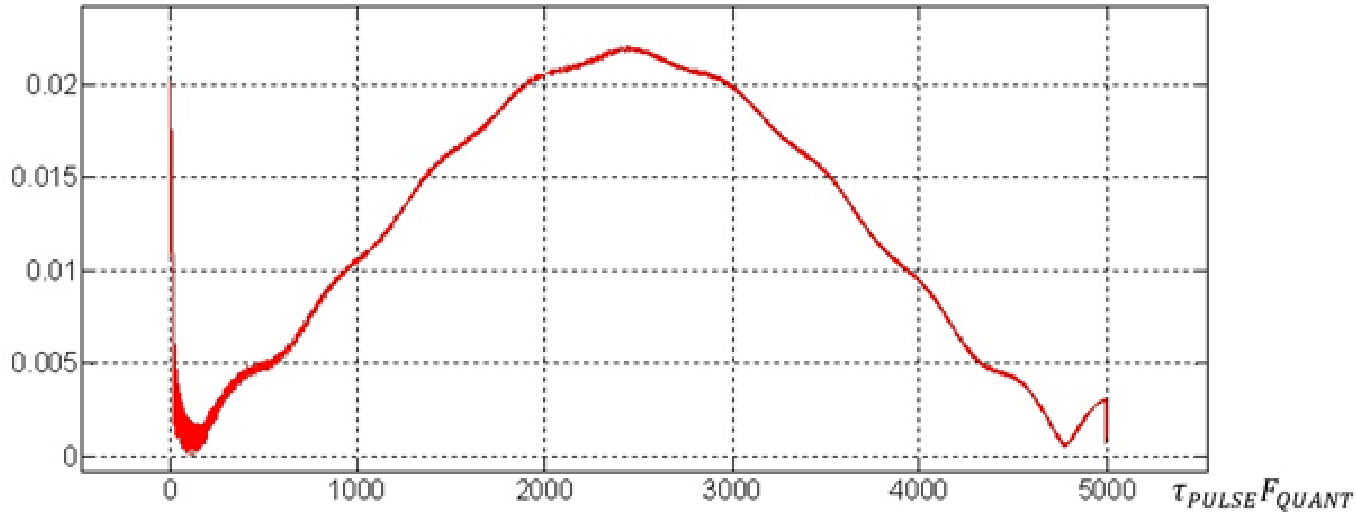

Fig. 4. Amplitude-frequency characteristics of the reference vector (physical simulating).

under the condition: $\left(\sum_{i=1;i\neq k}^{m} \alpha_i \overline{S}_{ij}, \overline{P}_{0j} \right) \begin{cases} < \varepsilon \\ or \\ = 0 \end{cases}$

If to consider that a set of signals under research has a correlation interval $\sim \dfrac{1}{\Delta F}$, and $f_{quant.} > 2\Delta F$ (ΔF is a signal band), so the matrix (S_{ij}) will have the dimension m x n, where $m<n$, the reference vector $\overline{P}_{0j}$ can be written as the following:

$$\overline{P}_{0j} = \left\{ E - (S_{ij})_{-k}^{T} \left[(S_{ij})_{-k} (S_{ij})_{-k}^{T} \right]^{-1} \cdot \right. \qquad (1)$$
$$\left. \cdot (S_{ij})_{-k} \right\} \cdot \overline{S}_{kj}^{T}$$

where $(S_{ij})_{-k}$ is the matrix (S_{ij}) without the k-th line.

The filter response built using (1) can be written as the following:

$$U(x/y) = \left(\alpha_k \overline{S}_{kj}, \overline{P}_{0j} \right) + \left(\sum_{i=1 i\neq \kappa}^{m} \alpha_i \overline{S}_{ij}, \overline{P}_{0j} \right) +$$
$$+ \left(\overline{w}(t_j) \cdot \overline{P}_{0j} \right).$$

To obtain an analytic base of the research, a number of experiments with various values of the listed parameters of the signal with LFM was carried out. A programme of the experiment was the following: only one

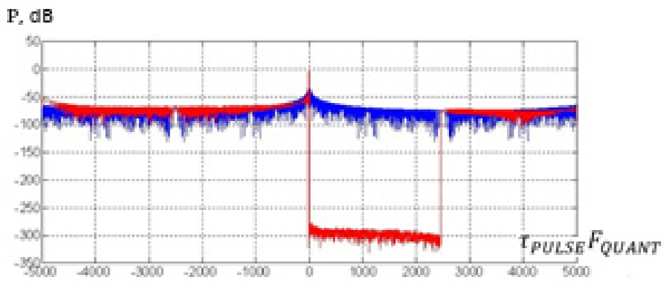

Fig. 5. The responses of the matched filter (blue colour) and the filter under research (red) for physical simulation.

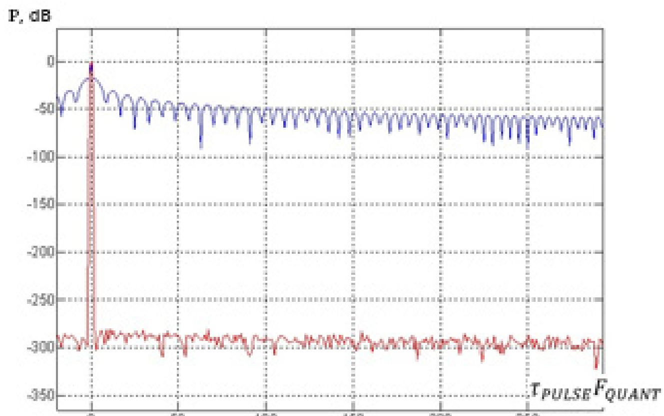

Fig. 6. The responses of the matched filter (blue colour) and the filter under research (red) for physical simulation.

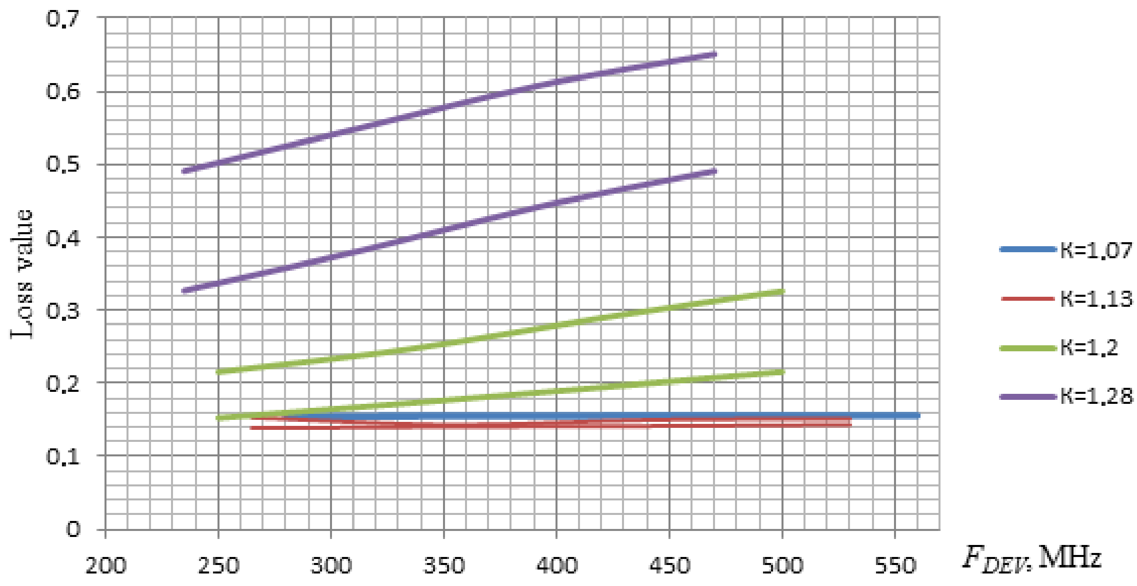

Fig. 7. Dependence of the loss level on deviation frequency for different K (a mathematical simulation).

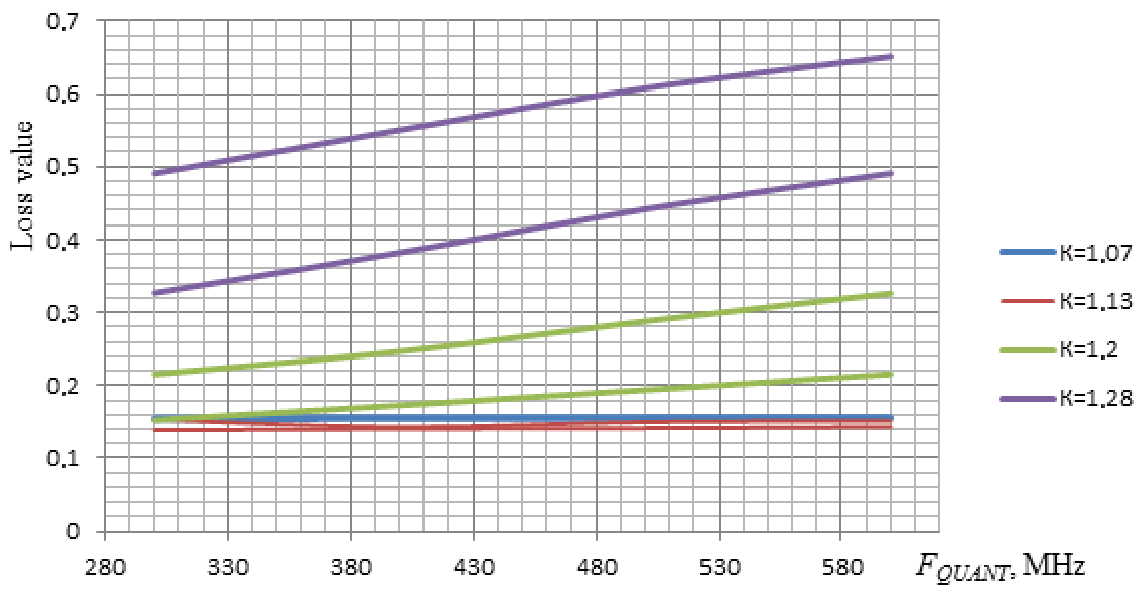

Fig. 8. Dependence of the loss level on quantitation frequency for different K (a mathematical simulation).

parameter varied on each stage, and others remained constant. It was performed to reveal a parameter among the others under investigation that determines to the full extent the result: to control the loss values and response function type. The corresponding analytical graphs were built for each experiment.

Simulation results

A model describes a received signal in the form of a matrix. Its lines are the reflected signals from the SC determined by the chosen correlation level between the neighbouring lines-signals of this matrix. Taking into

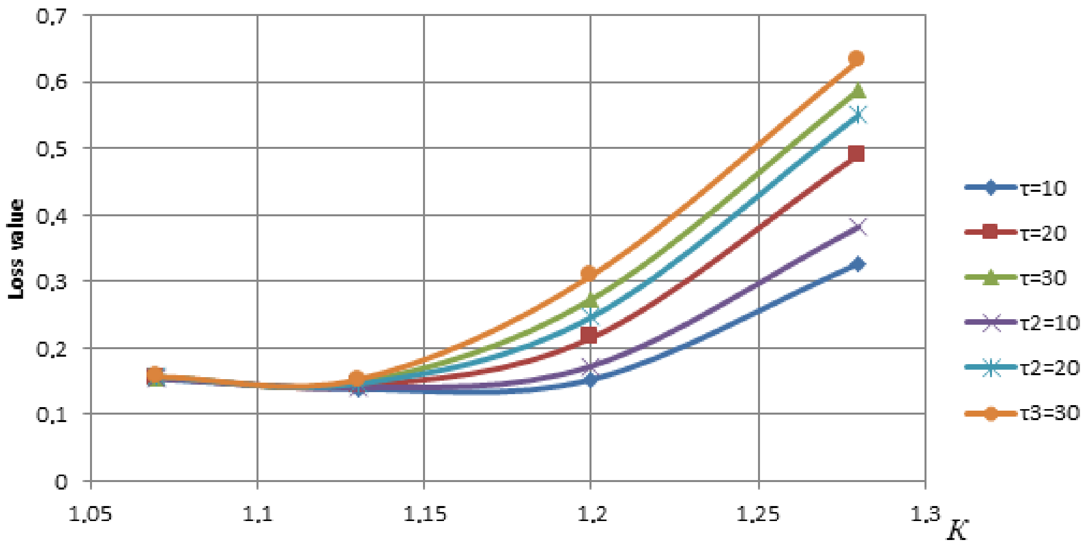

Fig. 9. Dependences for the quantization frequency 300 MHz (τ) and 400 MHz (τ2).

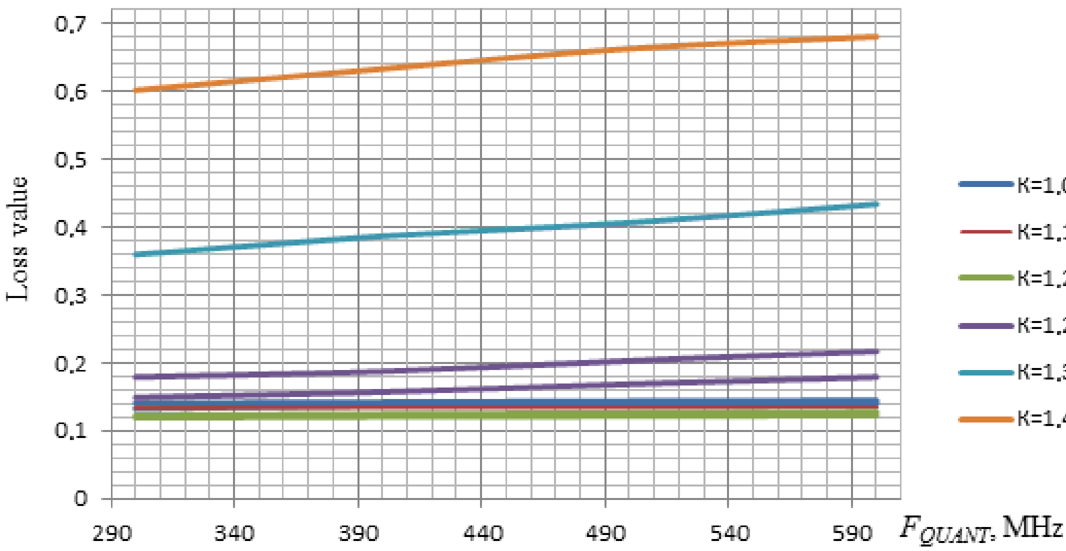

Fig. 10. Loss dependence on quantization frequency for different K during a physical simulation.

account a digital method for signal processing and presence of the quadrature mixers on the output of the receiver, signals of each line of this matrix can be given as numerical vectors in the complex space. The simulation task is determination of the technical parameter K depending on F_{DEV}, F_{QUANT} and τ_{PULSE} allowing one to obtain the minimum loss level of mismatching.

To get the character of the dependences and to reveal the parameters, which at the full extent influence, a number of experiments was conducted. Under these conditions, the varied parameters underwent "a net" of the values under analysis chosen a priori and built for deviation frequency, quantization frequency and pulse duration. The data varied in the range:

1. F_{QUANT} = 300–600 MHz.

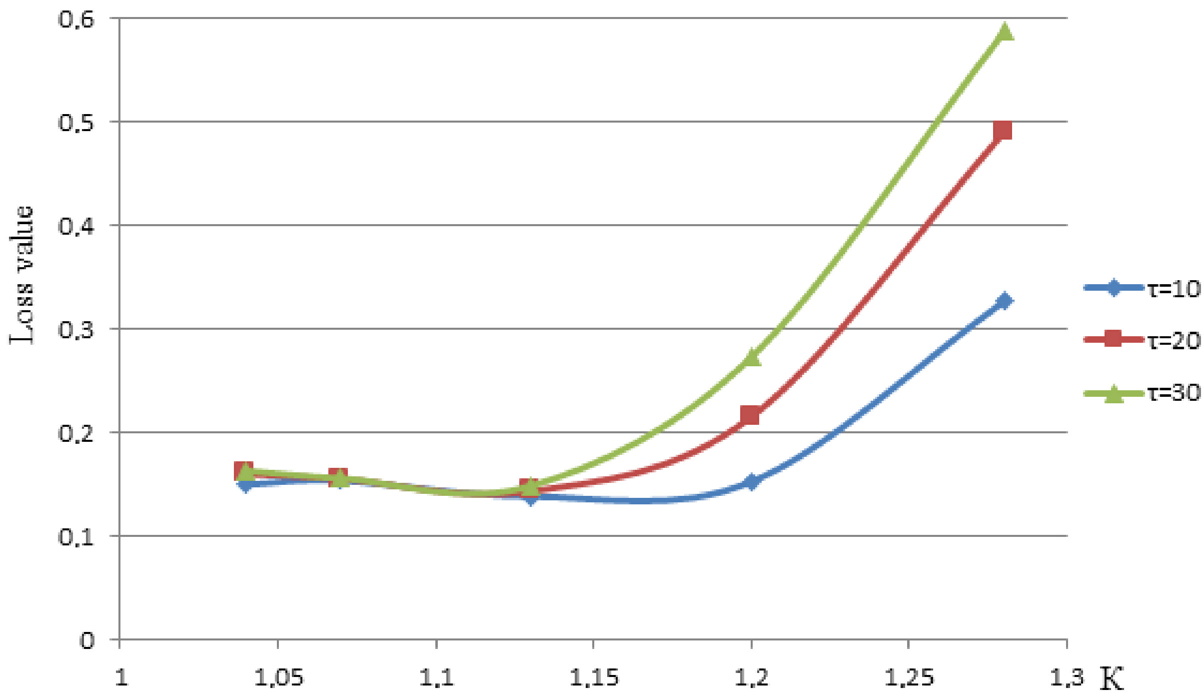

Fig. 11. A diagram of loss dependence on the ratio K=F_{QUANT}/f_{DEV}

2. F_{DEV} = 205–560 MHz (что соответствует значениям показателя K = 1.07–1.46).

3. τ = 10–40 μsec.

Further, the simulation results for a signal model with quantization frequency F_{QUANT}= 500 MHz, deviation frequcny F_{DEV} = 442 MHz (K=1.13) and pulse durability τ = 10 μsec.

Amplitude-frequency characteristics (Fig. 1) of the reference vector is distribution with the maximum in the area of the zero frequency and descending to the edges and tends to the maximum value in the area of the boundary points (the upper frequencies in the spectrum).

The response of the filter given in Fig. 2 is shown in comparison with the case of the matched filtration. The diagram shows that using the mismatched filtration (formula 1) it is possible to obtain a good area of the stable zone of the maximum suppression, about –300 dB.

A mathematical apparatus is the foundation of the algorithm for solution, which is used for solving a big (several thousands) system of linear equations. If an amount of equations in the system becomes more than a certain threshold, so the system turns into unstable, and suppression disappears. Fig. 3 shows with a red colour a response of the filter that is searched for under the amount of the equations in the system to be solved surpassing a third part from the value

The given diagrams show the character of the mathematical dependences when finding the signal symmetrically relative to zero on the time axis. In real conditions a signal exists in the time interval $t>0$, i.e., it is unsymmetrical relative to zero. The diagrams of the corresponding dependences are given below. Such simulating can be called physical.

It should be noted that for a physical simulating a condition of equations system solving is another: an amount of equations in the system should not exceed a half of the value . Fig. 5 shows a response of the filter, and Fig. 6. depicts its scaled area of the zone for the maximum suppression.

During each experiment, a level of a useful signal and loss level were registered.

The analysis of the data received

To obtain analytical data, a number of experiments for the values of the quantization frequencies lying in the range from 300 MHz to 600 MHz and deviation frequencies corresponding to them from 205 MHz to 560 MHz, the pulse duration τ varied from 10 μsec to 30 μsec.

The derived values were written in the summary table, the analysis of which was later given in the form of a diagram. The obtained distributions enable one to find out a frequency dependence of the results, determine the zones with the maximum signal level and the values of the parameters of the signal with LFM corresponding to them.

To demonstrate the results of the experiment, comparative diagrams for mathematical and physical simulation were built.

The results of a mathematical simulation

The diagrams of the loss dependences (in fractions, axis of coordinates) on the deviation frequency (axis of abscissas) (Fig. 7) and quantization frequency (Fig. 8) show the drop in signal amplitude with increasing the value of the K indicator. There is no frequency dependence for small values of the K indicator, while at K>1.2 with increase in frequency a level of the useful signal falls. In addition, there is a slight signal loss with increase in the duration τ.

Diagram 9 shows the dependence of the loss value on the K indicator. In case of a mathematical simulation, an area 1.07–1.15 is the smoothest and, consequently, recommended. Further, a significant drop in characteristics is seen that leads to the loss of a useful signal.

Analytical dependences for a physical distribution

A physical simulation permits one to obtain the same effect. The only difference is that an area of frequency independent results is at the indicator K≤1.2.

The results for the physical simulation is given in Figs. 10, 11.

The analysis of the diagrams received showed that at the small factor K (1.07–1.2) a loss value does not depend on the quantization frequency and is about 0.12–0.14%, while with increasing the K (K>1.2) loss of a useful signal increase by 20% with each increase of the K by 0.1. As the diagram above shows, at the value K=1.36, a loss value increased 3 times in comparison to the values obtained at small factors. At the K=1.46, the loss value increased 5 times. It can be concluded that the most useful, in terms of getting a useful information from the received signal, is an indicator of the quantization frequency-to-deviation frequency ratio equal to 1.07–1.2. With such indicator, the loss dependences on the quantization frequency in the recommended range are almost unobserved.

It should be concluded that the essential factor influencing the results is the indicator $K=F_{QUANT}/F_{DEV}$ (quantization frequency-to-deviation frequency ratio), optimum values of which lie is in the range 1.07–1.2. These results can be referred to the processing of the set of pulse signals with LFM. The results obtained in the foreign and domestic literature known to the authors were not found.

References

1. Voevodin V.V. *Vychislitel'nye osnovy lineynoy algebry* [Computing fundamentals of linear algebra]. Moscow, Nauka, 1977. (in Russian)
2. Kuk Ch., Bernfel'd. *Radiolokatsionnye signaly* [Radiolocating signals]. Moscow, Sov. radio, 1971, 214 p. (in Russian)
3. Marpl Jr. S.L. *Tsifrovoy spektral'nyy analiz i ego prilozheniya* [Digital spectral analysis with applications]. Moscow, Mir, 1990. (in Russian) (Translated from English)
4. Radiolokatsionnye ustroystva i sistemy. [Radiolocating devices and systems]. *Spravochnik po radiolokatsii* [Radiolocation manual]. Ed. M. Skolkin. Vol 3. Moscow, Sov. radio, 1978. (in Russian) (Translated from English)
5. Shishanov A.V., Shaposhnikov V.I. Povyshenie informatsionnoy effektivnosti i apriornaya otsenka kachestva raboty RSA [Increasing the information efficiency and an a priori estimate of quality of work of synthetic-aperture radars]. *Doklad na VI Vserossiyskoy nauchno-tekhnicheskoy konferentsii "Aktual'nye problemy raketno-kosmicheskogo priborostroeniya i informatsionnykh tekhnologiy"* [Report of the VI All-Russian scientific and technical conference "Current problems of rocket and space device engineering and information technologies"]. Moscow, AO "Rossiyskie kosmicheskie sistemy", 2013. (in Russian)

ROCKET-SPACE DEVICE ENGINEERING AND INFORMATION SYSTEMS
Vol. 3, Iss. 2, 2016, pp. 50–53

Development of the Scientific Equipment for Search and Localization of Air Leak Places from the ISS ROS Pressurized Compartments

N.M. Pushkin[1], S.V. Batsev[2], K.O. Leushin

[1]doctor of engineering science, [2]candidate of engineering science
Joint Stock Company "Scientific and Production Association of measuring equipment", Russia

e-mail: npoit@npoit.ru, otdel413@mail.ru

Abstract: The article describes the main results of the development of the scientific equipment intended for refinement of methods of searching the air leaks from the ISS pressurized compartments. It should be stressed that in the process of work the hardware and software scientific complex, consisting of the optical-electronic unit, control and monitor pane,l and laptop, was designed. The optical-electronic unit is an extravehicular part of the complex used for identification of various effects and anomalies taking place at depressurization of the station. The results of measurements and video data are transferred via the panel to the onboard laptop in which indications of the UV, IR and visible band cameras, UV-spectrometer, as well as vacuum control and electric field intensity devices, are fixed. Moreover, separate parts of the scientific equipment have passed factory and interdepartmental tests and verified their working capacity. The design and engineering documentation for the scientific equipment was issued. It should be noted that the scientific complex will allow one to optimize the most effective method of extravehicular search of air leak places from the pressurized compartments of the ISS ROS (the Russian Orbital Segment of the International Space Station).

Keywords: air leak, depressurization, research, device, equipment

The off-nominal situation leading to air leaking from the station pressurized compartments, for example, at collisions of the International Space Station (ISS) with another vehicle, at blow of a large meteoric particle or because of the collision with the elements of space debris can take place during the ISS operation. By means of the scientific "BAR-ARM" equipment developed by Joint Stock Company "Scientific and Production Association of Measurement Equipment" ("NPO IT") the space experiment (SE) "Express" is carried out at the ISS. The purpose of the experiment is working off the methods of air leakage search from the ISS compartments.

The "BAR-ARM" equipment consists of the optical-electronic unit, monitor and control panel, and onboard laptop, on the display of which the indications of sensors and images received by means of optical devices of the equipment are shown.

The optical-electronic unit (OEU) is an extravehicular part of a complex of the scientific "BAR-ARM" equipment. A 3D model of the OEU is shown in Fig. 1. The OEU is intended for identification of various effects and anomalies on an external surface of the ISS taking place at air leakage into the external environment. Change of pressure of own external atmosphere of the ISS, change of the temperature field of an external surface, luminescence of gases and vapors of water in the ultraviolet range, and change of the electric field intensity can be such effects. To control these factors the OEU includes the following devices:

- TV camera of visible range;
- TV camera of infrared (IR) range;
- camera of ultraviolet (UV) range;
- UV range spectrometer;
- vacuum control system with two space-separated sensors;
- intensity measurement system of alternating electric field.

In the course of the experiment, the OEU will move along the ISS surface by means of the operated manipulator. Before the experiment, the equipment is transferred from the stand-by mode to the operating mode. The stand-by mode includes the storage mode of the scientific "BAR-ARM" equipment on the board and periodic tests. The thermal stabilization system, which is built in the OEU, is involved in this mode. The connection of the payload adapter, on which the OEU is placed, to the active docking adaptor of the manipulator and its transfer to the measurement zone is carried out while transferring

Fig. 1. The prototype of the optical-electronic unit (OEU) of the scientific "BAR-ARM" equipment.

the equipment to the operating mode. Then opening of protective shutters of the optical windows of the OEU modules and carrying out the measurement sessions by each scientific equipment module is implemented. Upon termination of a measurement session, the protective shutters are closed, and the manipulator transfers the OEU to a storage zone. The payload adapter is connected to the passive docking adaptor to activate the thermal stabilization system of the OEU while storage.

The optical devices "Thompson" and "SOM" (Fig. 2 and Fig. 3) are placed in the pressurized compartments (Fig. 4) and are packed in the OEU frame. To pass the optical radiation of visible, IR and UV ranges, the OEU frame is supplied with quartz and germanium entrance windows. The windows are equipped with blends (hoods) for protection against the side illumination. The entrance windows have the operated blinds for protection against the external pollution caused by products of orientation and correction engines operation.

The results of thermal and ultraviolet radiation control will be put on the image received by the TV camera of the visible range. The corresponding scientific software for this purpose is under development. The experiment results are output onto the on-board computer (laptop).

The interface of the on-board computer to the OEU devices is carried out via the intermediate control panel, where necessary devices of digital signal transformation are placed.

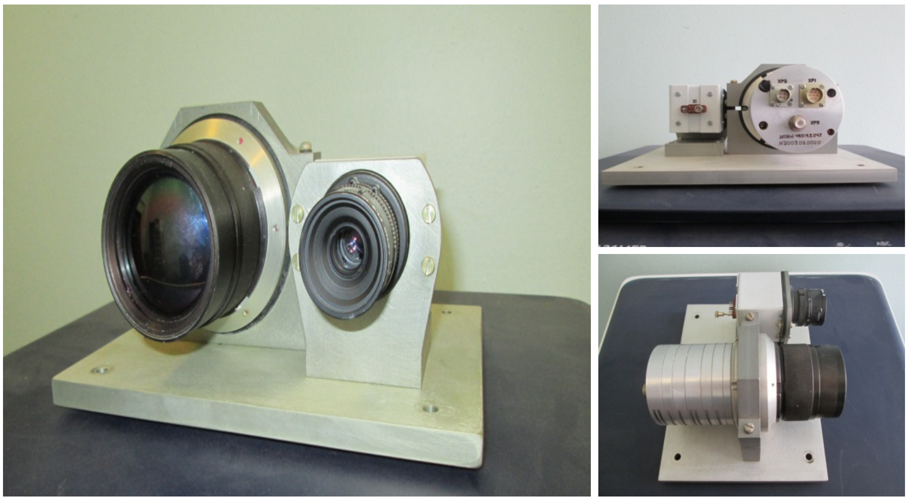

Fig. 2. A TV module “Tompson”

Fig. 3. A spectral optical module “SOM”

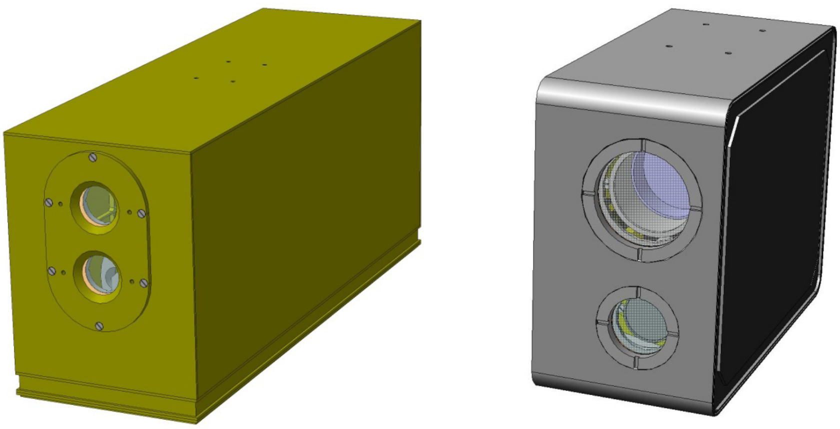

Fig. 4. Air-tight units of the optical devices to control the surface of the ISS in UV, IR and visible spectrum ranges.

Nowadays the components of the OEU and the "BAR-ARM" equipment are at various development stages. In particular, television modules of visible and infrared ranges have passed preliminary (factory) tests, and the vacuum monitoring system – interdepartmental tests.

The successful completion of the "BAR-ARM" equipment development will allow one to fulfill the most effective method of extravehicular search of air leakage places from the ISS pressurized compartments.

References

1. Tarasov V.V., Yakushenkov Yu.G. *Infrakrasnye sistemy "smotryashchego" tipa* [The IR Systems of the Image Spatial Sampling Type]. Moscow, Logos, 2004, 444 p. (in Russian)

2. Nesmelova I.M., Andreev V.A. Materialy dlya IK priemnikov izlucheniya, al'ternativnye CdHgTe [The Materials for the IR Detectors Alternative to CdHgTe]. *Opticheskiy zhurnal* [Journal of Optical Technology]. 2007, Vol. 74, No. 3, pp. 90-82. (in Russian)

3. Parvulyusov Yu.B., Soldatov V.P., Yakushenkov Yu.G. *Proektirovanie optiko-elektronnykh priborov* [Optical-Electronic Devices Engineering]. Moscow, Mashinostroenie, 1990, 425 p. (in Russian)

4. Pronin Yu.S., Plastinin Yu.A., Epishkin Yu.A., Shubralova E.V. Opredelenie oblika i struktury kompleksa instrumental'nykh sredstv poiska mest razgermetizatsii korpusa KS na baze priemlemykh diagnosticheskikh priznakov s uchetom etapnosti razmeshcheniya na bortu [The Determination of the Image and Structure of the Integrated Tool Set for Searching the Depressurization Places of the Spacecraft Body Based on the Admissible Diagnostic Signs Taking into Account the Stages of Placing on the Board]. FGUP "TsNIIMASh", NTO No. 851-5074/97-4124-12, NIR "Bar", 1999. (in Russian)

5. Epishkin Yu.A., Klepatskiy A.R., Kopyatkevich R.M., Mishin G.S., Novikov S.B. Issledovanie istecheniya strui v vakuum i temperaturnykh poley v zone mikrotechi v obolochke germootseka kosmicheskogo apparata [The Study of Stream Flow to Vacuum and the Temperature Filed in the Microleak Zone in the Pressurized Compartment Envelope of the Spacecraft]. *Kosmonavtika i raketostroenie* [Cosmonautics and Rocket Engineering], No. 23, TsNIImash, 2001. (in Russian)

ROCKET-SPACE DEVICE ENGINEERING AND INFORMATION SYSTEMS
Vol. 3, Iss. 2, 2016, pp. 54–59

The Information-Measuring System for Space Technology Monitoring

A.S. Shchevelev[1], V.V. Kikot, A.Yu. Udalov

[1]candidate of engineering science
Joint-Stock Company "Research institute of physical measurements", Russia

e-mail: persivald87@gmail.com, inbox@post.su, udaaleksandr@rambler.ru

Abstract. The purpose of the research was to validate the choice of fiber-optic measuring instruments for space technology. It is shown that the information-measuring system meets the requirements of the system being operated in the special conditions of rocket and space engineering and of the objects of the ground space infrastructure. In addition, the task was to research the fiber-optic information-measuring system to determine the metrological characteristics and further evaluation of the system efficiency. The developed information-measuring system includes a fiber-optic strain and temperature sensors. The sensing tip of the fiber forms fiber Bragg gratings (FBG). The temperature and strain readings are obtained by measuring the shift of the resonance FBG wavelength by the built-in spectrum analyzer. The results of the study showed that the sensitivity of the FBG was 11.2 pm /°C for the positive range (from 25 to 300 ° C) and 9.1 pm /°C - for the negative temperature range (from -80 to 25 ° C). The deformation ratio of FBG in the range up to 1200 μm (0.012 μm) was $K = 0.6 \pm 0.3[1/\mu\varepsilon]$. The comparison of the calculated and experimental data showed minor discrepancy between the predicted and experimental values, which confirms the correctness of the constructive decision and system efficiency of the developed information-measurement system.

Keywords: fiber Bragg grating, information-measuring system for monitoring, measuring cell, sensitivity

Introduction

The definition of the measurements occurring inside the technically difficult objects is of interest for various science fields. Among fiber-optical measuring systems one of the most widespread types are systems on the basis of sensors with Bragg gratings.

Sensors with Bragg gratings, as well as other fiber optic sensors (FOS), have a number of advantages, which favourably distinguish them from the sensors constructed on other physical principles. The main of them are the following: small weight and small dimensions of sensitive elements caused by the small diameter of the very optical waveguide (~100 μm); high reliability and reproducibility of measurements caused by stability of the used registration methods of optical radiation, including application of spectral methods; high fire safety caused by absence in designs of sensitive elements of electric currents and the heated areas and also a possibility of using non-flammable substances; high dielectric durability – tension of electric breakdown of quartz glass is ~10 kV/mm (20 °C) and ~2.5 kV/mm (500 °C); possibility of carrying out the multipoint and distributed measurements, including with using spectral and spatial multiplexing of the sensitive elements located in one or in several optical fibers.

The FOS sensitive element, on the basis of which the developed information and measuring system is built, is a fiber Bragg grating (FBG). It is created on optical fiber and is only several millimeters in length. Such sizes are very close to the sizes of point sensors, however, if the set of sensors with FBG is created on different wavelengths and demodulated by the system with temporary division, the total amount of such sensors on one fiber is limited by the width of a source range and a radiation detector. Up to one hundred sensitive elements with FBG for the creation of the distributed system intended for measurement both deformations and temperatures can be built on one fiber.

In fact, there is no object of control or production, which would not be affected by deformation and temperature loads. In this regard, the developed system is especially important and up-to-date in the field of monitoring of products of space equipment.

The operation principle of the converters with FBG

During the development efforts in Joint Stock Company "Research institute of physical measurements" development of the distributed microoptoelectromechanical measuring and functional modules providing measurement of temperature and deformation of the basic bearing designs of products of the missile and space equipment and objects of ground infrastructure (IFMOT and IFMOD) is conducted.

The design, formation methods, and the basic operation principles of FBG are described in [1-3]. The most important property of FBG is narrow-band reflection of optical radiation, which relative spectral width can make 10^{-6} and less. The radiation extending on optical fiber is possible to present in the form of combinations of its own modes: directed and radiating. If there is no disturbance in optical fiber, the modes extend without interaction with each other.

The structure of FBG is built in such a way to provide necessary resonant interaction between the chosen modes of an optical fiber. Interaction of modes in an optical fiber is usually described by means of the theory of the bound modes [2], where it is supposed that on a certain wavelength only two modes meet a condition of phase synchronism and can transfer effectively each other energy. FBG connect the main mode of an optical fiber with the mode extending in an opposite direction. Two modes interact on a uniform lattice of refractive index, that is on structure, in which the refractive index periodically changes with the constant period of L, if a condition of a phase synchronism is satisfied:

$$\beta_2 - \beta_1 = 2\pi N / \Lambda \quad (1)$$

where b1 and b2 are the propagation constants of the describing modes, N is an integer characterizing an order, where an interaction between modes is performed. Mode propagation constant is expressed by the ratio

$$\beta_i = 2\pi n_{eff}^i \big/ \lambda \quad (2)$$

where n_{eff}^i is an effective refractive index if the i-th mode, l is a wavelength in a vacuum.

Types of intermode interaction for N = 1 are given in Fig. 1. On a vertical axis the effective index of refraction of modes OV, where n_{co}, n_{cl} and next are the indices of a core refraction, cover and external environment respectively is laid. The positive and negative directions of a vertical axis characterize the modes of optical fiber extending in relation to initial main mode of HE11 in the direct and return directions respectively. Dispersion curves for the modes of the core ($n_{ext} < n_{eff} < n_{co}$) and cover

($n_{ext} < n_{eff} < n_{cl}$) are shown. A shaded area corresponds to the radiating modes of OB. 1 and 2 dashed lines are the values $n_{eff}^{co} - \lambda/\Lambda$ for the gratings with a small L_{BG} £ 1 μ and bigger (long-period fiber gratings) L_{LPG} ³ 100 μ periods respectively (n_{eff}^{co} is an effective refractive index of the main mode).

Crossings of curves with dispersive curves of various modes set lengths of waves, on which the condition of phase synchronism is satisfied (1)

$$\lambda_{BG} = 2n_{eff}^{co}\Lambda_{BG} \tag{3}$$

The properties of this reflection depend on the grating parameters. For a uniform grating of length L reflection coefficient R on the resonant wavelength of l_{BG} is expressed as $R = th^2(k_{BG}L)$, where $k_{BG} = pDn_{mod}h_{BG}/l_{BG}$ is coupling coefficient. Dn_{mod} is a modulation amplitude in the first order of decomposition of a stroke form into the Fourier series, a part of power of the main mode, which extends on a core of an optical fiber of radius of *a*. E_{co} is an amplitude of the electric field of the main mode.

Dependence of the Bragg wavelength on temperature differential can be written down as:

$$\Delta\lambda_{\mathbf{BG}} = \lambda_{BG}(\zeta + \alpha)\Delta T \tag{4}$$

where $\alpha = \left(\frac{1}{\Lambda}\right)\left(\frac{\partial\Lambda}{\partial T}\right)$ is a thermal coefficient ($0.55 \cdot 10^{-6}$ °C^{-1}); $\zeta = \left(\frac{1}{n}\right)\left(\frac{\partial n}{\partial T}\right)$ is a thermooptical coefficient ($8.6 \cdot 10^{-6}$ °C^{-1}) for a quartz core of the optical fiber with alloying by germanium.

For simultaneous measurement of deformation provided that temperature coefficients for them significantly differ from each other, a system of the equations

$$\begin{pmatrix} d\lambda_{BG}^1/\lambda_{BG}^1 \\ d\lambda_{BG}^2/\lambda_{BG}^2 \end{pmatrix} = \begin{pmatrix} K_\varepsilon^{01} & K_T^{01} \\ K_\varepsilon^{02} & K_T^{02} \end{pmatrix}\begin{pmatrix} d\varepsilon \\ dT \end{pmatrix} = \overline{K}\begin{pmatrix} d\varepsilon \\ dT \end{pmatrix} \tag{5}$$

has a determinant other than zero ($\det(\overline{K}) \neq 0$) and can be solved analytically relative to $d\varepsilon$ and dT:

$$\begin{pmatrix} d\varepsilon \\ dT \end{pmatrix} = \overline{K}^{-1}\begin{pmatrix} d\lambda_{BG}^1/\lambda_{BG}^1 \\ d\,\lambda_{BG}^2/\lambda_{BG}^2 \end{pmatrix} \tag{6}$$

Thus, when using two FBG (for measurement of temperature and deformation) the task is reduced to that the spectral response of gratings is various at change of temperature or at the application of deformation (compression / stretching force), the size of which is required to be measured.

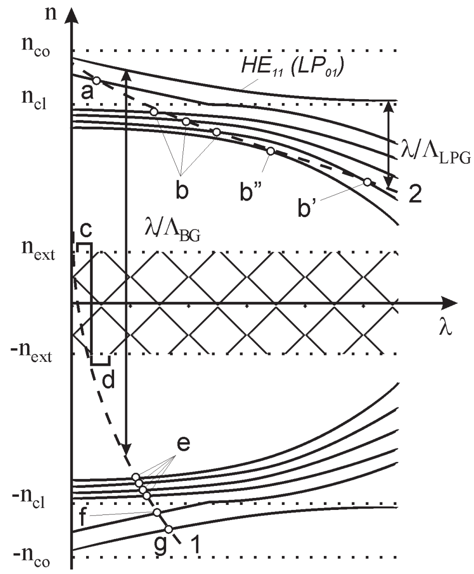

Fig 1. The chart showing the performance of a condition of phase synchronism between the main mode of HE_{11} (LP_{01}) and other modes of optical fiber.

Experimental studies

The block diagram of the monitoring measuring system is given in Fig. 2.

The source of radiation forms a light stream with wavelength in the range of 1550 … 1590 nm, which extends on an optical fiber. A spectrum analyzer is used as a radiation receiver. This analyzer is necessary for display and research of reflection ranges of the Bragg wavelengths. Measurement of reflection ranges was carried out on the Bragg wavelength of 1550±0.5 nm (for measurement of temperature) and 1538±0.5 nm (for deformation measurement) with reflection coefficient of 70% in normal climatic conditions.

Experimental studies on influence of the increased temperature in the range from 25 to 300 °C, the lowered temperature from -80 to +25 °C (Fig. 3 and 4) are conducted. At influence of the increased and lowered temperature, the shift of the Bragg wavelength towards increase and reduction respectively is observed. Load also leads to the shift of the Bragg wavelength of the measuring functional optical module of deformation.

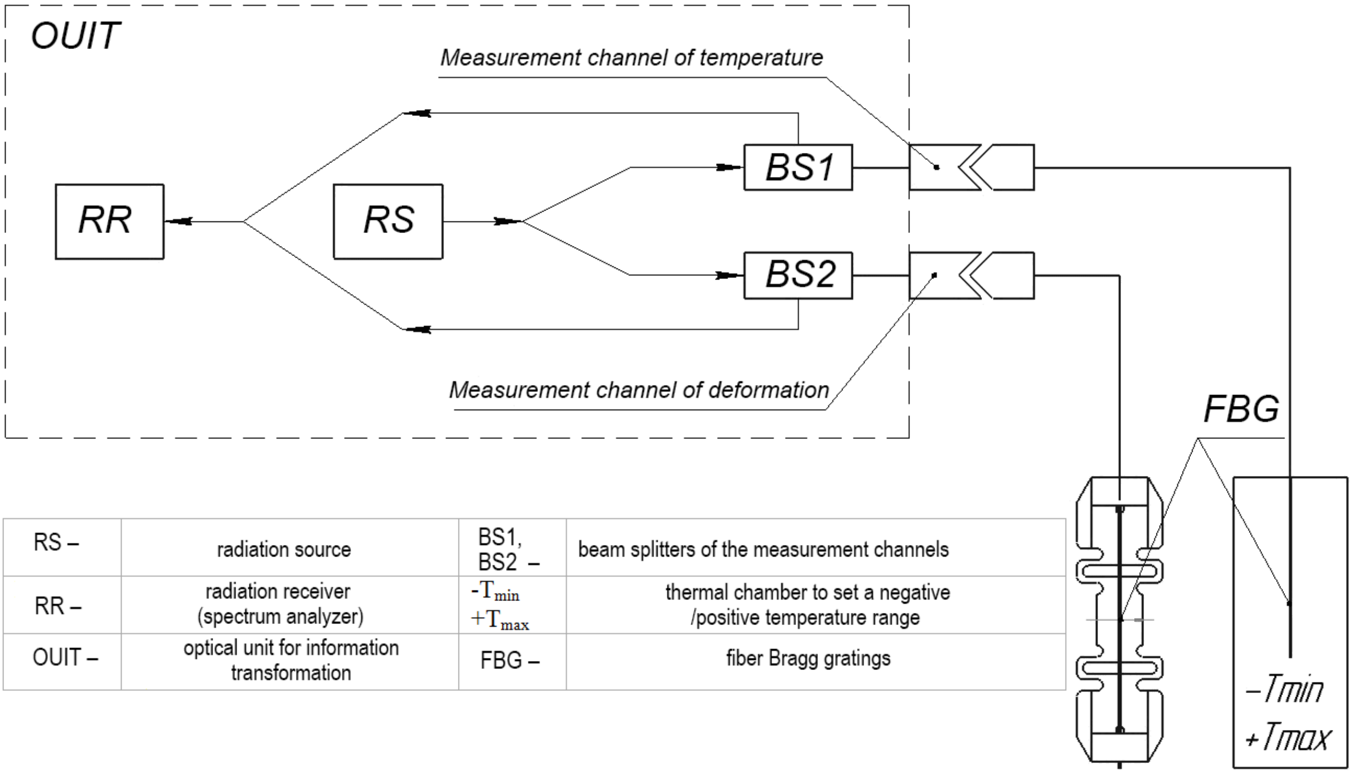

RS –	radiation source	BS1, BS2 –	beam splitters of the measurement channels
RR –	radiation receiver (spectrum analyzer)	$-T_{min}$ $+T_{max}$	thermal chamber to set a negative /positive temperature range
OUIT –	optical unit for information transformation	FBG –	fiber Bragg gratings

Fig. 2. A block diagram of the information and measuring system

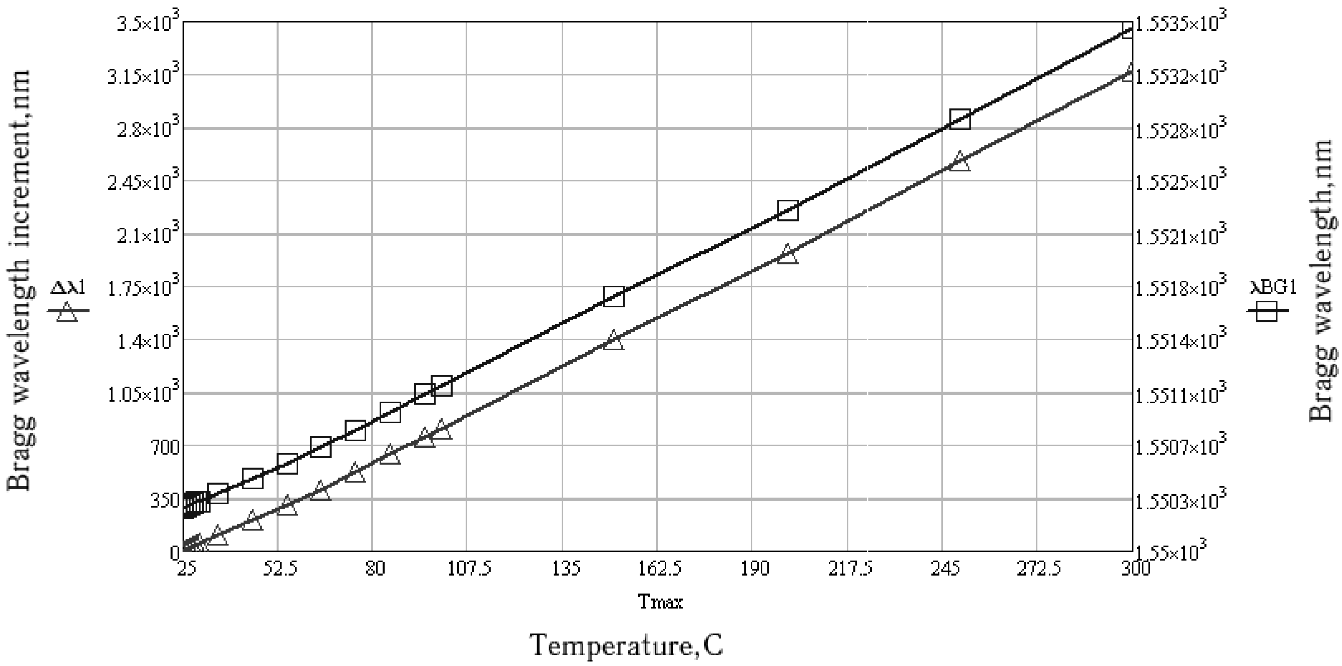

Fig. 3. Functional dependence of shift of the Bragg wavelength $\Delta\lambda_{\mathbf{BG1}}$ on temperature in the positive range

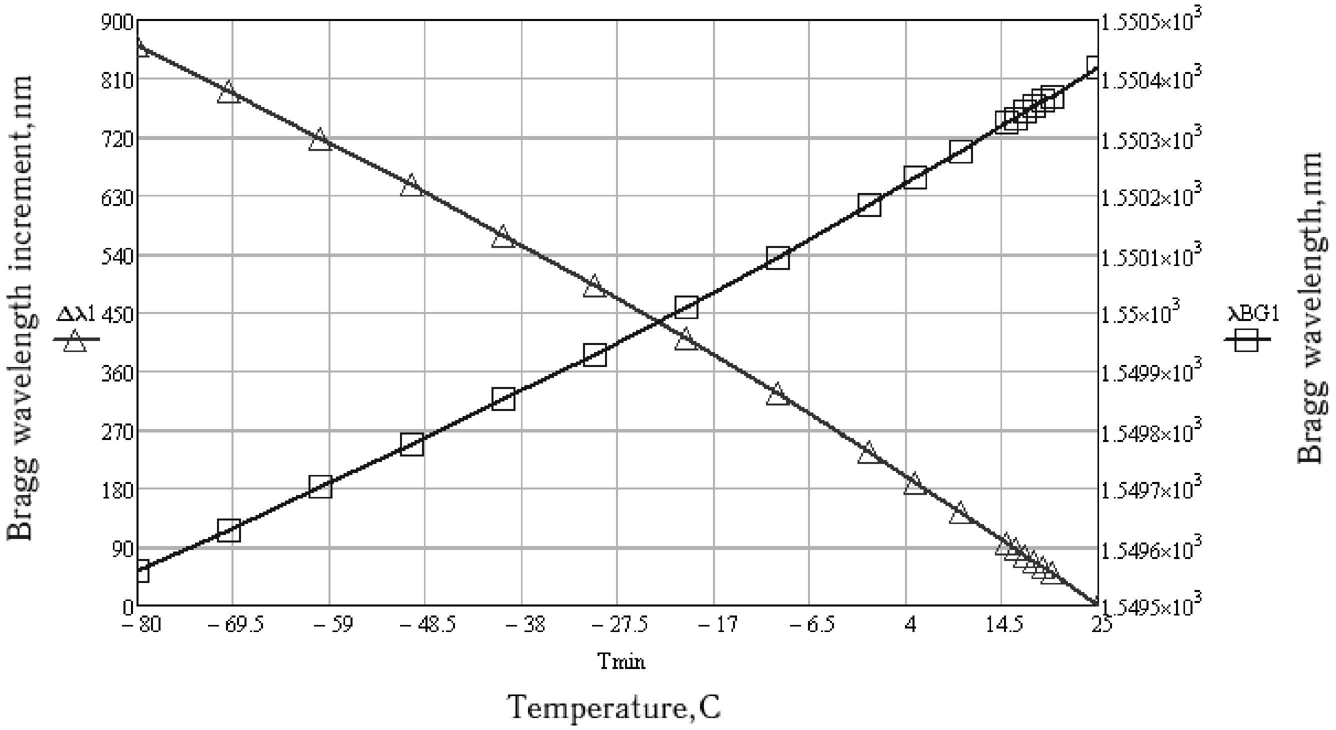

Fig. 4. Functional dependence of shift of the Bragg wavelength $\Delta\lambda_{\mathbf{BG1}}$ on temperature in the negative range

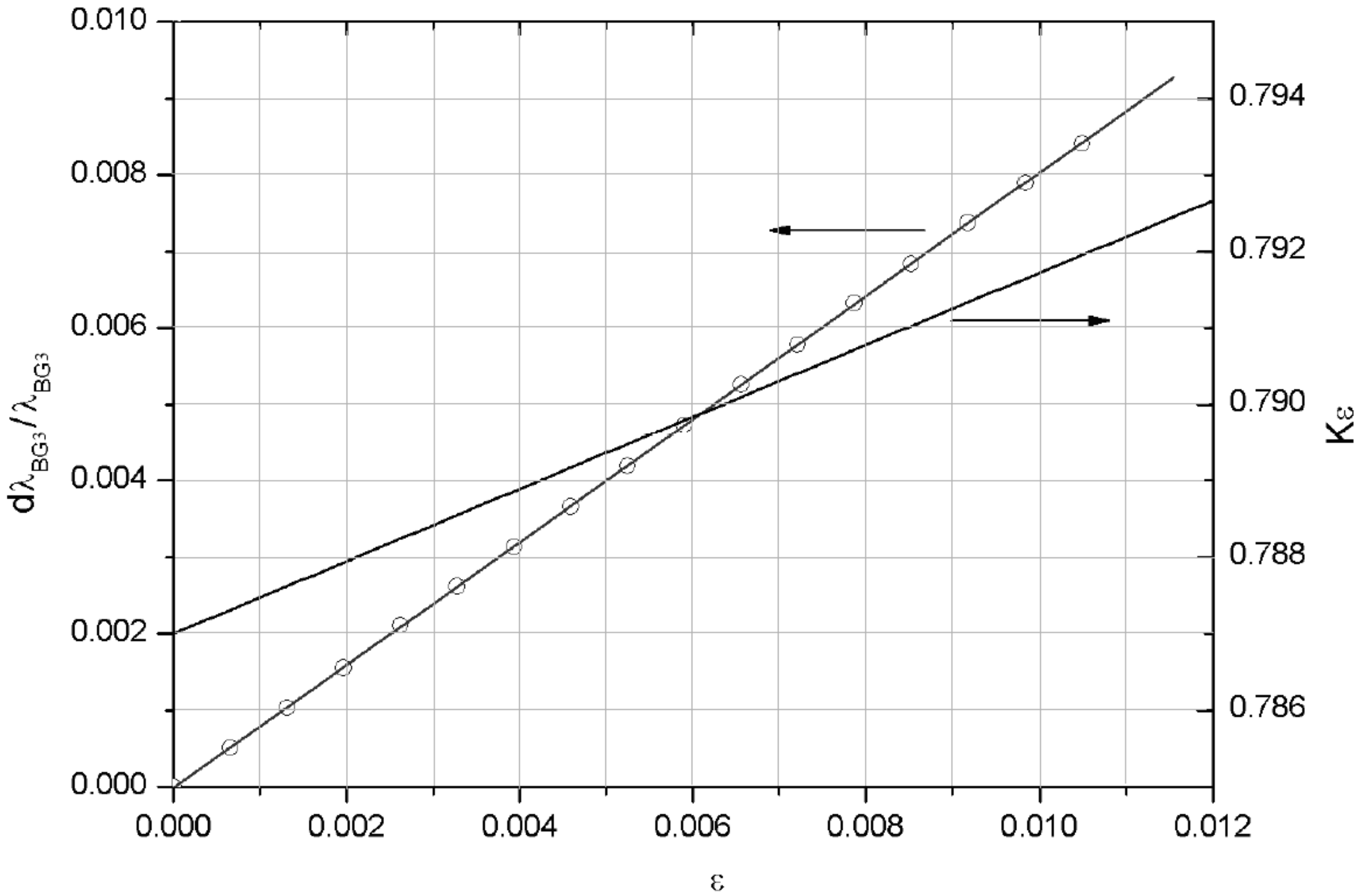

Fig. 5. Dependence of relative change of the Bragg wavelength $\Delta\lambda_{BG2}$

Dependencies $\Delta\lambda 1=f(T_{max})$ and $\lambda_{BG1}=f(T_{max})$ have a linear character in all temperature range (Fig. 3). According to the formula (4), sensitivity has made 11.9 pm/°C. The analysis of experimental dependence $\lambda_{BG1}=f(T_{max})$ has shown that sensitivity of the module in the positive range is 11.2 pm/°C. Divergence of experimental and settlement data is insignificant. As well as in case of the increased temperatures, dependences $\Delta\lambda 1=f(T_{min})$ and $\lambda_{BG1}=f(T_{min})$ have a linear character in the negative temperature range (Fig. 4). Theoretically, according to the formula (4), sensitivity is 11.9 pm/°C. The analysis of experimental dependence and $\lambda_{BG1}=f(T_{min})$ has shown that sensitivity of the sensor in the negative range is 9.1 pm/°C.

Measurement of deformation represents a certain complexity, since it demands high stability of fixing knots of a measuring part of optical fiber in the course of measurements. The dependence of relative change of wavelength on the deformation attached to optical fiber measured at normal climatic conditions is given in Fig. 5.

Experimental value of deformation coefficient $K = 0.6 \pm 0.3[1/\mu\varepsilon]$ $(K\varepsilon = 0.800 \pm 0.003[ppm/\mu\varepsilon])$ corresponds to the value of deformation coefficient received at imitating modeling $K\varepsilon = \dfrac{d\lambda_{BG2}/\lambda_{BG2}}{d\varepsilon} = 0.78[ppm/\mu\varepsilon]$.

Conclusions

The studies have shown that transformation functions $\lambda_{BG1}=f(T_{max})$ and $\lambda_{BG1}=f(T_{min})$ have a linear character. Sensitivity of IFMOT is 11.2 pm/°C for a positive range and 9.1 pm/°C for a negative range of temperatures. For IFMOD deformation coefficient is $K = 0.6 \pm 0.3[1/\mu\varepsilon]$.

Comparison of the indicators received at imitating modeling and experimental studies has revealed their practical full convergence that confirms efficiency of the developed information and a measuring system.

References

1. Kul'chin Yu.N. *Raspredelennye volokonno-opticheskie izmeritel'nye sistemy* [Distributed fiber-optic measuring systems]. Moscow, Fizmatlit, 2011, 272 p. (in Russian)

2. *Fiber Bragg Grating Sensors: Recent Advancements, Industrial Applications and Market Exploitation*. Eds. Cusano A, Cutolo A. and Albert J. Bentham Science Publishers, 2011.

3. *Bragg Gratings, Photosensitivity, and Poling in Glass Fibers and Waveguides: Applications and Fundamentals (BGPP).*

4. Kashyap R. *Fiber Bragg Gratings.* Academic Press, 1999.

5. Shu X., Allsop T., Gwandu B., Zhang L., Bennion I. *High-Temperature Sensitivity of Long-Period Gratings in B-Ge Codoped Fiber*. IEEE Phot. Lett., 2001, Vol. 13, No. 8, pp. 818–820.

6. Vasil'ev S.A., Dianov E.M., Medvedkov O.I., Protopopov V.N., Kostantini D.M., Iokko A., Limberger Kh.G., Salate R.P. *Kvantovaya elektronika* [Quantum Electronics], 1999, Vol. 26, No. 1, pp. 65-68. (in Russian)

ROCKET-SPACE DEVICE ENGINEERING AND INFORMATION SYSTEMS
Vol. 3, Iss. 2, 2016, pp. 60–65

The Analysis of the Potential for Applying the CCSDS Recommendations with a View to Improve Technical Characteristics of the Domestic Space Radio Links Intended for Transmitting Telemetry from Objects of Different Purposes

V.L. Vorontsov

candidate of engineering science
A branch of Joint Stock Company "United Rocket and Space Corporation"–"Institute of Space De-vice Engineering" ("ORKK"-"NII KP"), Russia

e-mail: a762642@yandex.ru

Abstract. The paper presents the analysis of the opportunities to use the CCSDS recommendations for building the domestic radio links to transmit telemetry in the absence of the required domestic teleme-try standards. Advantages and problematic issues are highlighted related to applying the CCSDS rec-ommendations for the domestic practice. The most important features of the CCSDS recommendations in force are related to integrating operations with data (signals) and combining data (signals) with a view to implement certain functions ensuring significant advantages and employed for developing space radio links. Good prospects apperar to get these advantages when building domestic space radio links. However, consideration should be given to specific features of domestic space radio links (there are notable differences) and to the procedure for applying the CCSDS recommendations (particularly, using the patented technical solutions).

Keywords: space agency, CCSDS recommendations, space radio link, telemetry, modulation tech-niques, noiseless coding techniques

The significance of the CCSDS recommendations (technical solutions given in the CCSDS documents) when solving practical tasks of the domestic telemetry, in particular, the coarse (field) of SLS is increasing (CCSDS – Consultative Committee for Space Data Systems; SLS – Space Link Services). This tendency is caused by the substantial improvement of the space radio links opportunities during the realization of these recommendations. In addition, a problem of the valid choice of the reasonable technical solutions in the CCSDS recommendations becomes urgent due to the constant growth of the CCSDS recommendations number, their constant correction and absence of the necessary domestic telemetry standards.

The aim of the paper is to determine the general approaches to the choice of the reasonable technical solutions contained in the CCSDS documents related to the space radio links used for transmitting telemetry data from the objects of various purpose being telemetered.

Usually, in the CCSDS practice, initiating new technical solutions by the space agencies and formulating the CCSDS documents provisions corresponding to them are caused by the following reasons:

– new tasks of the space agencies-members of the (relevant recommendations are usually written in the Blue Books; surveys are written in the Green Books; explanations of the provisions are in the Blue Books; and best practices are in the Purple Books);

– "rigid" requirements, which significance is expected in future (they are written in the Orange Books, or Experimental Specifications);

– necessity in coordination (correction) of the separate provisions of the recommendations (for example, if some contradictions are revealed) can arise at any development stage of the existing recommendations.

Under such conditions, following approaches regarding solving organizational and technical issues exist:

– ensuring succession. For instance, using the modulations that provide carrier suppression is more profitable from the energy point of view than to use a residual carrier. However, since many space agencies employ ground stations operating with the residual frequency, where they invested great sums of money (rec. 2.3.1 [1], rec. means a recommendation), so, according to the CCSDS recommendations [1], the phase-locked loop (PLL) means of the receiver used for work with both residual and suppressed frequencies can be applied;

– complexing the methods of operations on the data (signals) and of the data (signals) with allowance for their mutual dependence and variety of space radio links, as well as changing conditions of applying radio links (for example, changings in time of the jamming situation, changing of the distance between the source of information and the recipient);

– coordination of the corrected CCSDS documents provision with space agencies-members of the CCSDS to provide mutual support.

However, at times, separate technical solutions or their combinations and restrictions (requirements) corresponding to them can be applied in solving other tasks (the tasks, not initiated for CCSDS). i.e., they turn out to be universal in some way. Moreover, there is a tendency to universality (diversification). It reveals itself in complexing the methods of operation on the data (signals) and of the data (signals) to fulfil certain functions used for solving the building tasks of a space radio link.

A confirmation of the complexing should be further examined.

In case of carrier suppression, one of the following modulation method should be used (rec. 2.3.2A [1]):

– (filtered) BPSK,

– (filtered) QPSK,

– filtered OQPSK (rec. 2.4.17A and 2.4.17B [1]),

– GMSK (rec. 2.4.17A and 2.4.17B [1]),

when a system with a residual carrier surpasses the restrictions on power flux density (PFD) onto the Erath's surface providing the following values of the speed to transmit the symbols of the space-to-ground communication channels are not exceeded:

– 2 Msymb/s in the bands 2 and 8 GHz;

– 10 Msymb/s in the band 26 GHz;

– 20 Msymb/s in the band 32 GHz.

If the above-mentioned modulation methods are used (that provide carrier suppression), so data randomization should be used, as it is determined in rec. 2.3.2A [2].

It should be noted that at the symbol bit rate not more than 2 Msymb/s and frequency band 2200–2290 MHz, the BPSK methods with filtration, OQPSK with filtration and GMSK relate to the modulation methods ensuring carrier suppression. The OQPSK methods with filtration and GMSK therewith are the most preferred. At the symbol bit rate more than 2 Msymb/s and frequency band 2200–2290 MHz, the OQPSK methods with filtration and GMSK are also recommended.

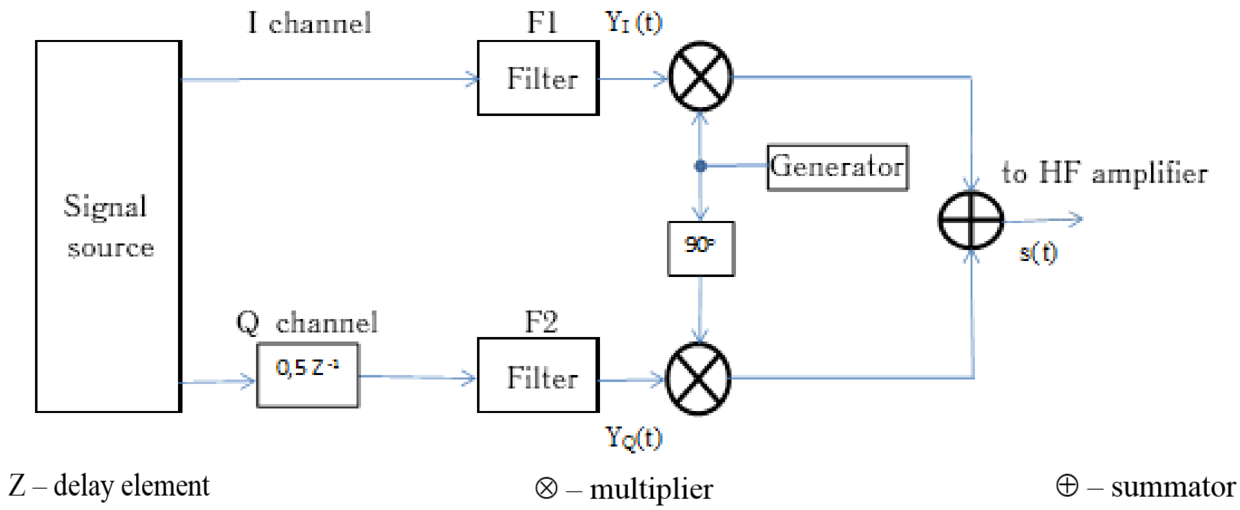

Fig. 1. A block diagram of the Q-I modulator with filtration of the main frequency band

In its turn, the OQPSK methods with filtration and GMSK are built according to the complexing principle [3]. As the OQPSK-modulator circuit (Fig. 1) [3] shows, that certain actions on the signals precede the carrier frequency modulation. Common-mode and quadrature signals are filtered by means of smoothing filters F1 и F2, and a signal delay in the Q channel is a half of the durability of the symbol interval T_S to create a phase shift between the I and Q channels. Signals of the I and Q channels on the output of the signal source are formed in the NRZ format.

VCM and ACM, presented in the DVB-S2 standard [4], aimed at increasing the resistance to jamming, are connected with complexing of the modulation methods and antinoise coding.

The essence of the Adaptive Coding and Modulation (ACM) is in well-timed change of the modulation type and (or) the speed of the antinoise code dependently on the jamming situation state evaluated on the recipient's side according to signal-to-noise ratio. In such conditions, parameters combinations of the modulation and antinoise coding, structure and meaning of the commands formed on the recipient's side for correct adjustment of the modulator and coder are determined a priori. The data formed on the information source's side for further sending to the recipient incorporate reference data on setting of the modulator and coder that enables one automatically change the adjustment of the modulator and decoder on the recipient's side. Change in the modulator and coder settings (as well as demodulator and decoder respectively) is carried out without loss of information.

In case of Variable Coding and Modulation (VCM), well-timed change of the modulation type and (or) the speed of the antinoise code is performed by the program.

Methods of the antinoise coding and conditions for their fulfilment are also connected to complexing (Fig. 2) [2].

Apart from showing the nature of the above-mentioned complexing, the results given (despite the fact that there are not many examples) show quite full that substantiation of the operation methods selection over the data (signals) and features of the data (signals) when building a certain space radio link is connected not to the obvious choice of the relevant CCSDS recommendations (providing the stated radio link correspond to the CCSDS requirements).

There are other aspects as well, regarding building a space radio link, connected to the necessity to fulfill specific CCSDS requirements.

In particular, there are the requirements of the electromagnetic capability (EMC) through limitation of the spurious emission level.

Following the CCSDS recommendation (rec 2.4.16 [1]), total power of any spurious emission should not exceed -60 dBc (dBc is measured relatively to the total power of the unmodulated carrier).

One of the methods to meet this requirement is to eliminate a symbol asymmetry of the digital signals in the modulator input. The essence of the CCSDS recommendation (rec. 2.4.8 [1]) is such: the symbol asymmetry should not exceed 0.2% (the recommendation gives the description of the parameter essences "Symbol asymmetry", i.e., a methodology to evaluate the asymmetry evaluation is given).

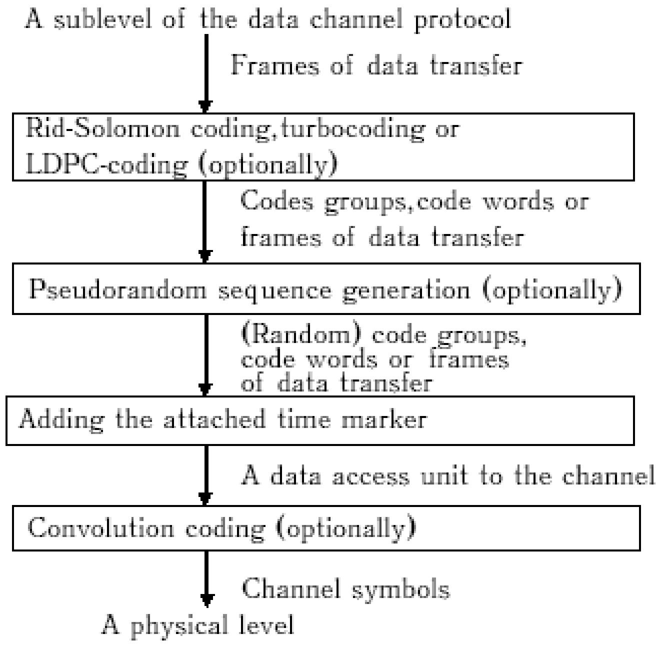

Fig. 2. An internal arrangement of the sublevel for synchronization and coding channels of the information source

Another way is to eliminate phase and amplitude instability. In the CCSDS recommendation (rec. 2.4.12A [1]; the BPSK/(O)QPSK/GMSK modulators, suppressed carrier, space-to-ground channels, category A) it is written the following: for the quadrature modulation when speed and power for data transfer for (I) channels and quadrature (Q) channels are the same, phase and amplitude instability are caused by mutual interference of channels due to impossibility to support interchannel orthogonality or because of imperfect tracking of the carrier. This unfavorably affects the system performance. Its essence is the following: instability of the modulator phase should not exceed 5 degrees, and amplitude instability should not exceed 0.5 dB between the constellation points.

Since in the basis of the recommended CCSDS modulation methods (in particular, the above-mentioned BPSK, QPSK, OQPSK, GMSK methods) there are phase manipulations methods, so corresponding specific requirements are aimed at eliminating a phase ambiguity of signals either through synchromarker or through the modulation insensitive to polarity (rec. 2.4.11 [1]).

Necessity to perform the above-mentioned (and other) specific requirements evaluating according to the accepted CCSDS techniques (type of the technique for evaluating the symbol asymmetry) makes certain limitations concerning the choice of the rational technical solutions from the CCSDS recommendations when building a space radio link.

At the same time, several CCSDS recommendations have descriptions of the limitations that significantly increase the opportunities of their structuring, create favourable conditions for their further consideration (or ignoring) at the early stages of the analysis. Such limitations are the following:

– altitude from the Earth where the tasks are solved (less than 2.0 ´ 10^6 km relate to the A category and not less than 2.0 ´ 10^6 km relate to the B category);

– data transfer direction (signals) (space-to-ground and ground-to-space);

– entities of the sematic composition of the signals (data) of the radio link [only telemetry data, telemetry data and telecommands; telemetry data and signals to measure the range (as described in [5], [6] or [7]); radiometry; etc.];

– separate software and hardware tools (SHT) that are the parts of the radio link [onboard means of spacecraft (SHT of an object being telemetered), ground station, transponder and so on];

– etc.

Several restrictions (additional to the listed above) are connected with the peculiarities of the development of the domestic telemetry. Thus, a usually typical radio line for the domestic practice is to be applied only for telemetry data transfer. Under such circumstances [in particular, for launchers], its combining with telecommands or signals transfer to measure the range (as described in [5] or [6]) is not carried out. All things considered, in the nearest future an autonomous flight control of a carrier-rocket will exist. Moreover, determination of its movement parameters by means of the customer navigation equipment (CNE) will exist as well. With such an approach, necessity in realization of the corresponding technical solutions described in the CCSDS recommendations does not arises [1] and completely in [5] and [6].

It should be noted that the CCSDS recommendations being in force should not be obligatory met. In the foreign practice, the provisions of the corresponding practice is the guide to action. They are formed not only based on the CCSDS recommendations, but also taking into consideration other documents, in particular, the ITU radio link regulations, SFCG frequencies distributions (ITU – International Telecommunications Union, SFCG – Space Frequency Coordination Group). That is why, for example, the ECSS-E-ST-50-05C recommendations of the ESA [8], regarding radio frequencies and modulation, is not a copy of the CCSDS recommendations [1].

There are no necessary domestic telemetry standards (see appendixes on the development of the standardization process of the domestic telemetry concerning rocket and space and rocket engineering [9]). If there are no any, it is possible to use CCSDS recommendations when developing SOW (Statement of Work) for building a space radio link. One should take into account the following condition peculiarities of the CCSDS practice for the domestic practice:

– mutual support (in case of joint projects with other space agencies, for example, with NASA and ESA);

– considerable benefits from using technical solutions given in the provisions of the CCSDS documents (for instance, significant improvement of the data); the following aggravating circumstances therewith appear:

a) the CCSDS requirements recommendations badly agree with the existing domestic practice (see the analysis given above regarding the entities of the CCSDS recommendations);

b) necessity in getting the right to lawful fulfillment of separate technical solutions, in particular:

1) a number of technical solutions given in the CCSDS recommendations being in force is patented, and one needs to get a license (see, for example, Sections 1.7, B3.1 and B3.2 of Appendix B [2] on turbocoding and coding by means of low density codes with control to evenness; Section 1.8 and Appendix B [4] on the DVB-S2 technology, as well as Section 3.4.1.7 [10] with the set approach to the patented technologies);

2) necessity in getting a right to the usage of the PN codes. There is a SNIP agreement between three agencies-members of the CCSDS (NASA, ESA and JAXA), which use the PN codes named "a family of SNIP codes" (SNIP stands for Space Network Interoperability Panel). Moreover, a new set of codes has been developed that named as "a set of PN codes of the CCSDS" [5];

– using common efforts in smb's interests – as it is accepted in the CCSDS practice – initiating by the Russian side the technical solutions (technologies) for the CCSDS-community (an example of such initiating: CCSDS-community is given a domestic technology for improvement the data reliability based on a more wide usage of the opportunities of the diverse reception [11]). In this case they should be approved by other space agencies (except Roscosmos). Hence, the following problematic issues arise:

a) necessity (expediency) of the joint tasks fulfilment corresponding to these technical solutions should be proved. Otherwise, approval is impossible (approval of the project by the space agency means undertaking the obligations for its funding);

b) to control the chosen technical solutions (to correct corresponding provisions of the certain CCSDS documents), it is necessary to agree specific interests of the Russian part with the technical CCSDS policy, which is very problematic (joint projects are necessary for this, otherwise there is nothing to do but conform);

c) strengths and means to work in the CCSDS to support and develop the relevant provisions of the CCSDS documents in the interests of the Russian part (in the interests of the domestic enterprises of the rocket and space field);

d) a problem of know-how associated with technical solutions, a problem of data confidentiality (for instance, in the military field) is possible. In these cases, the CCSDS-compatibility can turned out to be extremely undesirable.

It should be also noted that technical solutions important for building domestic space radio lines are possible out of the CCSDS recommendations (the developments of the Russian specialists described in the Russian sources can be among them).

Taking everything into account, in the existing conditions when there is a lack of necessary domestic telemetry standards, an essential condition of significance of the CCSDS recommendations when building domestic space radio lines used for telemetry data transfer is improvement of their technical characteristics. When justifying the CCSDS technical solutions (the CCSDS recommendations corresponding to them), it is expediently to take into consideration the peculiarities of the Russian practice for creating space radio links and the set CCSDS procedures for using the CCSDS recommendations.

References

1. Radio Frequency and Modulation Systems—Part 1: Earth Stations and Spacecraft, Recommendation for Space Data System Standards CCSDS 401.0-B-23, Issue 23, Blue Book, Consultative Committee for Space Data Systems, December 2013.

2. TM Synchronization and Channel Coding, Recommended Standard CCSDS 131.0-B-2, Issue 2, Blue Book, Consultative Committee for Space Data Systems, August 2011.

3. Bandwidth-Efficient Modulations: Summary of Definition, Implementation, and Performance, Informational Report CCSDS 413.0-G-2, Issue 2, Green Book, Consultative Committee for Space Data Systems, October 2009.

4. CCSDS Space Link Protocols over ETSI DVB-S2 Standard, Recommendation for Space Data System Standards CCSDS 131.3-B-1, Issue 1, Blue Book, Consultative Committee for Space Data Systems, March 2013.

5. Data Transmission and PN Ranging for 2 GHz CDMA Link via Data Relay Satellite, Recommended Standard CCSDS 415.1-B-1, Issue 1, Blue Book, Consultative Committee for Space Data Systems, September 2011.

6. Pseudo-Noise (PN) Ranging Systems, Recommended Standard CCSDS 414.1-B-1, Issue 1, Blue Book, Consultative Committee for Space Data Systems, March 2009.

7. Pseudo-Noise (PN) Ranging Systems, Informational Report CCSDS 414.0-G-1, Issue 1, Green Book, Consultative Committee for Space Data Systems, March 2010.

8. European cooperation for space standardization. ECSS-E-ST-50-05C – Space engineering – Radio frequency and modulation, July 2008.

9. Artem'ev V.Yu., Vorontsov V.L. O standartizatsii, effektivnosti, tselyakh i stimulakh, kasayushchikhsya razvitiya otechestvennoy telemetrii, otnosyashcheysya k raketno-kosmicheskoy i raketnoy tekhnike [On standartization, effectiveness, aims, and stimuli regarding development of domestic telemetry concerning rocket and space rocket engineering]. «*Trudy MAI*» [Trudy MAI]. 2011, No. 44, pp. 1–15. (in Russian)

10. CCSDS Publications Manual, CCSDS Record, A20.0-Y-3, Issue 3, Yellow Book, Consultative Committee for Space Data Systems, December 2011.

11. Correlated Data Generation, Research and Development for Space Data System Standards CCSDS 551.1-O-1, Issue 1, Orange Book, Consultative Committee for Space Data Systems, July 2015.

ROCKET-SPACE DEVICE ENGINEERING AND INFORMATION SYSTEMS
Vol. 3, Iss. 2, 2016, pp. 66–71

Development of Microwave Monolithic Integrated Circuits of 5 mm Wavelength Range for Application in Promising Space Systems

Yu.V. Fedorov, P.P. Mal'tsev[1], D.L. Gnatyuk[2], O.S. Matveenko[3], D.V. Krapukhin, S.A. Gamkrelidze[4]

[1,4]doctor of engineering science, professor, [2,3]candidate of engineering science
Federal State Budgetary Scientific Establishment Institute of Super High-Frequency Semiconductor Electronics of the Russian Academy of Sciences (IUHFSE RAS), Russia

e-mail: iuhfseras2010@yandex.ru

Abstract. A set of monolithic integrated circuits (MIC) to be applied in the transmitter receiver modules (TRM) with rigid restrictions for the mass-dimensional characteristics and power consumption, and increased requirements to the resistance to the external and special factors, and operating in the frequency range of 57–64 GHz was developed based on nitride heterostructures at IUHFSE RAS. Technical and operational characteristics of the stated products are presented. The developed MIC can be used in severe service conditions and, owning to their functionalities, they can be applied in the communication and control systems of spacecraft.

Keywords: electronic component base, super high frequency, monolithic integrated circuit, nitride heterostructure

Introduction

Creation of the functionally complete range of products of the electronic component base (ECB) meeting to the full extent the requirements of the rocket and space technology for functional parameters, reliability and resistance to radiation is one of the priority problems solved by the entities of a radio electronic complex and the relevant organizations of the Russian Academy of Sciences.

This problem has become very urgent because of the wide use of the import ECB in new samples of space technology (up to 43% of all the range for some satellite systems) and a tough policy of sanctions promoted by the western countries.

The components of the microwave technology belong to the ECB products, which, on the one hand, determine tactical, technical and operational characteristics of modern space systems, and on the other one, are almost unavailable for domestic manufacturers in the international market, since there are considerable restrictions on their export and severe prohibitive measures on distribution of the appropriate technologies.

The list of the main objectives for import substitution of the microwave ECB includes the following:

- creating a scientific and technical base in the field of the microwave devices in providing promising samples of the ground and onboard space systems;
- ensuring technological independence of domestic manufactures and producers of the radio electronic equipment on foreign suppliers of the ECB, special materials, manufacturing process equipment and control and measuring equipment.

The main course of research and development in the field of the microwave technology are [1]:

- producing the optimized heterostructures on the basis of gallium nitride (GaN) and other broadband materials for powerful microwave devices in ultra high, super high and extremely high frequency bands;
- development and introduction of manufacturing techniques of the microwave transistors and monolithic integrated circuits (MIC) on the basis of broadband semiconductor materials (GaN, SiC, InP, polydiamond and graphene), including extremely high frequency (EHF) band (60 … 200 GHz);
- development and introduction of manufacturing techniques of the multipurpose single-crystal microwave MIC ("system on a chip" type), including analog, switching and digital schemes.

Application of the high-integrated multipurpose ECB products is a basis for producing potential low weight dimensional spacecraft (no more than 120–150 kg.) as crucial elements of the space segment for the domestic industry. It is connected with the main tendency of space engineering development at the present stage, which is based on essential expenditures reduction on development, deployment and operation of space based systems through microminiaturization, integration of nanotechnologies and nanoelectronics. Creation of such spacecraft allows one to deploy orbital groups by means of rather inexpensive lightweight carrier rockets that can lead to expenditure reduction on launch services for 10–15%.

Therefore, increase in operating frequencies and level of integration in case of simultaneous support of high resistance to the external and special influencing factors becomes a defining trend in developing the ECB of a very high frequency.

The development results of promising microwave MIC on GaN heterostructures

Federal State Budgetary Scientific Establishment Institute of Super High-Frequency Semiconductor Electronics of the Russian Academy of Sciences (IUHFSE RAS) has developed a frameless MIC set of the 5 mm wavelength range (Fig. 1).

The developed MIC set of 5411 series (the characteristics of the crystals are given below) has a low-noise amplifier (LNA) with a built-in antenna on an input (5411UV01AN) and without antenna (5411UV01N), power amplifier (PA) with a built-in antenna on an output (5411UV02AN) and without antenna (5411UV02N) and signal converter 5411HC01H (SC). It is to be applied as a part of the TRM with rigid restrictions on weight dimension characteristics and power consumption, increased requirements on resistance to external and special factors operating in the frequency range of 57–64 GHz.

Fig. 2 illustrates the microwave parameters of LNA; Fig. 3 shows the microwave parameters of the intermediate frequency amplifier (i-f amplifier).

The specified frequency range of 57–64 GHz has the following advantages:

- makes it possible to work in broadband of frequencies and provides data transmission rate up to 5 Gbit/s and more;

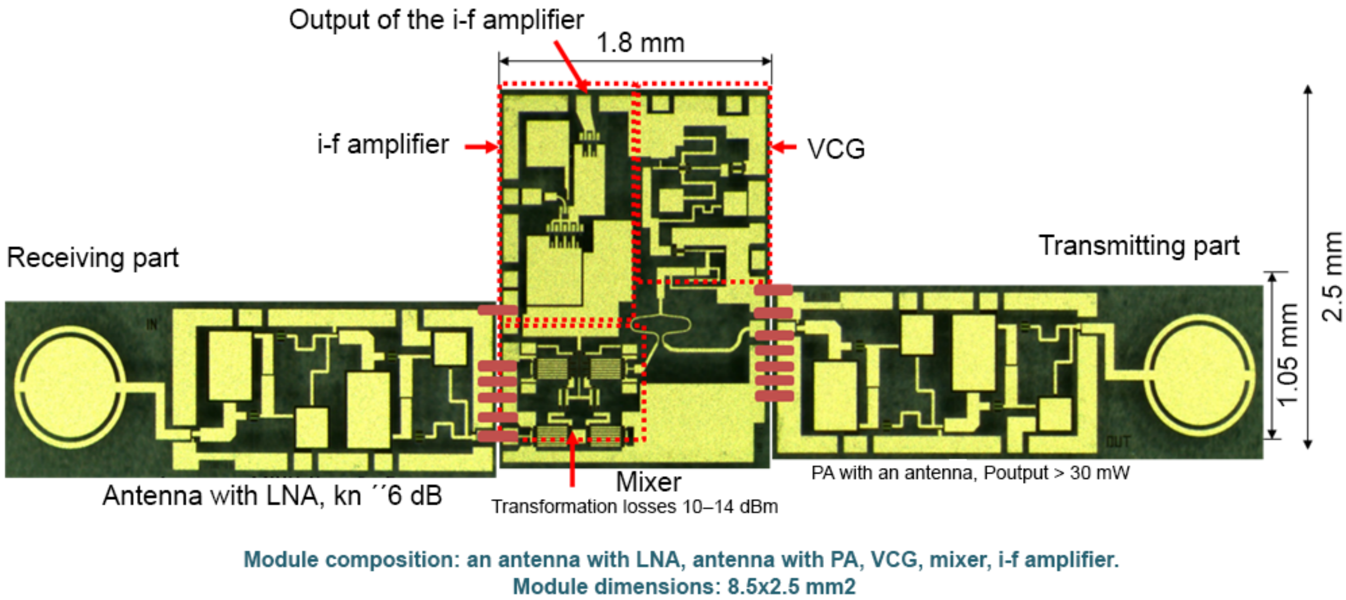

Fig. 1. A TRM for frequency ranges of 57–64 GHz on the heterostructure AlGaN/GaN/Sapphire

- it is characterized by a high degree of absorptivity in the atmosphere that enables one to create the isolated communication channels;

- a small wavelength integrates antennas and whole antenna grids on one crystal.

In the range of 57–64 GHz, it is possible to create transmiter receiver devices of broadband jam-resistance communication providing a high speed and hidden data transfer between electronic subscribers and also to transfer to creation of mobile broadband communication networks 5G [2].

MIC are built on NEMT-transistors formed on nitride heterostructures of AlGaN/GaN with a sapphire substrate of 340 microns thick with technological regulations of 110 nm. It should be noted that using GaN heterostructures provides potential benefits of the developed MIC in comparison with traditional products on gallium arsenide (GaAs) owning to the bigger width of the forbidden GaN zone (3.4 eV), including providing higher electric durability, power, resistance to impact of external and special factors, and integration of elements on a crystal.

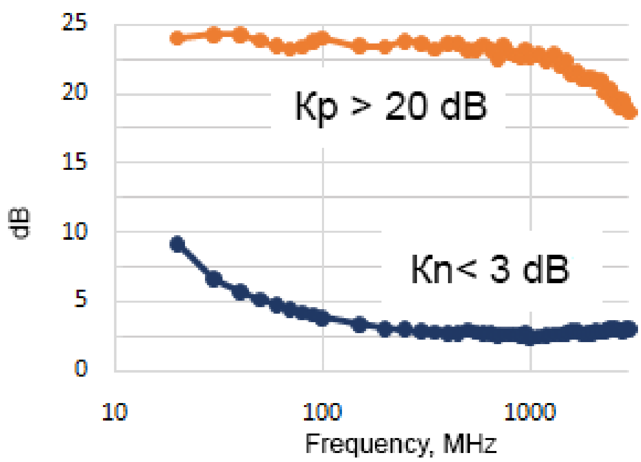

Fig. 3. The microwave parameters of the i-f amplifier

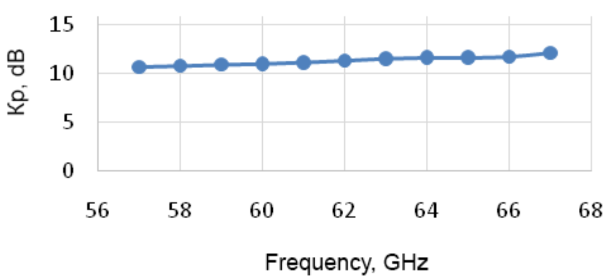

Fig. 2. The microwave parameters of LNA

It is no coincidence that leading European organizations of aerospace industry chose GaN heterostructures as the main technological direction for creating radar equipment of the next generation and its components, including high power amplifiers and TRM.

The main technical characteristics of the developed MIC are presented in Table 1.

Table 1. Technical characteristics of the GaN MIC set

Parameter name, unit of measurement	**Parameter symbol**	**Parameter value**	
		Not less than	**Not more than**
Operating frequency range of the input signal, GHz Lower frequency value Upper frequency value	f_{input}	 64	 57
Low-noise amplifier (LNA)			
Noise factor, dB	k_n		6.5
Transmission factor, dB	k_{trans}	16	
VSWR of input and output	SWR_{Un}		2
Current consumption, mA	I_{cons1}		100
Dimensions of MIC of LNA, mm x mm	S_{LNA}		1.15 x 2.26 ±0.1
Dimensions of MIC of LNA with the antenna, mm x mm*	S_{LNA2}		1.15 x 3.4 ± 0.1
Power amplifier (PA)			
Amplification factor by power, dB	K_p	20	
Output power of PA, mW	P_{output}	100	
VSWR of input and output	SWR_{Un}		2
Current consumption, mA	I_{cons2}		200
Dimensions of MIC of PA, mm x mm*	S_{PA}		1.15 x 2.26 ± 0.1
Dimensions of MIC of PA with the antenna, mm x mm*	S_{PA2}		1.15 x 3.4 ± 0.1
Signal converter (SC)			
Operating frequency range of the output signal of i. f, GHz Lower frequency value Upper frequency value	$f_{i.f}$	 2	 0
Conversion coefficient, dB	K_{conv}	0	15
VSWR of input and output	SWR_{Un}		2
Current consumption, mA	I_{cons3}		100
Dimensions of MIC of SC, mm x mm*	S_{SC}		1.9 x 2.26 ± 0.1
* MIC dimensions are given with allowance for tolerance on the cut line			

The parameters of the products resistance to the influence of climatic and mechanical factors are given in Table 2.

It should be noted that the developed MIC perform their function and have the parameters value within the limits of the set norms during and after the influence of the special factors 7.И with the characteristics values 7.$И_1$-7.$И_7$, 7.$И_{10}$, and 7.$И_{11}$ according to GOST PB 20.39.414.2 for the performance group 3$У_c$.

A TRM based on the developed MIC set has two antennas operating to transmit and receive signals.

Figs. 4 and 5 show calculated and measured diagrams of antenna radiation pattern.

Under such conditions, both transmitted and received signals are sent to the balance mixer involved in the SC, where subtraction of one signal from another takes place, and their difference is sent to the i-f amplifier. This diagram is common for the devices that determine the distance to the target and the object movement velocity. Antennas integration on one crystal with amplifiers deceases the losses in the path that, in its turn, decreases noise factor in the receiving path and increases the transmitted power of the transmission path. An antenna radiation area is above the crystal. Radiation maximum is perpendicular to the crystal plane. A voltage-controlled generator (VCG) retunes the signal in the range of 2 GHz

Table 2. The parameters of the MIC resistance to the influence of climatic and mechanical factors

Name of the external influencing factor	Name of the factor characteristic, unit of measure	Characteristic value of the influencing factor
Mechanical factors		
Mechanical shocks of single action	Peak impact acceleration, m/s² (g)	15 000 (1500)*
	Action durability of shock acceleration, msec	0.1–2
Climatic factors		
Increased ambient temperature	Maximum value during operation, °C	minus 85
Decreased ambient temperature	Minimum value during operation, °C	minus 60
	Minimum value during transportation and storage, °C	minus 60
* Resistance requirement to the influencing factor is imposed only for strength		

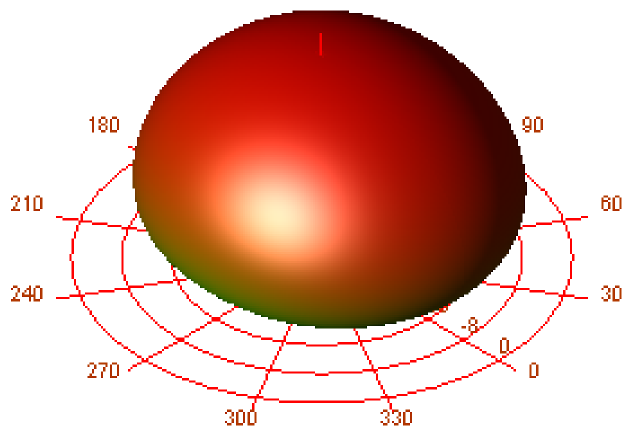

Fig. 4. Radiation pattern (calculation)

owning to the control voltage (initial value of the VCG frequency therewith lies in the range of 57–64 GHz) and power from 10 to 20 mW. The high frequency signal range received from the receiving antenna to the mixer is 57–64 GHz. In such a way, VCG fine-tune makes it possible to receive an output signal of the intermediate frequency in the range from 0 to 2 GHz.

The dependence of the VCG generation frequency on the control voltage and microwave parameters of the PA are shown in Figs. 6 and 7.

The analysis of the present state of the similar developments of the microwave MIC abroad has shown that in this range, the MIC built according to CMOS or SiGe technologies on the silicon substrate are employed [3, 4]. Only separate components (amplifiers, mixers, etc.) are built on AlGaN/GaN/Al_2O_3 heterostructures.

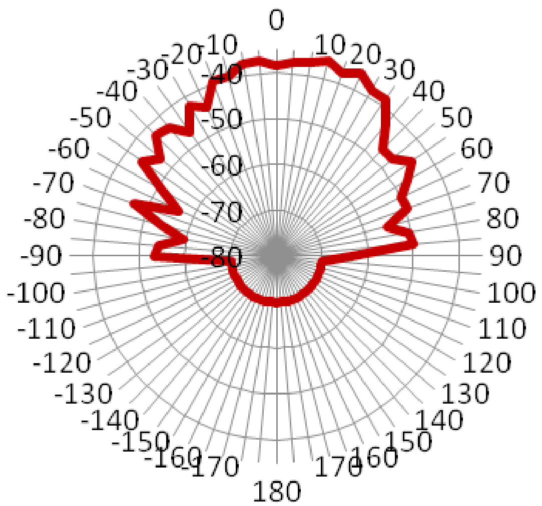

Fig. 5. Radiation pattern (measurement)

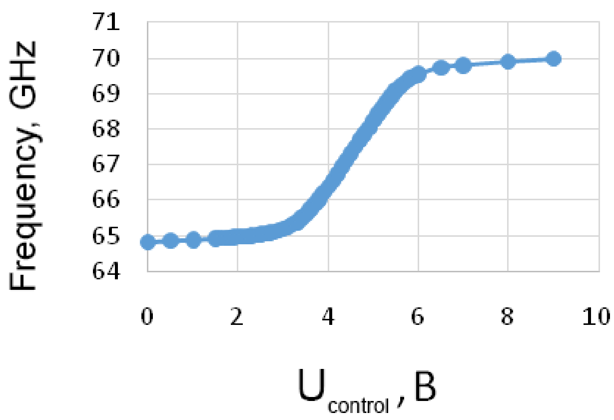

Fig. 6. Dependence of the VCG oscillation frequency

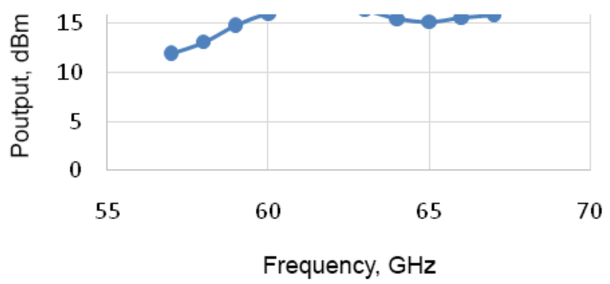

Fig. 7. Microvawe parameters of PA

Conclusion

The technology developed in IUHFSE RAS allows one to create MIC amplifiers of increased power and low noise factor, as well as to integrate on one crystal all components of the transmitter receiver devices: VCG, mixer, amplifiers and antennas.

In future, in the terms of mass production of microwave MIC, it will be possible to transfer to silicon substrates to reduce products cost. IUHFSE RAS is actively carrying out research to solve the problem of production of GaN heterostructures on silicon.

The created basic technology and design solutions have become the basis to fulfil future efforts on building promising microwave ECB in the interests of space technology [5].

References

1. Mal'tsev P.P., Shakhnovich I.V. SVCh-tekhnologii – osnova elektroniki budushchego. Tendentsii i rynki [Microwave technologies - the basis of future electronics. Trends and markets]. *Elektronika. Nauka, tekhnologiya, biznes* [Electronics: Science, Technology, Business]. 2015, No. 8, pp. 78–84. (in Russian)

2. Mal'tsev P.P., Fedorov Yu.V., Galiev R.R., Mikhaylovich S.V., Gnatyuk D.L. Nitridnye pribory millimetrovogo diapazona [Millimetre range nitride devices]. *Nanoindustriya* [Nanoindustry]. 2014, No. 3, pp. 40–51. (in Russian)

3. Ghaffar F.A. 60 GHz system-on-chip (SoC) with built-in memory and an on-chip antenna. Antennas and Propagation (EuCAP). 2014, 8th European Conference on Antennas and Propagation (EuCAP), pp. 531–532.

4. Jian Zhang. Low noise amplifier with integrated balanced antenna for 60 GHz wireless communications. Antennas and Propagation. 2014, IEEE Transactions, Vol. 62, No. 6 pp. 3407–3411.

5. Mal'tsev P.P., Matveenko O.S., Fedorov Yu.V., Gnatyuk D.L., Krapukhin D.V., Zuev A.V., Bunegina S.L. Monolitnaya integral'naya skhema usilitelya so vstroennoy antennoy dlya pyatimillimetrovogo diapazona dlin voln [5 mm-Wave Amplifier Monolithic Integrated Circuit with Integrated Antenna]. *Nano- i mikrosistemnaya tekhnika* [Nano and microsystem technique]. 2014, No. 9, pp. 12–15. (in Russian)